THE EUROPEAN
PHYSICAL JOURNAL C

$\eta^{(\prime)}$-meson twist-2 distribution amplitude within QCD sum rule approach and its application to the semi-leptonic decay $D_s^+ \rightarrow \eta^{(\prime)}\ell^+\nu_\ell$

Dan-Dan Hu[1], **Hai-Bing Fu**[1,3,a] , **Tao Zhong**[1], **Long Zeng**[2,3], **Wei Cheng**[4], **Xing-Gang Wu**[2,3,b]

[1] Department of Physics, Guizhou Minzu University, Guiyang 550025, People's Republic of China
[2] Department of Physics, Chongqing University, Chongqing 401331, People's Republic of China
[3] Chongqing Key Laboratory for Strongly Coupled Physics, Chongqing 401331, People's Republic of China
[4] School of Science, Chongqing University of Posts and Telecommunications, Chongqing 400065, People's Republic of China

Abstract In this paper, we make a detailed discussion on the η and η'-meson leading-twist light-cone distribution amplitude $\phi_{2;\eta^{(\prime)}}(u, \mu)$ by using the QCD sum rules approach under the background field theory. Taking both the non-perturbative condensates up to dimension-six and the next-to-leading order (NLO) QCD corrections to the perturbative part, its first three moments $\langle \xi_{2;\eta^{(\prime)}}^n \rangle|_{\mu_0}$ with $n = (2, 4, 6)$ can be determined, where the initial scale μ_0 is set as the usual choice of 1 GeV. Numerically, we obtain $\langle \xi_{2;\eta}^2 \rangle|_{\mu_0} = 0.231_{-0.013}^{+0.010}$, $\langle \xi_{2;\eta}^4 \rangle|_{\mu_0} = 0.109_{-0.007}^{+0.007}$, and $\langle \xi_{2;\eta}^6 \rangle|_{\mu_0} = 0.066_{-0.006}^{+0.006}$ for η-meson, $\langle \xi_{2;\eta'}^2 \rangle|_{\mu_0} = 0.211_{-0.017}^{+0.015}$, $\langle \xi_{2;\eta'}^4 \rangle|_{\mu_0} = 0.093_{-0.009}^{+0.009}$, and $\langle \xi_{2;\eta'}^6 \rangle|_{\mu_0} = 0.054_{-0.008}^{+0.008}$ for η'-meson. Next, we calculate the $D_s \rightarrow \eta^{(\prime)}$ transition form factors (TFFs) $f_+^{\eta^{(\prime)}}(q^2)$ within QCD light-cone sum rules approach up to NLO level. The values at large recoil region are $f_+^{\eta}(0) = 0.476_{-0.036}^{+0.040}$ and $f_+^{\eta'}(0) = 0.544_{-0.042}^{+0.046}$. After extrapolating TFFs to the allowable physical regions within the series expansion, we obtain the branching fractions of the semi-leptonic decay, i.e. $D_s^+ \rightarrow \eta^{(\prime)}\ell^+\nu_\ell$, i.e. $\mathcal{B}(D_s^+ \rightarrow \eta^{(\prime)}e^+\nu_e) = 2.346_{-0.331}^{+0.418}(0.792_{-0.118}^{+0.141}) \times 10^{-2}$ and $\mathcal{B}(D_s^+ \rightarrow \eta^{(\prime)}\mu^+\nu_\mu) = 2.320_{-0.327}^{+0.413}(0.773_{-0.115}^{+0.138}) \times 10^{-2}$ for $\ell = (e, \mu)$ channels respectively. And in addition to that, the mixing angle for $\eta - \eta'$ with φ and ratio for the different decay channels $\mathcal{R}_{\eta'/\eta}^\ell$ are given, which show good agreement with the recent BESIII measurements.

1 Introduction

The D_s^+-meson, which is composed of a charm quark and a strange antiquark, has been discovered in year 1993. There are rich physics contents in D_s^+-meson decays. The D_s^+-meson semileptonic or exclusive decay processes provide important heavy-to-light theoretical bases for studying heavy quark decays, investigating light meson spectroscopy and supplying a bridge between weak and strong interaction couplings of quarks. More and more experimental results have been reported from the BABAR, the CLEO, the BESIII collaborations, and etc., such as the $D_s^+ \rightarrow (\eta, \eta', K^0, a_0(980), f_0(980), \phi, K^{*0})\ell^+\nu_\ell$ decays' branching fractions are within the range of $[0.12, 2.61]\%$ [1–6]. Total semileptonic branching fractions provide useful discrimination on the different theoretical evaluations of hadronic matrix elements, which sizably affect the charm quark semileptonic decays. The $D_s \rightarrow \eta^{(\prime)}\ell^+\nu_\ell$ is different from the usually considered channels with final state containing light-quark composition only, and it has attracted much attention from both theoretical and experimental groups. Moreover, the $\eta^{(\prime)}$-mesons, composed by $s\bar{s}$ quark pair, are especially intriguing, since the s-quark plays an important role for the flavor physics. In deep leaning of those two processes, one can obtain useful information on the CKM matrix element $|V_{cs}|$ and the heavy-to-light transition form factors (TFFs).

Experimentally, the semileptonic decay processes for $D_s^+ \rightarrow \eta^{(\prime)}\ell^+\nu_\ell$ have been found by the CLEO collaboration early in year 1995, and their measured value of the ratio of branching fractions $\mathcal{B}(D_s^+ \rightarrow \eta'e^+\nu_e)/\mathcal{B}(D_s^+ \rightarrow \eta e^+\nu_e)$ is $0.35 \pm 0.09 \pm 0.07$ [7]. Then, the CLEO collaboration issued the measured value of the branching fractions in years 2009

[a] e-mail: fuhb@cqu.edu.cn (corresponding author)
[b] e-mail: wuxg@cqu.edu.cn

and 2015, i.e. $\mathcal{B}(D_s^+ \to \eta e^+ \nu_e) = (2.48 \pm 0.29 \pm 0.13)\%$, $\mathcal{B}(D_s^+ \to \eta e^+ \nu_e) = (2.28 \pm 0.14 \pm 0.20)\%$, $\mathcal{B}(D_s^+ \to \eta' e^+ \nu_e) = (0.91 \pm 0.33 \pm 0.05)\%$, and $\mathcal{B}(D_s^+ \to \eta' e^+ \nu_e) = (0.68 \pm 0.15 \pm 0.06)\%$ [8,9]. In year 2017, the BESIII collaboration measured the branching fractions by using the same channels based on the integrated luminosity of 482 pb^{-1} of the $e^+ e^-$ collision at the center-of-mass energy $\sqrt{s} = 4.009$ GeV, and they issued $\mathcal{B}(D_s^+ \to \eta \mu^+ \nu_\mu) = (2.42 \pm 0.46 \pm 0.11)\%$, $\mathcal{B}(D_s^+ \to \eta' \mu^+ \nu_\mu) = (1.06 \pm 0.54 \pm 0.07)\%$, $\mathcal{B}(D_s^+ \to \eta e^+ \nu_e) = (2.30 \pm 0.31 \pm 0.08)\%$, and $\mathcal{B}(D_s^+ \to \eta' e^+ \nu_e) = (0.93 \pm 0.30 \pm 0.05)\%$ [10,11]. In year 2019, the BESIII collaboration finished the improved measurements on the branching fractions by using $e^+ e^-$ annihilation data corresponding to an integrated luminosity of 3.19 fb^{-1} collected at a center-of-mass energy of 4.178 GeV and then gave the first determination of $D_s \to \eta^{(\prime)}$ TFF, e.g. $\mathcal{B}(D_s^+ \to \eta e^+ \nu_e) = (2.323 \pm 0.063 \pm 0.063)\%$, $\mathcal{B}(D_s^+ \to \eta' e^+ \nu_e) = (0.824 \pm 0.073 \pm 0.027)\%$, $f_+^\eta(0)|V_{cs}| = 0.4455 \pm 0.0053 \pm 0.0044$, and $f_+^{\eta'}(0)|V_{cs}| = 0.477 \pm 0.049 \pm 0.011$ [12]. There are large discrepancies for $D_s^+ \to \eta^{(\prime)} \ell^+ \nu_\ell$ among different experimental collaborations. With more and more data accumulated in the near future, the experimental precision shall be greatly improved and the gap among different measurements could be shrunk.

Theoretically, the decay widths or branching fractions for the semileptonic decay $D_s^+ \to \eta^{(\prime)} \ell^+ \nu_\ell$ depends heavily on the precision of the $D_s \to \eta^{(\prime)}$ TFFs. At present, the $D_s \to \eta^{(\prime)}$ TFFs have been studies under various approaches, such as the lattice QCD (LQCD) [13], the traditional and covariant light-front quark model (LFQM) [14–16], the constituent quark model (CQM) [17], the covariant confined quark model (CCQM) [18,19], the light-cone sum rules (LCSR) [20,21], the QCD sum rules (QCD SR) [22]. The LCSR approach is based on the operator product expansion (OPE) near the light-cone $x^2 \rightsquigarrow 0$ and parameterizes all the non-perturbative dynamics into the light-cone distribution amplitudes (LCDAs), which have been applied for dealing with many semileptonic decay processes [23–39]. One may observe that the predicted values of $D_s \to \eta^{(\prime)}$ TFFs behave differently from various groups. Those discrepancies indicate that it is important to improve the accuracy of theoretical calculation. In this paper, we will calculate the $D_s \to \eta^{(\prime)}$ TFFs by using the LCSR approach up to next-to-leading order (NLO) QCD corrections.

It is well known that the states η and η' are considered as candidates for mixing. The mixing among pseudoscalar mesons is of great theoretical interests and significance for understanding the dynamics and hadronic structures, which is caused by the QCD anomaly and related to the chiral symmetry breaking. Thus, one can gain a better insight into the dynamics if the mixing parameters are more accurately determined. The semileptonic decays $D_s^+ \to \eta^{(\prime)} \ell^+ \nu_\ell$ probe the

$s\bar{s}$ components of η and η', which can well separate the strong and weak effects in theory, are expected to be sensitive to $\eta - \eta'$ mixing angle [40]. Many measurements on the processes, where η and η' are involved, have been carried out to fix the mixing parameters. The $\eta - \eta'$ mixing can be described in different forms. To investigate the $\eta - \eta'$ mixing, two schemes have been suggested in the literature [41–47], i.e. the singlet-octet (SO) mixing scheme and the quark-flavor (QF) mixing scheme. The SO mixing angle θ between η and η' is known to be in the range of $\theta \in [-10°, -23°]$. In this scheme, The η and η' are the mixtures of the flavor SU(3) octet η_8 and single η_0 states:

$$\begin{pmatrix} \eta \\ \eta' \end{pmatrix} = \begin{pmatrix} \cos\theta & -\sin\theta \\ \sin\theta & \cos\theta \end{pmatrix} \begin{pmatrix} \eta_8 \\ \eta_0 \end{pmatrix}, \tag{1}$$

where $\eta_8 = (u\bar{u} + d\bar{d} - 2s\bar{s})/\sqrt{6}$ and $\eta_0 = (u\bar{u} + d\bar{d} + s\bar{s})/\sqrt{3}$. Analogously, information could be gathered on the mixing scheme in the QF basis, which is consists with the form η and η' states as combinations of $|\eta_q\rangle = |\bar{u}u + \bar{d}d\rangle/\sqrt{2}$ and $|\eta_s\rangle = |\bar{s}s\rangle$:

$$|\eta\rangle = \cos\varphi|\eta_q\rangle - \sin\varphi|\eta_s\rangle,$$
$$|\eta'\rangle = \sin\varphi|\eta_q\rangle + \cos\varphi|\eta_s\rangle. \tag{2}$$

It has been shown that in this scheme a single angle is essentially required. In year 2007, the KLOE Collaboration provides the value $\varphi = (41.5 \pm 0.3_{\text{stat}} \pm 0.7_{\text{syst}} \pm 0.6_{\text{th}})°$ by extracting the pseudoscalar mixing angle φ in the QF basis by measuring the radio $\mathcal{B}(\phi \to \eta'\gamma)/\mathcal{B}(\phi \to \eta\gamma)$ [48]. Some theoretical groups have calculated the single mixing angle φ [21,22,47,49], their predicted values are within the range of $\varphi \in [39°, 41.8°]$. One can put forward the ratio $\mathcal{R}_{\eta'/\eta} = \mathcal{B}(D_s \to \eta'\ell^+\nu_\ell)/\mathcal{B}(D_s \to \eta\ell^+\nu_\ell)$ to access the $\eta - \eta'$ mixing angle through the ratio of the TFFs $f_+^\eta(q^2)/f_+^{\eta'}(q^2)$ [22], which are related to the $\eta - \eta'$ mixing scheme. In particular, information could be gathered on the mixing scheme in the QF basis. In this paper, we will use the QF basis with the single mixing angle φ to analyze the $D_s \to \eta^{(\prime)}$ decay modes, and the corresponding TFFs satisfy the relation

$$\tan\varphi = \frac{|f_+^\eta(q^2)|}{|f_+^{\eta'}(q^2)|}. \tag{3}$$

One usually takes the large recoil point of the squared momentum transfer $q^2 = 0$ to do the calculation, i.e. $\tan\varphi = |f_+^\eta(0)|/|f_+^{\eta'}(0)|$. A more accurate $D_s^+ \to \eta^{(\prime)}\ell^+\nu_\ell$ LCSR analysis is important.

The η and η' mesons full of rich phenomenology, which are predominantly flavor-singlet states. This means that their wave functions are approximately symmetric in the three

lightest quark types (up, down, and strange), which build up the light-hadron spectroscopy. Thus, the LCDAs for $\eta^{(\prime)}$-meson, as one of the most important parameters, composed by $s\bar{s}$ are significant to the $D_s \rightarrow \eta^{(\prime)}$ TFFs, which can be expanded as a Gegenbauer polynomial series:

$$\phi_{2;\eta^{(\prime)}}(u, \mu) = 6u\bar{u}\left[1 + \sum_{n=1}^{\infty} a^n_{2;\eta^{(\prime)}}(\mu) C^{3/2}_n(\xi)\right], \qquad (4)$$

where $a^n_{2;\eta^{(\prime)}}(\mu)$ stands for the nth-order Gegenbauer moment, $\bar{u} = (1 - u)$ and $\xi = (2u - 1)$. When the factorization scale μ is large enough, the twist-2 LCDAs $\phi_{2;\eta^{(\prime)}}(u, \mu)$ tends to the asymptotic form $\phi_{2;\eta^{(\prime)}}(u, \infty) = 6u\bar{u}$. There are some theoretical and experimental predictions for the Gegenbauer moments $a^n_{2;\eta}(\mu)$, such as the fitting results coming from CLEO collaboration $a^2_{2;\eta}(\mu_0) = -0.07 \pm 0.03$ [50], the fitting results from BABAR result $a^2_{2;\eta}(\mu_0) = -0.05 \pm 0.02$ [51], the results predicted by Kroll and Passek-Kumericki $a^2_{2;\eta}(\mu_0) = -0.05 \pm 0.02$ [52], and the fitting results from a sum rule analysis $a^2_{2;\eta}(\mu_0) = 0.25 \pm 0.15$ [20]. By taking the approximation with π, K-meson, Ball and Zwicky predicted $a^2_{2;\eta}(\mu_0) = 0.115$ and $a^4_{2;\eta}(\mu_0) = -0.015$ [53]. At present, few works have been done to calculate the second and higher order moment. Particularly, the twist-2 LCDA of η'-meson is rarely studied. So it is important and meaningful to make a more accurate calculation on the second order moment and the higher order moments for $\eta^{(\prime)}$-meson LCDAs within the QCD sum rule approach.

An effective way to calculate the nth-order moments of the $\eta^{(\prime)}$-meson LCDAs is to use the following definition,

$$\langle\xi^n_{2;\eta^{(\prime)}}\rangle|_\mu = \int_0^1 du\, \xi^n\, \phi_{2;\eta^{(\prime)}}(u, \mu). \qquad (5)$$

$\langle\xi^n_{2;\eta^{(\prime)}}\rangle|_\mu$ can be calculated by using the Shifman–Vainshtein–Zakharov (SVZ) sum rules [54–59]. In which, the perturbative QCD is established on the assumption that the perturbative vacuum and the short-distance interaction are not affected by the long-distance structure of the non-Abelian gauge field. The QCD physical vacuum contains a series of vacuum condensates, such as the quark condensate $\langle q\bar{q}\rangle$, the gluon condensate $\langle G^2\rangle$, and etc. These vacuum condensates reflect the non-perturbation characteristics of QCD. The QCD sum rules based on the background field theory (BFTSR) method gives a possible way to consider the non-perturbation effect, which also provides a systematic description of these vacuum condensates from the field theory point of view. At present, the BFTSR has been used in calculating the twist-2 or twist-3 LCDAs for π, K, D, D_s, a_0, K_0^*, f_0, ρ, J/ψ, $a_1(1260)$-mesons [60–72]. Besides, other methods in studying the LCDAs can be found in Refs. [73–81]. In this paper, we will calculate the $\eta^{(\prime)}$-meson twist-2 LCDAs within the BFTSR approach for the first time.

The rest of the paper are organized as follows. In Sect. 2, we present the basic idea of the QCD background field theory, the detailed BFTSR procedures for calculating the moments of $\phi_{2;\eta^{(\prime)}}(u, \mu)$, the branching fractions and the transition form factors involved in the semileptonic decay $D_s^+ \rightarrow \eta^{(\prime)}\ell^+\nu_\ell$. In Sect. 3, we present our numerical results and make a detailed comparison with other experimental and theoretical predictions. Section 4 is reserved for a summery. The intermediate processes for calculating the moments of $\eta^{(\prime)}$-meson LCDA within the BFTSR and the basic definition of $\eta^{(\prime)}$-meson twist-2, 3, 4 LCDAs are given in the Appendixes A, B and C.

2 Calculation technology

2.1 Basic idea and formulas for background field theory

The important aspect for the SVZ sum rules approach is the OPE, which has been introduced by using the QCD physical vacuum $\langle 0|\mathcal{O}_N|0\rangle_{\text{phys.}}$. Its special property is the non-perturbation effect, which can be described by the classical background field satisfying the equations of motion. The main idea of the background field theory method is to describe the non-perturbation effect with the classical background field satisfying the equation of motion and to describe the quantum fluctuation, namely the perturbation effect, on this basis within the frame of the quantum field theory. More specifically, one can use the following substitution in the theoretical Lagrangian and Green's functions [55,82,83]

$$\mathcal{A}^a_\mu(x) \rightarrow \mathcal{A}^a_\mu(x) + \phi^a_\mu(x),$$
$$\psi(x) \rightarrow \psi(x) + \eta(x), \qquad (6)$$

where $\mathcal{A}^a_\mu(x)$ and $\psi(x)$ stand for the gluon and quark background fields, $\phi^a_\mu(x)$ and $\eta(x)$ represent their quantum fluctuations, respectively. In the presence of background fields, the quantization of $\phi^a_\mu(x)$ and $\eta(x)$ has been completed in Ref. [84]. Among them, the gluon quantum field satisfies the background field gauge,

$$D^{ab}_\mu(\mathcal{A})\phi^\mu_b = 0,$$
$$D^{ab}_\mu(\mathcal{A}) = \delta^{ab}\partial_\mu - g_s f^{abc}\mathcal{A}^c_\mu, \qquad (7)$$

where the color indices $a, b, c = (1, 2, \ldots, 8)$, g_s is the coupling constant of strong interactions, f^{abc} is the structure constant of the $SU_f(3)$ group. The advantage of choosing the background field gauge is that it makes the theory be invariant under the background field gauge, making the calculated physical quantity independent of the gauge. With the help of Eq. (6), one can obtain the following effective Lagrangian [54]

$$\mathcal{L}_{\text{eff}} = \mathcal{L}_{\text{QCD}}(\mathcal{A}, \psi) + \mathcal{L}(\text{ghosts}) + \bar{\eta}(i\not{D} - m)\eta$$
$$+ \frac{1}{2}\phi_\mu^a \left\{ g^{\mu\nu} D_{ac}^2 - \left(1 - \frac{1}{\alpha}\right)[D^\mu D^\nu]_{ac} \right.$$
$$\left. + 2g_s f^{abc} G_b^{\mu\nu} \right\} \phi_\nu^c + g_s(\bar{\psi}\phi^a T^a \eta + \bar{\eta}\phi^a T^a \eta)$$
$$- g_s^2 f^{adf} f_{abc} \mathcal{A}_d^\mu \phi_f^\nu \phi_\mu^b \phi_\nu^c - g_s f^{abc}$$
$$\times (\partial_\mu \phi_\nu^a)\phi_b^\mu \phi_c^\nu - \frac{1}{4}g_s^2 f^{abc} f_{acf} \phi_b^\mu \phi_c^\nu \phi_\mu^d \phi_\nu^f$$
$$+ g_s \bar{\eta}\phi^a T^a \eta, \tag{8}$$

where the $\mathcal{L}_{\text{QCD}}(\mathcal{A}, \psi)$ with $\mathcal{A}_\mu^a(x)$, $\psi(x)$ has the usual form of QCD Lagrangian and can be minimized to zero when the classical fields $\mathcal{A}_\mu^a(x)$ and $\psi(x)$ are the solutions of the equation of motion, and α is the gauge-fixing parameter. The $\mathcal{L}(\text{ghosts})$ is the contribution of the ghost particle term. Especially, in order to describe the various quark-antiquark pairs and gluons in a vacuum, one can follow the classical QCD Lagrangian [54]

$$\mathcal{L}_{\text{QCD}}(\mathcal{A}, \psi) = -\frac{1}{4}G_{\mu\nu}^a G^{a\mu\nu} + \bar{\psi}(i\not{D} - m)\psi, \tag{9}$$

with $G_{\mu\nu}^a = \partial_\mu \mathcal{A}_\nu^a - \partial_\nu \mathcal{A}_\mu^a + g_s f^{abc} \mathcal{A}_\nu^b \mathcal{A}_\mu^c$ stands for the gluon field strength tensor. The gluon field $\mathcal{A}_\mu^a(x)$ and quark field $\psi(x)$ satisfy the QCD equations of motion,

$$(i\not{D} - m)\psi(x) = 0,$$
$$\widetilde{D}_\mu^{ab} G_b^{\nu\mu}(x) = g_s \bar{\psi}(x)\gamma^\nu T^a \psi(x), \tag{10}$$

where $D_\mu = \partial_\mu - i g_s T^a \mathcal{A}_\mu^a(x)$ with $a, b, c = (1, 2, \ldots, 8)$ and $\widetilde{D}_\mu^{ab} = \delta^{ab}\partial_\mu - g_s f^{abc} \mathcal{A}_\mu^c(x)$ are fundamental and adjoint representations of the gauge covariant derivative, respectively. As an advantage of using the background field theory, one can take different gauges for dealing with the quantum fluctuations and background fields. More specifically, one can adopt the background gauge, i.e. $\widetilde{D}_\mu^{AB}\phi^{B\mu}(x) = 0$ for the gluon quantum field [85–87], the Schwinger gauge or the fixed-point gauge, i.e. $x^\mu \mathcal{A}_\mu^A(x) = 0$ for the background field [88].

As the background field satisfies the motion equation (10), at least one background field is included in the coupling between the quantum fluctuation field and the background field. In the effective Lagrangian, there is no contribution from the vertex $g_s \bar{\psi}\gamma^\mu \phi_\mu^a T^a \psi$, and it only has the vertex $g_s \bar{\psi}\phi_\mu^a T^a \eta$ and its conjugate contributions. According to the effective Lagrangian, the quantum quark and gluon propagators in the background field are [67]

$$S_F(x) = i[i\gamma^\mu D_\mu - m]^{-1}, \tag{11}$$
$$S_{\mu\nu}^{ab}(x) = i[g_{\mu\nu}(D^2)^{ab} + 2g_s f^{abc} G_{\mu\nu}^c]^{-1}, \tag{12}$$

where the gauge-fixing parameter is taken as $\alpha = 1$. Within the framework of BFT, the quark propagator will be affected by the background quark and/or gluon fields, which satisfies the equation

$$(i\not{D} - m)S_F(x, 0) = \delta^4(x). \tag{13}$$

If taking

$$S_F(x, 0) = (i\not{D} + m)\mathcal{D}(x, 0), \tag{14}$$

Eq. (13) can be changed as

$$(\Box - \mathcal{P}_\mu \partial^\mu - \mathcal{Q} + m^2)\mathcal{D}(x, 0) = \delta^4(x), \tag{15}$$

where $\Box = \partial^2$, and

$$\mathcal{P}_\mu = 2i\mathcal{A}_\mu(x),$$
$$\mathcal{Q} = \gamma^\nu \gamma^\mu \mathcal{A}_\nu(x)\mathcal{A}_\mu(x) + i\gamma^\nu \gamma^\mu \partial_\nu \mathcal{A}_\mu(x). \tag{16}$$

Moreover, after applying the fixed-point gauge, the gluon background field can be expressed by using the gauge invariant $G_{\mu\nu;\alpha_1\cdots\alpha_n}$ as

$$\mathcal{A}_\mu(x) = \frac{1}{2}x^\nu G_{\nu\mu} + \frac{1}{3}x^\nu x^\alpha G_{\nu\mu;\alpha}$$
$$+ \frac{1}{8}x^\nu x^\alpha x^\beta G_{\nu\mu;\alpha\beta} + \frac{1}{30}x^\nu x^\alpha x^\beta x^\gamma G_{\nu\mu;\alpha\beta\gamma}$$
$$+ \frac{1}{144}x^\nu x^\alpha x^\beta x^\gamma x^\delta G_{\nu\mu;\alpha\beta\gamma\delta} + \cdots, \tag{17}$$

where $G_{\mu\nu;\alpha_1\cdots\alpha_n}$ is the notation for $(D_{\alpha_1}\cdots D_{\alpha_n}G_{\mu\nu})(0)$, where the indexes $\alpha_1\cdots\alpha_n$ indicates the covariant derivative up to n-th order. Substituting Eq. (17) into Eq. (15), we obtain the expressions for $\mathcal{D}(x, 0)$. By further using Eq. (14), we obtain the required quark propagators in the background field, i.e.,

$$S_F(x, 0) = S_F^0(x, 0) + S_F^2(x, 0)$$
$$+ S_F^3(x, 0) + \sum_{i=1}^{2} S_F^{4(i)}(x, 0)$$
$$+ \sum_{i=1}^{3} S_F^{5(i)}(x, 0) + \sum_{i=1}^{5} S_F^{6(i)}(x, 0). \tag{18}$$

We present the quark propagators with various gauge invariant tensors $G_{\mu\nu;\alpha_1\cdots\alpha_n}$ that shall result in up to dimension-six operators in the Appendix A1. Because the fixed-point gauge violates the translation invariance, the quark propagator from x to 0, $S_F(0, x)$, can not be directly obtained by applying the replacement $x \to -x$ in Eq. (18). However, it can be related with $S_F(x, 0)$ via the relation [59]

$$S_F(0, x|\mathcal{A}) = C S_F^{\text{T}}(x, 0| - \mathcal{A}^{\text{T}})C^{-1}, \tag{19}$$

where C stands for the charge conjugation matrix and the symbol T indicates transposition of both the Dirac and the color matrices.

Furthermore, one will encounter the vertex operator $\Gamma(z \cdot \overset{\leftrightarrow}{D})^n$ with Γ indicates all kinds of Dirac matrices for heavy/light-meson twist-2, 3 LCDAs. Generally, we have the following expansion [60]

$$(z \cdot \overset{\leftrightarrow}{D})^n = (z \cdot \overrightarrow{D} - z \cdot \overleftarrow{D})^n = (z \cdot \overset{\leftrightarrow}{\partial} + z \cdot B)^n + \cdots, \tag{20}$$

where the ellipsis denotes for the higher-order terms, which are irrelevant for our present analysis and

$$
\begin{aligned}
z \cdot B &= -2iz \cdot \mathcal{A} \\
&= -ix^\mu z^\nu G_{\mu\nu} - \frac{2i}{3}x^\mu x^\rho z^\nu G_{\mu\nu;\rho} \\
&\quad - \frac{i}{4}x^\mu x^\rho x^\sigma z^\nu G_{\mu\nu;\rho\sigma} - \frac{i}{15}x^\mu x^\rho x^\sigma x^\lambda z^\nu G_{\mu\nu;\rho\sigma\lambda} \\
&\quad - \frac{i}{72}x^\mu x^\rho x^\sigma x^\lambda x^\tau z^\nu G_{\mu\nu;\rho\sigma\lambda\tau} + \cdots.
\end{aligned}
\tag{21}
$$

We can expand the operator $(z \cdot \overset{\leftrightarrow}{D})^n$ into series of the operators $(z \cdot \overset{\leftrightarrow}{\partial})^n$ and $G_{\mu\nu;\rho\dots}$. For the purpose, we first expand $(z \cdot \overset{\leftrightarrow}{D})^n$ as

$$
\begin{aligned}
(z \cdot \overset{\leftrightarrow}{D})^0 &= 1, \\
(z \cdot \overset{\leftrightarrow}{D})^1 &= z \cdot \overset{\leftrightarrow}{\partial} + z \cdot B, \\
(z \cdot \overset{\leftrightarrow}{D})^2 &= (z \cdot \overset{\leftrightarrow}{\partial})^2 + 2(z \cdot \overset{\leftrightarrow}{\partial})(z \cdot \underline{B}) + (z \cdot B)^2, \\
(z \cdot \overset{\leftrightarrow}{D})^3 &= (z \cdot \overset{\leftrightarrow}{\partial})^3 + 3(z \cdot \overset{\leftrightarrow}{\partial})^2(z \cdot \underline{B}) \\
&\quad + \left[(z \cdot \partial)^2(z \cdot B)\right] + 3(z \cdot \overset{\leftrightarrow}{\partial})(z \cdot \underline{B})^2 + (z \cdot B)^3, \\
&\cdots,
\end{aligned}
\tag{22}
$$

where, the operator "underline" below symbol "B" (or "x" in the Appendix A2) indicates that the operation $\overset{\leftrightarrow}{\partial}$ does not act on it. In deriving those equations, the following equation has been adopted,

$$(z \cdot \overset{\leftrightarrow}{\partial})^n(z \cdot B) = \sum_{k=0}^{n} \frac{n!}{k!(n-k)!}(z \cdot \overset{\leftrightarrow}{\partial})^{n-k}\left[(z \cdot \partial)^k(z \cdot \underline{B})\right]. \tag{23}$$

By keeping only those terms that shall leads to operators up to dimension-six, we can obtain the full expression for the vertex operator, which are listed in the Appendix A2.

2.2 SVZ sum rules for the moments of $\phi_{2;\eta^{(\prime)}}(x, \mu)$

Following the traditional way of constructing the light pseudoscalar meson, we take the following definition

$$
\begin{aligned}
&\langle 0|\bar{s}(0)\mathcal{C}_s \not{z} \gamma_5[z, -z](iz \cdot \overset{\leftrightarrow}{D})^n s(0)|\eta^{(\prime)}(q)\rangle \\
&= i(z \cdot q)^{n+1} f_{\eta^{(\prime)}} \langle \xi^n_{2;\eta^{(\prime)}}\rangle|_\mu,
\end{aligned}
\tag{24}
$$

where z_μ stand for the light-like vector and $[z, -z]$ is the path-ordered gauge connection, $f_{\eta^{(\prime)}}$ are the η and η'-meson decay constant, $(iz \cdot \overset{\leftrightarrow}{D})^n = (iz \cdot \overrightarrow{D} - iz \cdot \overleftarrow{D})^n$. Basis on the QF scheme, the flavour content is $\mathcal{C}_s = (\mathcal{C}_1 - \sqrt{2}\mathcal{C}_8)/\sqrt{3}$ with SO basis $\mathcal{C}_1 = \mathbf{1}/\sqrt{n_f}$ and $\mathcal{C}_8 = \lambda_8/\sqrt{2}$ [21,47]. In which the λ_i is the standard $\mathrm{SU}_f(3)$ Gell-Mann matrix and $\mathbf{1}$ is the 3×3 unit matrix. As a special case, the 0th-order LCDA's moment for Eq. (5) satisfies the normalization condition

$$\langle \xi^0_{2;\eta^{(\prime)}}\rangle|_\mu = \int_0^1 du \phi_{2;\eta^{(\prime)}}(u, \mu) = 1. \tag{25}$$

To derive the SVZ sum rules for the moments $\langle \xi^n_{2;\eta^{(\prime)}}\rangle|_\mu$, we introduce the following correlation function,

$$
\begin{aligned}
\Pi^{(n,0)}_{2;\eta^{(\prime)}}(z, q) &= i \int d^4x e^{iq \cdot x} \langle 0|T\{J_n(x), J_0^\dagger(0)\}|0\rangle \\
&= (z \cdot q)^{n+2} I^{(n,0)}_{2;\eta^{(\prime)}}(q^2),
\end{aligned}
\tag{26}
$$

where $J_n(x) = \bar{s}(x)\mathcal{C}_s \not{z} \gamma_5 (iz \cdot \overset{\leftrightarrow}{D})^n s(x)$, $J_0^\dagger(0) = \bar{s}(0)\mathcal{C}_s \not{z} \gamma_5 s(0)$ and $z^2 \rightsquigarrow 0$. Only even moments are non-zero and the odd moments of the LCDA are zero because of G-parity, i.e. $n = (0, 2, 4, 6, \dots)$ will contribute to the final results.[1] At one hand, in deep Euclidean region $q^2 \ll 0$, one can apply the OPE for the correlation function Eq. (26).

$$
\begin{aligned}
\Pi^{(n,0)}_{2;\eta^{(\prime)}}(z, q) &= i \int d^4x e^{iq \cdot x} \mathrm{Tr}[\mathcal{C}_s\mathcal{C}_s] \\
&\times \Big\{ - \mathrm{Tr}\langle 0|S_F^s(0, x)\not{z}\gamma_5(iz \cdot \overset{\leftrightarrow}{D})^n S_F^s(x, 0)\not{z}\gamma_5|0\rangle \\
&+ \mathrm{Tr}\langle 0|\bar{s}(x)s(0)\not{z}\gamma_5(iz \cdot \overset{\leftrightarrow}{D})^n S_F^s(x, 0)\not{z}\gamma_5|0\rangle \\
&+ \mathrm{Tr}\langle 0|S_F^s(0, x)\not{z}\gamma_5(iz \cdot \overset{\leftrightarrow}{D})^n \bar{s}(0)s(x)\not{z}\gamma_5|0\rangle \\
&+ \cdots \Big\},
\end{aligned}
\tag{27}
$$

where $\mathrm{Tr}[\mathcal{C}_s\mathcal{C}_s] = 1$. In the detailed OPE calculation, we adopt the $\overline{\mathrm{MS}}$-scheme to deal with the infrared divergences. Lorentz invariant scalar function $I^{(n,0)}_{2;\eta^{(\prime)}}(q^2)$ in Eq. (26) depends on the condensation parameter and will encounter the vacuum matrix elements of the following form,

$$
\begin{aligned}
&\langle 0|G^a_{\mu\nu}G^b_{\mu\nu}|0\rangle, \ \langle 0|G^a_{\mu\nu}G^b_{\rho\sigma}G^c_{\lambda\tau}|0\rangle, \\
&\langle 0|G^a_{\mu\nu;\lambda}G^b_{\rho\sigma;\tau}|0\rangle, \ \langle 0|G^a_{\mu\nu}G^b_{\rho\sigma;\lambda\tau}|0\rangle, \\
&\langle 0|G^a_{\mu\nu;\lambda\tau}G^c_{\rho\sigma}|0\rangle, \ \langle 0|\bar{q}^a_\alpha(x)q^b_\beta(y)|0\rangle, \\
&\langle 0|\bar{q}^a_\alpha(x)q^b_\beta(y)G^A_{\mu\nu}|0\rangle, \ \langle 0|\bar{q}^a_\alpha(0)q^b_\beta(0)G^A_{\mu\nu;\rho}|0\rangle.
\end{aligned}
\tag{28}
$$

The full expression for the vacuum condensates which one may encounter in the following calculations are listed in the

---

[1] This point can also been seen in Eq. (16) of Ref. [47].

Appendix A3, which can also be found in our previous work [60]. On the other side, the correlation function (26) can be treated by inserting a complete set of intermediate hadronic states in physical region to obtain its hadronic representation

$$
\begin{aligned}
\mathrm{Im} I^{(n,0)}_{2;\eta^{(\prime)},\mathrm{Had}}(q^2) = {}& \pi \delta(q^2 - m^2_{\eta^{(\prime)}}) f^2_{\eta^{(\prime)}} \langle \xi^n_{2;\eta^{(\prime)}} \rangle|_\mu \\
& + \pi \frac{3}{4\pi^2(n+1)(n+3)} \theta(q^2 - s_{\eta^{(\prime)}}),
\end{aligned}
\tag{29}
$$

in which $s_{\eta^{(\prime)}}$ stand for the continuum threshold for the lowest continuum state. The first term is the contribution of $\eta^{(\prime)}$-meson poles, and the second term is the contribution of continuum states above poles. Then both of the OPE part and the hadronic representation of the invariant function $I^{(n,0)}_{2;\eta^{(\prime)}}(q^2)$ can be marched with the following dispersion relation

$$
\frac{1}{\pi} \int_{4m_s^2}^\infty ds \frac{\mathrm{Im} I^{(n,0)}_{2;\eta^{(\prime)},\mathrm{Had}}(s)}{s - q^2} = I^{(n,0)}_{2;\eta^{(\prime)},\mathrm{QCD}}(q^2).
\tag{30}
$$

The Borel transform helps to reduce the contribution from the continuum states on the left of Eq. (30) and the contribution of the higher-dimension condensates on the right, and finally the sum rules can be obtained,

$$
\frac{1}{\pi} \frac{1}{M^2} \int ds e^{-s/M^2} \mathrm{Im} I^{(n,0)}_{2;\eta^{(\prime)},\mathrm{had}}(s) = \hat{\mathcal{B}}_{M^2} I^{(n,0)}_{2;\eta^{(\prime)},\mathrm{QCD}}(q^2),
\tag{31}
$$

where M^2 is Borel parameter, $\hat{\mathcal{B}}_{M^2}$ is Borel transformation operator,

$$
\hat{\mathcal{B}}_{M^2} = \lim_{\substack{-q^2, n \to \infty \\ -q^2/n = M^2}} \frac{1}{(n-1)!} (-q^2)^n \left(-\frac{d}{d(-q^2)} \right)^n.
\tag{32}
$$

In order to deal with the s-quark mass (m_s) contribution to $\langle \xi^n_{2;\eta^{(\prime)}} \rangle|_\mu$, we take the expansion according to different orders of m_s^k with $k = (0, 2, 4, \ldots)$, i.e. $I_{m_s^k}(n, M^2)$, since m_s is closer to Λ_{QCD}, which is different from our previous treatment for the heavy quark such as $q = (c, b)$ in Refs. [62,63]. Here, we take the first two orders of the squared s-quark mass, i.e. $I_{m_s^0}(n, M^2)$ and $I_{m_s^2}(n, M^2)$. The reason lies in the suppression of $m_s^4 < 0.1\%$ for the third-order, which are quite small and can be safely neglected. Recently, we have suggested a new method for renormalization of various moments, i.e. the 0th-order moment $\langle \xi^0_{2;\eta^{(\prime)}} \rangle|_\mu$ should be considered to the total results. The reason lies in the accuracy is often up to dimension-six condensates and the NLO QCD corrections for the perturbative part instead of the infinite dimension or infinite-order perturbative parts [89]. The final expression for $\langle \xi^n_{2;\eta^{(\prime)}} \rangle|_\mu$ can then be written as

$$
\begin{aligned}
& \frac{f^2_{\eta^{(\prime)}} \langle \xi^n_{2;\eta^{(\prime)}} \rangle|_\mu \langle \xi^0_{2;\eta^{(\prime)}} \rangle|_\mu}{M^2 e^{m^2_{\eta^{(\prime)}}/M^2}} \\
={}& \frac{1}{\pi} \frac{1}{M^2} \int_{4m_s^2}^{s_{\eta^{(\prime)}}} ds e^{-s/M^2} \frac{3v^{n+1}}{8\pi(n+1)(n+3)} \\
& \times \left(1 + \frac{\alpha_s}{\pi} A'_n \right) \left\{ [1 + (-1)^n] \right. \\
& \times (n+1) \frac{1 - v^2}{2} + [1 + (-1)^n] \left.\right\} + \frac{2m_s \langle \bar{s}s \rangle}{M^4} \\
& + \frac{\langle \alpha_s G^2 \rangle}{12\pi M^4} \frac{1 + n\theta(n-2)}{n+1} - \frac{8n+1}{9} \\
& \times \frac{m_s \langle g_s \bar{s}\sigma T Gs \rangle}{M^6} + \frac{\langle g_s \bar{s}s \rangle}{81M^6} 4(2n+1) \\
& - \frac{\langle g_s^3 f G^3 \rangle}{48\pi^2 M^6} n\theta(n-2) + \frac{\sum \langle g_s^2 \bar{q}q \rangle^2}{486\pi^2 M^6} \left\{ -2(51n \right. \\
& + 25) \left(-\ln \frac{M^2}{\mu^2} \right) + 3(17n + 35) \\
& + \theta(n-2) \left[2n \left(-\ln \frac{M^2}{\mu^2} \right) - 25(2n+1) \tilde{\psi}(n) \right. \\
& \left. + \frac{1}{n}(49n^2 + 100n + 56) \right] \left.\right\} + I_{m_s^2}(n, M^2).
\end{aligned}
\tag{33}
$$

Due to the mass of s quark is heavier than u, d-quark, the $I_{m_s^2}(n, M^2)$-terms should be considered in this paper, which are

$$
\begin{aligned}
I_{m_s^2}(n, M^2) = m_s^2 \Bigg\{ & -\frac{\langle \alpha_s G^2 \rangle}{6\pi M^6} \Big[\theta(n-2)(n\tilde{\psi}(n) - 2) \\
& + 2n \left(-\ln \frac{M^2}{\mu^2} \right) - n - 2 \Big] + \frac{\langle g_s^3 f G^3 \rangle}{288\pi^2 M^8} \\
& \times \Big\{ -10\delta^{n0} + \theta(n-2) \Big[4n(2n-1) \left(-\ln \frac{M^2}{\mu^2} \right) \\
& -4n\tilde{\psi}(n) + 8(n^2 - n + 1) \Big] + \theta(n-4) \\
& \times [2n(8n-1)\tilde{\psi}(n) - (19n^2 + 19n + 6)] \\
& + 8n(3n-1) \left(-\ln \frac{M^2}{\mu^2} \right) - (21n^2 + 53n - 6) \Big\} \\
& - \frac{\sum \langle g_s^2 q\bar{q} \rangle^2}{972\pi^2 M^8} \Big\{ 6\delta^{n0} \Big[16 \left(-\ln \frac{M^2}{\mu^2} \right) - 3 \Big] \\
& + \theta(n-2) \Big[8(n^2 + 12n - 12) \left(-\ln \frac{M^2}{\mu^2} \right) - 2 \\
& \times (29n + 22) \tilde{\psi}(n) + 4 \left(5n^2 - 2n - 33 + \frac{46}{n} \right) \Big] \\
& + \theta(n-4) \Big[2 \left(56n^2 - 25n + 24 \right) \tilde{\psi}(n) \\
& - \left(139n^2 + 91n + 54 \right) \Big] + 8 \left(27n^2 - 15n - 11 \right)
\end{aligned}
$$

$$\times \left(-\ln \frac{M^2}{\mu^2} \right) - 3(63n^2 + 159n - 50) \Bigg\}$$
$$+ \frac{4(n-1)}{3} \frac{m_s \langle \bar{s}s \rangle}{M^6} + \frac{8n-3}{9} \frac{m_s \langle g_s \bar{s}\sigma TGs \rangle}{M^8}$$
$$- \frac{4(2n+1)}{81} \frac{\langle g_s \bar{s}s \rangle^2}{M^8} \Bigg\}. \tag{34}$$

For convenience, we put the detailed terms contribute to the BFTSR $\langle \xi_{2;\eta^{(\prime)}}^n \rangle |_\mu$ in the Appendix B. By taking the index n to zero, we get the sum rule of the 0th-order moment, which takes the following form,

$$\frac{(\langle \xi_{2;\eta^{(\prime)}}^0 \rangle |_\mu)^2 f_{\eta^{(\prime)}}^2}{M^2 e^{m_{\eta^{(\prime)}}^2/M^2}} = \frac{1}{\pi} \frac{1}{M^2} \int_{4m_s^2}^{s_{\eta^{(\prime)}}} ds\, e^{-s/M^2} \frac{v(3-v^2)}{8\pi}$$
$$+ \frac{2m_s \langle \bar{s}s \rangle}{M^4} - \frac{m_s \langle g_s \bar{s}\sigma TGs \rangle}{9M^6} + \frac{\langle \alpha_s G^2 \rangle}{12\pi M^4}$$
$$+ \frac{4\langle g_s \bar{s}s \rangle^2}{81M^6} + \frac{\sum \langle g_s^2 \bar{q}q \rangle^2}{M^6} \frac{1}{486\pi^2}$$
$$\times \left[-50 \left(-\ln \frac{M^2}{\mu^2} \right) + 105 \right] + m_s^2 \left\{ \frac{\langle \alpha_s G^2 \rangle}{3\pi M^6} - \frac{\langle g_s^3 f G^3 \rangle}{72\pi^2 M^8} \right\}$$
$$- \frac{\sum \langle g_s^2 \bar{q}q \rangle^2}{972\pi^2 M^8} \left[8\left(-\ln \frac{M^2}{\mu^2} \right) - 132 \right]$$
$$- \frac{4}{3} \frac{m_s \langle \bar{s}s \rangle}{M^6} - \frac{1}{3} \frac{m_s \langle g_s \bar{s}\sigma TGs \rangle}{M^8} - \frac{4}{81} \frac{\langle g_s \bar{s}s \rangle^2}{M^8} \Bigg\}, \tag{35}$$

where

$$\widetilde{\psi}(n) = \psi\left(\frac{n+1}{2}\right) - \psi\left(\frac{n}{2}\right) + \ln 4, \tag{36}$$

with $v^2 = 1 - 4m_s^2/s$ and $A_0' = 0$, $A_2' = 5/3$, $A_4' = 59/27$, $A_6' = 353/135$ are the NLO correction to the perturbative part [90]. The 0th-order derivative of the digamma function $\psi(n+1) = \Sigma_{k=1}^n 1/k - \gamma_E$, where the Euler's constant $\gamma_E = 0.557216$. Furthermore, in order to get the Gegenbauer moment $a_{2;\eta^{(\prime)}}^n$, one can expand $\phi_{2;\eta^{(\prime)}}(u,\mu)$ into a Gegenbauer polynomial series by using Eq. (4) and the basic definition of $\langle \xi_{2;\eta^{(\prime)}}^n \rangle |_\mu$ (5). Then, one can get the following relations up to 6th-order,

$$\langle \xi_{2;\eta^{(\prime)}}^2 \rangle |_\mu = \frac{1}{5} + \frac{12}{35} a_{2;\eta^{(\prime)}}^2(\mu),$$
$$\langle \xi_{2;\eta^{(\prime)}}^4 \rangle |_\mu = \frac{3}{35} + \frac{8}{35} a_{2;\eta^{(\prime)}}^2(\mu) + \frac{8}{77} a_{2;\eta^{(\prime)}}^4(\mu),$$
$$\langle \xi_{2;\eta^{(\prime)}}^6 \rangle |_\mu = \frac{1}{21} + \frac{12}{77} a_{2;\eta^{(\prime)}}^2(\mu) + \frac{120}{1001} a_{2;\eta^{(\prime)}}^4(\mu)$$
$$+ \frac{64}{2145} a_{2;\eta^{(\prime)}}^6(\mu). \tag{37}$$

Following this method, one can get higher-order Gegenbauer moments.

2.3 The semileptonic decay $D_s^+ \to \eta^{(\prime)} \ell^+ \nu_\ell$

All the following calculations are performed under the Standard Model (SM). In order to derive the full analytical LCSR expressions for the TFFs, we use the traditional current method to calculate the TFFs. The correlation function for the TFFs of $D_s \to \eta^{(\prime)}$ is defined as [28]:

$$\Pi_\mu(p,q) = i \int d^4x\, e^{iqx} \langle \eta^{(\prime)}(p)|T\{\bar{s}(x)\gamma_\mu c(x), \bar{c}(0)i\gamma_5 s(0)\}|0\rangle$$
$$= \Pi[q^2, (p+q)^2] p_\mu + \tilde{\Pi}[q^2, (p+q)^2] q_\mu. \tag{38}$$

Following the basic procedure of LCSR approach, the correlation function can be treated by inserting complete intermediate states with the same quantum numbers as the current operator $(\bar{c}i\gamma_5 s)$ in the time-like $(p+q)^2$-region. After isolating the pole term of the lowest pseudoscalar D_s-meson, one can reach the following expression,

$$\Pi_\mu^{\text{had}}(p,q) = \frac{\langle \eta^{(\prime)}(p)|\bar{s}\gamma_\mu c|D_s(p+q)\rangle \langle D_s(p+q)|\bar{c}i\gamma_5 q|0\rangle}{m_{D_s}^2 - (p+q)^2}$$
$$+ \sum_{\text{H}} \frac{\langle \eta^{(\prime)}(p)|\bar{s}\gamma_\mu c|D_s^{\text{H}}(p+q)\rangle \langle D_s^{\text{H}}(p+q)|\bar{c}i\gamma_5 q|0\rangle}{m_{D_s^{\text{H}}}^2 - (p+q)^2}$$
$$= \Pi^{\text{had}}[q^2, (p+q)^2] p_\mu + \tilde{\Pi}^{\text{had}}[q^2, (p+q)^2] q_\mu, \tag{39}$$

with the superscript "had" and "H" stand for the hadronic expression of the correlation function and higher-excited state of D_s-meson, respectively. The decay constant of D_s-meson can be defined via the relation, $\langle D_s|\bar{c}i\gamma_5 q|0\rangle = m_{D_s}^2 f_{D_s}/m_c$. The definition of transition matrix element for $D_s \to \eta^{(\prime)}$ has the following form

$$\langle \eta^{(\prime)}(p)|\bar{s}\gamma_\mu c|D_s(p+q)\rangle = 2f_+^{\eta^{(\prime)}}(q^2) p_\mu + \tilde{f}^{\eta^{(\prime)}}(q^2) q_\mu. \tag{40}$$

with $\tilde{f}^{\eta^{(\prime)}} = f_+^{\eta^{(\prime)}}(q^2) + f_-^{\eta^{(\prime)}}(q^2)$. Then one can take the imaginary part of the invariant amplitude $\Pi^{\text{had}}[q^2, (p+q)^2]$ and $\tilde{\Pi}^{\text{had}}[q^2, (p+q)^2]$ which has the following form,

$$\text{Im}\Pi^{\text{had}}(q^2, s) = \pi \delta(s - m_{D_s^2})$$
$$\times \frac{2m_{D_s^2} f_{D_s} f_+^{\eta^{(\prime)}}}{m_c} + \pi \rho^{\text{H}}(s)\theta(s - s_0)$$
$$\text{Im}\tilde{\Pi}^{\text{had}}(q^2, s) = \pi \delta(s - m_{D_s^2})$$
$$\times \frac{m_{D_s^2} f_{D_s} \tilde{f}_+^{\eta^{(\prime)}}}{m_c} + \pi \tilde{\rho}^{\text{H}}(s)\theta(s - \tilde{s}_0) \tag{41}$$

where $\rho^{\text{H}}(s)$ and $\tilde{\rho}^{\text{H}}(s)$ denote the spectral density of higher resonance and the continuum states D_s^{H}, which can be approximated by invoking the so-called quark-hadron duality ansatz $\varrho^{\text{H}}(s) = \varrho^{\text{QCD}}(s)$ with $\varrho(s) = (\rho(s), \tilde{\rho}(s))$ and

the perturbative spectral density $\rho^{\rm QCD}$ and $\tilde{\rho}^{\rm QCD}$, the usual step-function $\theta(x)$. Here, the s_0 $(\tilde{s}_0)$ are effective parameters, which characterize the lower limit of continuum state, namely the continuum threshold parameters. After extracting the pole terms, the $s_0(\tilde{s}_0)$ can separate the ground state D_s and the excited state $D_s^{\rm H}$. When taking the limit for the interval between the two adjacent excited states, the sum of excited states is transformed into the integral of continuum states and $s_0(\tilde{s}_0)$ will be changed into the lower limit of the integration. Traditionally, the continuum threshold are often taken as the magnitude that is close to the squared mass of the first excited state. The ground state of D_s-meson is calculated by the LCSR approach. The excited states' contribution can be highly suppressed when making the Borel transformation. Meanwhile, the continuum states, contribution is usually required to be less than 30% so as to make the LCSR calculation more accurate and reliable. Then, one can use a general dispersion relation in the momentum squared $(p + q)^2$, which can establish a relationship with the QCD parts, i.e.

$$\Pi^{\rm QCD}(q^2, s) = \frac{1}{\pi} \int_{m_c^2}^{\infty} \frac{{\rm Im}\Pi^{\rm had}(q^2, s)}{s - (p + q)^2} ds,$$

$$\tilde{\Pi}^{\rm QCD}(q^2, s) = \frac{1}{\pi} \int_{m_c^2}^{\infty} \frac{{\rm Im}\tilde{\Pi}^{\rm had}(q^2, s)}{s - (p + q)^2} ds. \tag{42}$$

Here, we shall only deal with ${\rm Im}\Pi^{\rm had}[q^2, s]$ for the TFFs $f_+^{\eta^{(\prime)}}(q^2)$, which are the only TFFs contribute to the required branching fractions.

On the other hand, when the correlation function (38) is dominated by the light-like distances, it can be expanded around the light-cone. The light-cone expansion is performed by integrating out the transverse and minus degrees of freedom and leaving only the longitudinal momenta of the partons as the relevant degrees of freedom. The integration over the transverse momenta is done up to a cutoff, $\mu_{\rm IR}$, all momenta below which are included in the $\eta^{(\prime)}$-meson LCDAs. Large transverse momenta are calculated in perturbative theory. Thus, the correlation function can be separated into perturbative and nonperturbative contributions, both of which depend on the longitudinal parton momenta and the factorization scale $\mu_{\rm IR}$ [47].

In order to make our result more accurate, we consider both the leading-order (LO) for all the LCDAs' part and gluon radiative corrections to the dominant twist-2, 3 parts of the correlation function. The OPE result for the correlation function $\Pi^{\rm OPE}$ is then represented as a sum of LO and NLO parts,

$$\Pi^{\rm OPE}[q^2, (p + q)^2] = F_0(q^2, (p + q)^2)$$
$$+ \frac{\alpha_s C_F}{4\pi} F_1(q^2, (p + q)^2). \tag{43}$$

To calculate the invariant amplitude $F_0(q^2, (p + q)^2)$ and $F_1(q^2, (p + q)^2)$, one needs to know the expression for the c-quark propagator, i.e.

$$\langle 0|T\{c(x)\bar{c}(0)\}|0\rangle = i \int \frac{d^4k}{(2\pi)^4} e^{-ik\cdot x} \frac{m_c + \not{k}}{k^2 - m_c^2}$$

$$- ig \int \frac{d^4k}{(2\pi)^4} e^{-ik\cdot x} \int_0^1 dv \left[\frac{m_c + \not{k}}{2(m_c^2 - k^2)^2} \right.$$

$$\left. \times G^{\mu\nu}(vx)\sigma_{\mu\nu} + \frac{v}{m_c^2 - k^2} x_\mu G^{\mu\nu}(vx)\gamma_\nu \right]. \tag{44}$$

To do the calculation, the expression of twist-2, 3, 4 LCDAs matrix elements are needed, which are displayed in the Appendix C. To get the final LCSR expression, we need to use the Borel transformation to transform the variable $(p+q)^2$ into Borel parameter M^2. Then the expression of the $D_s \to \eta^{(\prime)}$ TFFs up to NLO gluon radiation correction to the twist-2, 3 LCDAs can be obtained by equating the two types of representation of the correlation function and by subtracting the contribution from higher resonances and continuum states, i.e.,

$$f_+^{\eta^{(\prime)}}(q^2) = \frac{e^{m_{D_s}^2/M^2}}{2m_{D_s}^2 f_{D_s}} \left[F_0(q^2, M^2, s_0) + \frac{\alpha_s C_F}{4\pi} F_1(q^2, M^2, s_0) \right]. \tag{45}$$

where $F_{0(1)}(q^2, M^2, s_0)$ originates from the OPE result for the LO (NLO) invariant amplitude $F_{0(1)}(q^2, (p + q)^2)$. Finally, the LCSR for $D_s \to \eta^{(\prime)}$ TFFs have the following form,

$$f_+^{\eta^{(\prime)}}(q^2) = \frac{m_c^2 f_{\eta^{(\prime)}}}{2m_{D_s}^2 f_{D_s}} e^{m_{D_s}^2/M^2} \int_{u_0}^1 du\, e^{-s(u)/M^2} \left\{ \frac{\phi_{2;\eta^{(\prime)}}(u)}{u} \right.$$

$$+ \frac{1}{2m_s m_c} \left[\phi_{3;\eta^{(\prime)}}^p(u) + \frac{1}{6} \left(2 \frac{\phi_{3;\eta^{(\prime)}}^\sigma(u)}{u} \right. \right.$$

$$- \frac{m_c^2 + q^2 - u^2 m_{\eta^{(\prime)}}^2}{m_c^2 - q^2 + u^2 m_{\eta^{(\prime)}}^2} \frac{d}{du} \phi_{3;\eta^{(\prime)}}^\sigma(u)$$

$$\left. \left. + \frac{4u m_{\eta^{(\prime)}}^2 m_c^2}{(m_c^2 - q^2 + u^2 m_{\eta^{(\prime)}}^2)^2} \phi_{3;\eta^{(\prime)}}^\sigma(u) \right) \right] + \frac{1}{m_c^2 - q^2 + u^2 m_{\eta^{(\prime)}}^2}$$

$$\times \left[u\psi_{4;\eta^{(\prime)}}(u) + \left(1 - \frac{2u^2 m_{\eta^{(\prime)}}^2}{m_c^2 - q^2 + u^2 m_{\eta^{(\prime)}}^2} \right) \right.$$

$$\times \int_0^u dv\, \psi_{4;\eta^{(\prime)}}(v) - \frac{m_c^2}{4} \frac{u}{m_c^2 - q^2 + u^2 m_{\eta^{(\prime)}}^2} \left(\frac{d^2}{du^2} \right.$$

$$- \frac{6u m_{\eta^{(\prime)}}^2}{m_c^2 - q^2 + u^2 m_{\eta^{(\prime)}}^2} \frac{d}{du} + \frac{12u m_{\eta^{(\prime)}}^4}{(m_c^2 - q^2 + u^2 m_{\eta^{(\prime)}}^2)^2} \right)$$

$$\times \phi_{4;\eta^{(\prime)}}(u) - \left(\frac{d}{du} - \frac{2u m_{\eta^{(\prime)}}^2}{m_c^2 - q^2 + u^2 m_{\eta^{(\prime)}}^2} \right)$$

$$\times \left(\frac{f_{3\eta^{(\prime)}}}{f_{\eta^{(\prime)}} m_c} I_{3;\eta^{(\prime)}}(u) + I_{4;\eta^{(\prime)}}(u) \right) - \frac{2u m_{\eta^{(\prime)}}^2}{m_c^2 - q^2 + u^2 m_{\eta^{(\prime)}}^2}$$

$$\times \left(u \frac{d}{du} - \frac{2u^2 m_{\eta^{(\prime)}}^2}{m_c^2 - q^2 + u^2 m_{\eta^{(\prime)}}^2} + 1 \right)$$

$$\times \bar{I}_{4\eta^{(\prime)}}(u) + \frac{2u m_{\eta^{(\prime)}}^2 (m_c^2 - q^2 - u^2 m_{\eta^{(\prime)}}^2)}{(m_c^2 - q^2 + u^2 m_{\eta^{(\prime)}}^2)^2}$$

$$\times \left(\frac{d}{du} - \frac{6u m_{\eta^{(\prime)}}^2}{m_c^2 - q^2 + u^2 m_{\eta^{(\prime)}}^2} \right) \int_u^1 d\xi \, \bar{I}_{4\eta^{(\prime)}}(\xi) \Bigg] \Bigg\}$$

$$+ \frac{m_c^4 f_{\eta^{(\prime)}} e^{-m_c^2/M^2}}{4(m_c^2 - q^2 + m_{\eta^{(\prime)}}^2)^2}$$

$$\times \left(\frac{d}{du} \phi_{4;\eta}(u) \right) \Bigg|_{u \to 1} + \frac{\alpha_s C_F e^{m_{D_s}^2/M^2}}{8\pi m_{D_s}^2 f_{D_s}} F_1(q^2, m^2, s_0), \quad (46)$$

with $s(u) = m_c^2 - (q^2 - m_{\eta^{(\prime)}}^2 u)\bar{u}/u$. The LO invariant amplitudes include twist-2, 3, 4 contributions. The NLO QCD corrections to the invariant amplitudes $F_1(q^2, (p+q)^2)$ include twist-2, 3 contributions, which can be separated into the following form,

$$F_1(q^2, m^2, s_0) = \frac{1}{\pi} \int_{m_c^2}^{s_0} ds \, e^{-s(u)/M^2} \text{Im} F_1(q^2, s)$$

$$= \frac{f_{\eta^{(\prime)}}}{\pi} \int_{m_c^2}^{s_0} ds \, e^{-s(u)/M^2}$$

$$\times \int_0^1 du \Big\{ \text{Im} T_1(q^2, s, u) \phi_{2;\eta^{(\prime)}}(u)$$

$$+ \frac{\mu_{\eta^{(\prime)}}}{m_c} \Big[\text{Im} T_1^p(q^2, s, u) \phi_{3;\eta^{(\prime)}}^p(u)$$

$$+ \text{Im} T_1^\sigma(q^2, s, u) \phi_{3;\eta^{(\prime)}}^\sigma(u) \Big] \Big\}, \quad (47)$$

where $\mu_{\eta^{(\prime)}} = m_{\eta^{(\prime)}}^2/2m_s$. The imaginary parts of the amplitudes $T_1(q^2, s, u)$, $T_1^p(q^2, s, u)$ and $T_1^\sigma(q^2, s, u)$ are the hard-scattering amplitudes calculated by the 6 diagrams for the gluon corrections. The final detailed expressions agree with those of Refs. [21,28], which are not listed here. The lower limit of integral

$$u_0 = \Big(q^2 - s_0 + m_{\eta^{(\prime)}}^2$$

$$+ \sqrt{(q^2 - s_0 + m_{\eta^{(\prime)}}^2)^2 - 4m_{\eta^{(\prime)}}^2(q^2 - m_c^2)} \Big) / (2m_{\eta^{(\prime)}}^2) \quad (48)$$

and for the final expression, we need a brief introduction to the integrals over three-particle LCDAs, i.e.

$$I_{3;\eta^{(\prime)}}(u) = \frac{d}{du} \left[\int_0^u d\alpha_1 \int_\Delta^1 dv \, \Phi_{3;\eta^{(\prime)}}(\alpha_i) \right],$$

$$I_{4;\eta^{(\prime)}}(u) = \frac{d}{du} \left\{ \int_0^u d\alpha_1 \int_\Delta^1 \frac{dv}{v} \left[2\Psi_{4;\eta^{(\prime)}}(\alpha_i) \right. \right.$$

$$- \Phi_{4;\eta^{(\prime)}}(\alpha_i) + 2\widetilde{\Psi}_{4;\eta^{(\prime)}}(\alpha_i) - \widetilde{\Phi}_{4;\eta^{(\prime)}}(\alpha_i) \Big] \Big\},$$

$$\bar{I}_{4;\eta^{(\prime)}}(u) = \frac{d}{du} \left\{ \int_0^u d\alpha_1 \int_\Delta^1 \frac{dv}{v} \left[\Psi_{4;\eta^{(\prime)}}(\alpha_i) \right. \right.$$

$$+ \Phi_{4;\eta^{(\prime)}}(\alpha_i) + \widetilde{\Psi}_{4;\eta^{(\prime)}}(\alpha_i) + \widetilde{\Phi}_{4;\eta^{(\prime)}}(\alpha_i) \Big] \Big\}, \quad (49)$$

where $\Delta = (u - \alpha_1)/(1 - \alpha_1)$, $\alpha_2 = 1 - \alpha_1 - \alpha_3$ and $\alpha_3 = (u - \alpha_1)/v$. Due to the contributions from three-particle parts are quite small, i.e. $< 0.1\%$, we can safely neglect these parts in this paper. We would like to figure out that the decay branching fraction for the considered decay. Using the parametrization of the transition matrix elements in terms of TFFs, in massless lepton case, we get

$$\frac{d\Gamma}{dq^2}(D_s^+ \to \eta^{(\prime)} \ell^+ \nu_\ell) = \frac{G_F^2 |V_{cs}|^2}{192\pi^3 m_{D_s}^3} \Big[\left(m_{D_s}^2 + m_{\eta^{(\prime)}}^2 - q^2 \right)^2$$

$$- 4m_{D_s}^2 m_{\eta^{(\prime)}}^2 \Big]^{3/2} |f_+^{\eta^{(\prime)}}(q^2)|^2, \quad (50)$$

where the fermi coupling constant $G_F = 1.166 \times 10^{-5}$ GeV^{-2}.

3 Numerical discussions

3.1 Input parameters

We adopt the following parameters to do the numerical calculation. The current charm-quark mass is $m_c = 1.27 \pm 0.02$ GeV, the masses of D_s, η and η'-meson $m_{D_s} = 1.9685$ GeV, $m_\eta = 0.5478$ GeV, $m_{\eta'} = 0.9578$ GeV and s-quark mass $m_s = 0.093$ GeV. All of them are taken from the Particle Data Group (PDG) [91]. The D_s, η, η'-meson decay constants are taken as $f_{D_s} = 0.274 \pm 0.013 \pm 0.007$ GeV [49], $f_\eta = 0.130 \pm 0.003$ GeV [53] and $f_{\eta'} = 0.157 \pm 0.003$ GeV [92]. The values of non-perturbative vacuum condensates up to 6-dimension are taken as follows [88,93,94],

$$\langle \alpha_s G^2 \rangle = 0.038 \pm 0.011 \text{ GeV}^4,$$

$$\langle g_s^3 f G^3 \rangle = 0.045 \pm 0.007 \text{ GeV}^6,$$

$$\langle g_s \bar{q} q \rangle^2 = (2.082_{-0.697}^{+0.734}) \times 10^{-3} \text{ GeV}^6,$$

$$\langle g_s^2 \bar{q} q \rangle^2 = (7.420_{-2.483}^{+2.614}) \times 10^{-3} \text{ GeV}^6,$$

$$\langle q\bar{q} \rangle = (-2.417_{-0.114}^{+0.227}) \times 10^{-2} \text{ GeV}^3,$$

$$\langle \bar{s}s \rangle = (-1.789_{-0.084}^{+0.168}) \times 10^{-2} \text{ GeV}^3,$$

$$\langle g_s s \bar{s} \rangle^2 = (1.541_{-0.516}^{+0.543}) \times 10^{-3} \text{ GeV}^6,$$

$$\sum \langle g_s^2 \bar{q} q \rangle^2 = (1.891_{-0.633}^{+0.665}) \times 10^{-2} \text{ GeV}^6. \quad (51)$$

Table 1 The criteria for determining Borel windows, and the resultant Borel windows and the corresponding values of the η and η'-meson leading twist LCDA moments $\langle \xi^n_{2;\eta^{(\prime)}} \rangle|_\mu$. "Con." represents the continuum contribution and "Six." represents the dimension-six condensates' contribution

	n	0	2	4	6
η-meson	Con.	$< 20\%$	$< 25\%$	$< 30\%$	$< 35\%$
	Six.	$< 5\%$	$< 5\%$	$< 5\%$	$< 5\%$
	M^2	[0.535, 1.188]	[1.026, 1.402]	[1.368, 1.759]	[1.677, 2.194]
	$\langle \xi^n_{2;\eta} \rangle|_\mu$	[0.952, 1.168]	[0.231, 0.230]	[0.110, 0.102]	[0.067, 0.059]
η'-meson	Con.	$< 30\%$	$< 35\%$	$< 40\%$	$< 45\%$
	Six.	$< 5\%$	$< 5\%$	$< 5\%$	$< 5\%$
	M^2	[1.049, 1.137]	[1.026, 1.233]	[1.368, 1.627]	[1.677, 2.082]
	$\langle \xi^n_{2;\eta'} \rangle|_\mu$	[1.076, 1.061]	[0.221, 0.201]	[0.099, 0.086]	[0.059, 0.047]

The quark-gluon mixture condensate $\langle g_s \bar{q} \sigma T G q \rangle = m_0^2 \langle \bar{q} q \rangle$ with $m_0^2 = 0.80 \pm 0.02 \text{GeV}^2$, which leads to

$$\langle g_s \bar{s} \sigma T G s \rangle = (-1.431^{+0.139}_{-0.076}) \times 10^{-2} \text{ GeV}^5. \tag{52}$$

Here, the ratio $\kappa = \langle \bar{s} s \rangle / \langle \bar{q} q \rangle = 0.74 \pm 0.03$ has been used. Meanwhile, the typical scale in this paper is $\mu_{IR} = (m_{D_s}^2 - m_c^2)^{1/2} \approx 1.5$ GeV. So the renormalization group equations (RGEs) should be used for running the quark masses and each vacuum condensates appearing in the BFTSR from the initial scale $\mu_0 = 1$ GeV to the typical scale μ_{IR}. The RGE can be found in Refs. [95–97], which are not listed here.

3.2 Determination for the Gegenbauer moments of $\eta^{(\prime)}$-meson twist-2 LCDA

One of the significant parameters in BFTSR is the continuum threshold $s_{\eta^{(\prime)}}$ for the moments of $\eta^{(\prime)}$-meson twist-2 LCDAs. Following our previous works, we can determine $s_\eta = 1.3 \pm 0.1$ GeV and $s_{\eta'} = 0.8 \pm 0.1$ GeV by setting the 0th-order of Gegenbauer moment into 1, i.e. $\langle \xi^0_{2;\eta} \rangle|_\mu = \langle \xi^0_{2;\eta'} \rangle|_\mu = 1$. Meanwhile, in order to determine the allowable range of the Borel parameter M^2 (i.e. the Borel Window), we adopt the following three criteria

- The continuum contributions are less than 45% of the total results;
- The contributions from the dimension-six condensates do not exceed 5%;
- We require the variations of $\langle \xi^n_{2;\eta^{(\prime)}} \rangle|_\mu$ within the Borel window to be less than 10%.
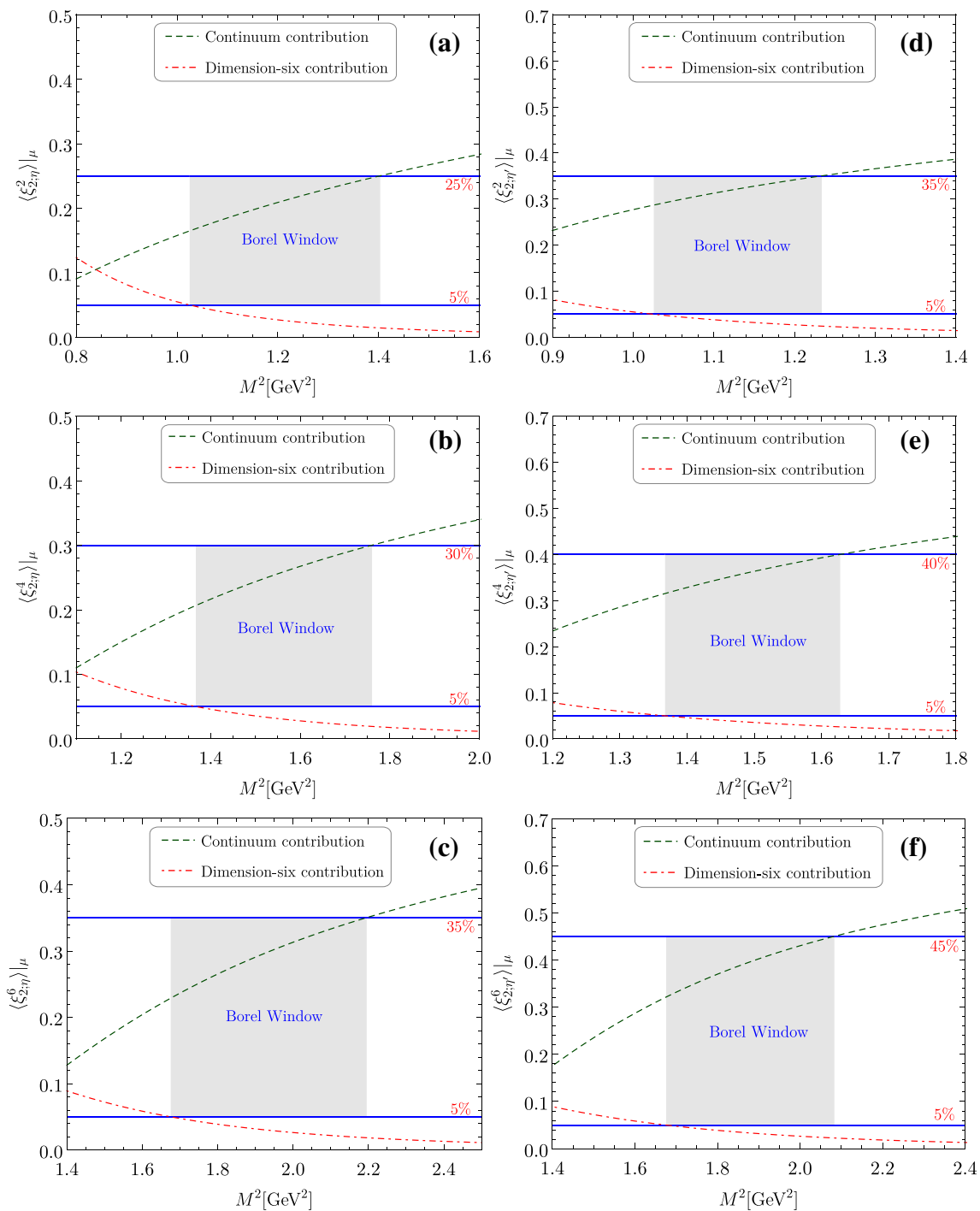
For the first four Gegenbauer moments $\langle \xi^n_{2;\eta^{(\prime)}} \rangle|_\mu$ with $n = (0, 2, 4, 6)$, we list the allowable Borel region and their corresponding $\langle \xi^n_{2;\eta^{(\prime)}} \rangle|_\mu$ in Table 1. When $n = (0, 2, 4, 6)$, we have set the continuum contributions to be less than 20%, 25%, 30%, 35% for $\langle \xi^n_{2;\eta} \rangle|_\mu$ and 30%, 35%, 40%, 45% for $\langle \xi^n_{2;\eta'} \rangle|_\mu$, respectively, and the dimension-six condensates' contributions to be less than 5% for all the order of

$\langle \xi^n_{2;\eta^{(\prime)}} \rangle|_\mu$. Then, the determined continuum's and dimension-six condensates' contribution for $\langle \xi^n_{2;\eta} \rangle|_\mu$ and $\langle \xi^n_{2;\eta'} \rangle|_\mu$ with $n = (2, 4, 6)$ are shown in the left and right panel of Fig. 1, respectively. In which, the shaded region stand for the Borel windows.

In order to provide a deeper insight into the flatness of the LCDA moments versus the Borel parameter M^2, we present the first three curves for the moments of $\eta^{(\prime)}$-meson twist-2 LCDA at the initial scale, i.e. $\langle \xi^n_{2;\eta^{(\prime)}} \rangle|_\mu$ with $n = (2, 4, 6)$ in Fig. 2. The determined Borel window are $M^2 \in [1.0, 2.5]$ GeV^2 for η-meson and $M^2 \in [1.0, 2.4]$ GeV^2 for η'-meson. It is noted that within this range, the moments $\langle \xi^2_{2;\eta^{(\prime)}} \rangle|_\mu, \langle \xi^4_{2;\eta^{(\prime)}} \rangle|_\mu$ and $\langle \xi^6_{2;\eta^{(\prime)}} \rangle|_\mu$ are almost flat, which vary less than 10% for the total results in the Borel window.

By taking the squared average of all the uncertainty sources into consideration and making use of the relations between the Gegenbauer moments $a^n_{2;\eta^{(\prime)}}(\mu)$ and the LCDA moments $\langle \xi^n_{2;\eta^{(\prime)}} \rangle|_\mu$, i.e. Eq. (37), we obtain the first three $a^n_{2;\eta^{(\prime)}}(\mu_0)$ and $\langle \xi^n_{2;\eta^{(\prime)}} \rangle|_{\mu_0}$ with $n = (2, 4, 6)$ for the leading-twist $\eta^{(\prime)}$-meson LCDA $\phi_{2;\eta^{(\prime)}}(u, \mu_0)$ predicted from BFTSR in Table 2. The factorization scale is taken as the initial scale $\mu_0 = 1$ GeV. As a comparison, we also list the LCSR given in year 2013 [20], the CLEO fit [50], the BABAR fit [51], the ones given by Kroll [52] and Ball [53], respectively. For the Ball's results, it is calculated by using the approximation $a^n_{2;\eta}(\mu) = a^n_{2;K}(\mu) = a^n_{2;\pi}(\mu)$. Our results for the second and fourth order η-meson LCDA's moments, e.g. $\langle \xi^2_{2;\eta} \rangle|_{\mu_0}$ and $\langle \xi^4_{2;\eta} \rangle|_{\mu_0}$ agree with the Ball's predictions within errors. But there still exist discrepancy for $a^4_{2;\eta}(\mu_0)$ with Ball's prediction. The main reason lies in the fourth order of equations between Gegenbauer and LCDA moments, i.e. Eq. (37) have large coefficients which will enlarge the small discrepancy of LCDA moments, even appears the opposite sign. At present, there are few studies on η'-meson's twist-2 LCDA.
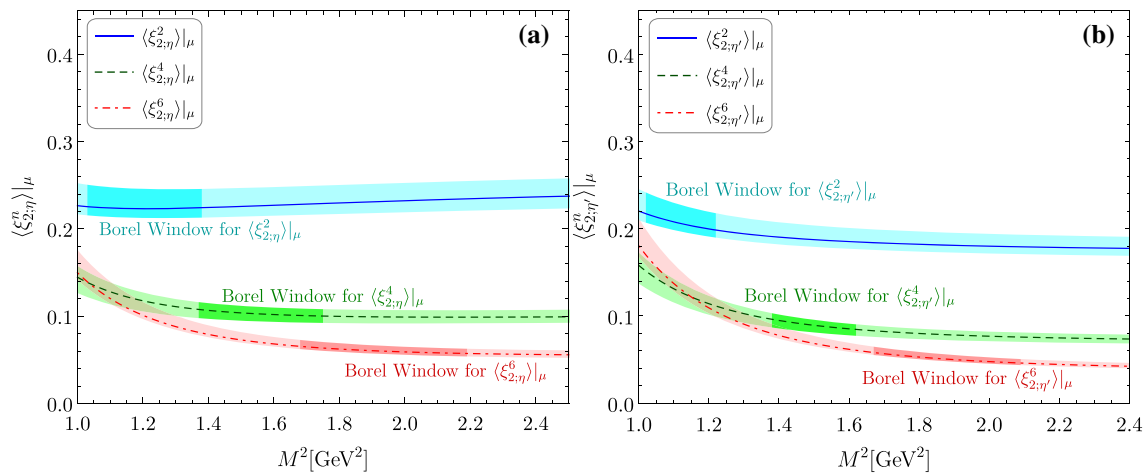
After considering the Gegenbauer moments $a^n_{2;\eta^{(\prime)}}(\mu)$ up to 6th-order into the conformal expansion of the Gegenbauer polynomial at initial scale, i.e. Eq. (4), we present the η and η'-meson twist-2 LCDAs in Fig. 3a, b separately.

Fig. 1 Contributions from the continuum state and dimension-six condensates for the $\eta^{(\prime)}$-meson leading-twist LCDA moments $\langle\xi^n_{2;\eta^{(\prime)}}\rangle|_\mu$ versus the Borel parameter M^2, where all input parameters are set to be their central values

For $\phi_{2;\eta}(u, \mu_0)$, we present the asymptotic form, the CLEO [50], the BABAR [51], Kroll's prediction [52], the SR fit [20] and the Ball's prediction [53] as a comparison. Figure 3a shows that the LCSR 2013 and Ball's results prefer a double-peaked behavior. The reason lies in that they adopt the π, K-meson's LCDAs as those of η-meson LCDAs.

Conversely, the CLEO [50], the BABAR [51] and the fitting results by Kroll indicate a single-peaked behavior. Our prediction tends to a double-peaked behavior. For $\phi_{2;\eta'}(u, \mu_0)$, we only exhibit the asymptotic form due to there are less results from references, which is shown in Fig. 3b. Furthermore, in order to have a look at the evolution $\phi_{2;\eta^{(\prime)}}(u, \mu_0)$

Fig. 2 The first three moments $\langle\xi^n_{2;\eta^{(\prime)}}\rangle|_\mu$ with $(n = 2, 4, 6)$ versus the Borel parameter M^2. The darker shaded bands indicate the Borel windows for $\langle\xi^n_{2;\eta^{(\prime)}}\rangle|_\mu$, respectively

Table 2 First three Gegenbauer and LCDA moments $a^n_{2;\eta^{(\prime)}}(\mu_0)$ and $\langle\xi^n_{2;\eta^{(\prime)}}\rangle|_{\mu_0}$ with $n = (2, 4, 6)$ for the leading-twist $\eta^{(\prime)}$-meson LCDA $\phi_{2;\eta^{(\prime)}}(u, \mu_0)$, where the errors are squared averages of those from all the input parameters. Other theoretical predictions are also given as a comparison

	η-meson			η'-meson		
	$\langle\xi^2_{2;\eta}\rangle|_{\mu_0}$	$\langle\xi^4_{2;\eta}\rangle|_{\mu_0}$	$\langle\xi^6_{2;\eta}\rangle|_{\mu_0}$	$\langle\xi^2_{2;\eta'}\rangle|_{\mu_0}$	$\langle\xi^4_{2;\eta'}\rangle|_{\mu_0}$	$\langle\xi^6_{2;\eta'}\rangle|_{\mu_0}$
BFTSR (this work)	$0.231^{+0.010}_{-0.013}$	$0.109^{+0.007}_{-0.007}$	$0.066^{+0.006}_{-0.006}$	$0.211^{+0.015}_{-0.017}$	$0.093^{+0.009}_{-0.009}$	$0.054^{+0.008}_{-0.008}$
CLEO fit [50]	0.176 ± 0.010	–	–	–	–	–
BABAR fit [51]	0.183 ± 0.007	–	–	–	–	–
P. Kroll [52]	0.183 ± 0.007	–	–	–	–	–
SR fit [20]	0.286 ± 0.051	–	–	–	–	–
P. Ball [53]	0.239	0.110	–	–	–	–

	η-meson			η'-meson		
	$a^2_{2;\eta}(\mu_0)$	$a^4_{2;\eta}(\mu_0)$	$a^6_{2;\eta}(\mu_0)$	$a^2_{2;\eta'}(\mu_0)$	$a^4_{2;\eta'}(\mu_0)$	$a^6_{2;\eta'}(\mu_0)$
BFTSR (this work)	$0.090^{+0.031}_{-0.037}$	$0.025^{+0.003}_{-0.010}$	$0.033^{+0.055}_{-0.058}$	$0.033^{+0.042}_{-0.050}$	$-0.002^{+0.007}_{-0.016}$	$0.043^{+0.067}_{-0.072}$
CLEO fit [50]	-0.07 ± 0.03	–	–	–	–	–
BABAR fit [51]	-0.05 ± 0.02	–	–	–	–	–
P. Kroll [52]	-0.05 ± 0.02	–	–	–	–	–
SR fit [20]	0.25 ± 0.15	–	–	–	–	–
P. Ball [53]	0.115	-0.015	–	–	–	–

with $n = (2, 4, 6)$, we present the different curves in Fig. 4. If we take $n = (2, 4)$, the behavior of LCDAs shall be closer to the asymptotic form. Furthermore, a small shake is observed when taking the 6th-order LCDA moment into consideration.
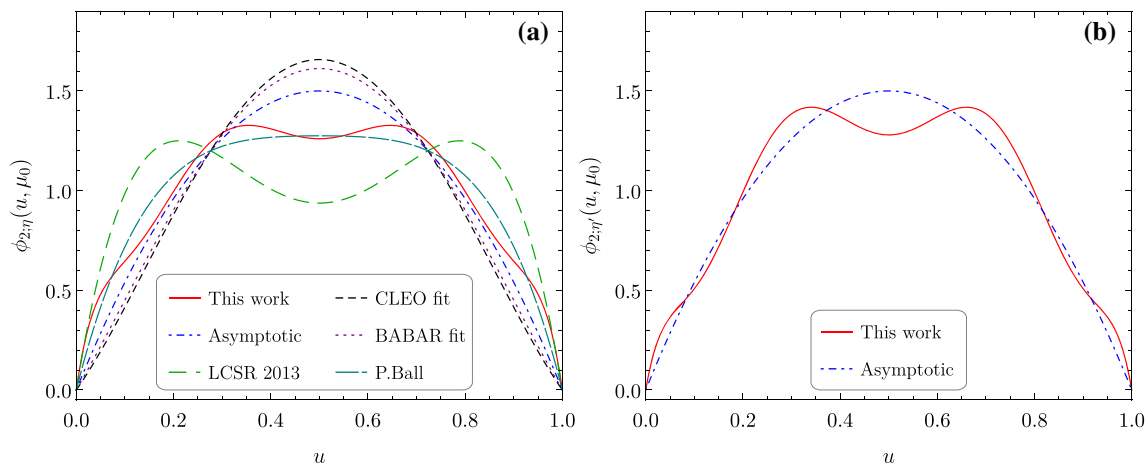
Other two-particle Fock state twist-3 and twist-4 LCDAs $\phi^p_{3;\eta^{(\prime)}}(u)$, $\phi^\sigma_{3;\eta^{(\prime)}}(u)$, $\psi_{4;\eta^{(\prime)}}(u)$ and $\phi_{4;\eta^{(\prime)}}(u)$ are defined as follows

$$\phi^p_{3;\eta^{(\prime)}}(u) = 1 + \left(30\eta^{\eta^{(\prime)}}_3 - \frac{5}{2}\rho^2_{\eta^{(\prime)}}\right)C^{1/2}_2(\xi)$$
$$+ \left(-3\eta^{\eta^{(\prime)}}_3\omega^{\eta^{(\prime)}}_3 - \frac{27}{20}\rho^2_{\eta^{(\prime)}} - \frac{81}{10}\rho^2_{\eta^{(\prime)}}a^2_{2;\eta^{(\prime)}}\right)$$
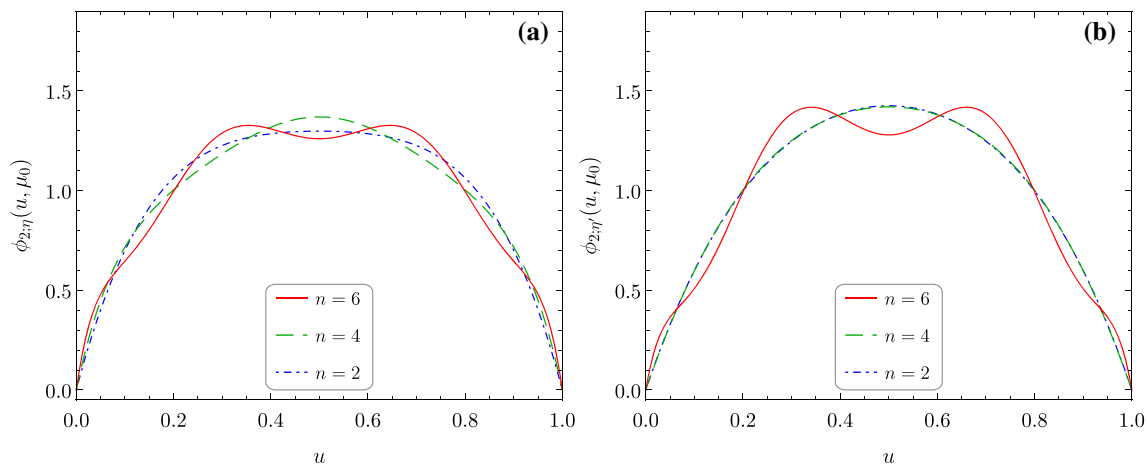
$$\times C^{1/2}_4(\xi), \tag{53}$$

$$\phi^\sigma_{3;\eta^{(\prime)}}(u) = 6u\bar{u}\left(1 + 5\eta^{\eta^{(\prime)}}_3 - \frac{1}{2}\eta^{\eta^{(\prime)}}_3\omega^{\eta^{(\prime)}}_3\right.$$
$$\left. - \frac{7}{20}\rho^2_{\eta^{(\prime)}} - \frac{3}{5}\rho^2_{\eta^{(\prime)}}a^2_{2;\eta^{(\prime)}}\right)C^{3/2}_2(\xi), \tag{54}$$

$$\psi_{4;\eta^{(\prime)}}(u) = \frac{5}{2}\varepsilon^2u^2\bar{u}^2 + \frac{1}{2}\varepsilon\delta^2$$
$$\left[u\bar{u}(2 + 13u\bar{u}) + 10u^3\ln u\ln\bar{u}(2 - 3u + \frac{6}{5}u^2)\right.$$
$$\left. + 10\bar{u}^3\left(2 - 3\bar{u} + \frac{6}{5}\bar{u}^2\right)\right], \tag{55}$$

Fig. 3 The $\eta^{(\prime)}$-meson leading-twist LCDA $\phi_{2;\eta^{(\prime)}}(u, \mu_0)$ predicted from the BFTSR. We make a comparison with the asymptotic form, the CLEO [50], SR fit [20], the BABAR [51], and the predictions of Kroll [52] and Ball [53]

Fig. 4 The curves of η and η'-meson twist-2 LCDA with $n = (2, 4, 6)$ respectively

$$\phi_{4;\eta^{(\prime)}}(u) = \frac{10}{3}\delta^2 u\bar{u}(u - \bar{u}), \tag{56}$$

where, the values for the twist-3, 4 LCDAs parameters are taken from Refs. [98,99]. In order to run the hadronic parameters of the $\eta^{(\prime)}$-meson twist-2, 3, 4 LCDAs from the initial factorization scale to any other scale, especially for typical scale $\mu_{\rm IR}$, the renormalization group equation should be used, which has the form

$$c_i(\mu_{\rm IR}) = \mathcal{L}^{\gamma_{c_i}/\beta_0} c_i(\mu_0), \tag{57}$$

where $\mathcal{L} = \alpha_s(\mu_{\rm IR})/\alpha_s(\mu_0)$, $\beta_0 = 11 - 2/3 n_f$, and the one-loop anomalous dimensions γ_{c_i} can be seen in our previous work [100]. Taking the hadronic parameters at initial scale μ_0 and using the renormalization function (57), one can achieve the corresponding values at the typical scale $\mu_{\rm IR}$.

3.3 TFFs and series expansion

In order to determine the continuum threshold s_0 for the $D_s \to \eta^{(\prime)}$ TFFs within LCSR approach, i.e. Eq. (46), one can follow the four criteria

- The continuum contributions are less than 30% of the total results;
- The contributions from the twist-4 LCDAs do not exceed 5%;
- We require the variations of the TFF within the Borel window be less than 10%;
- The continuum threshold s_0 should be closer to the squared mass of the first excited state of D_s-meson.

Based on the fourth term of the criteria, we take s_0 to be close to the squared mass of the excited state of D_s-meson $D_{s1}(2460)$, i.e. $s_0 = 6.1(3)$ GeV^2. Furthermore, the Borel parameter is taken as $M^2 = 25(1)$ GeV^2. Furthermore, we

Fig. 5 The TFFs $f_+^{\eta^{(\prime)}}(0)$ versus the Borel parameters M^2, where the shaded band is induced by the variations of squared average of all input parameters

can obtain the sum rule for m_{D_s} by differentiating the form factors $f_+^{\eta^{(\prime)}}(q^2) f_{D_s}$ with respect to $-1/M^2$ [101]. The resultant $m_{D_s}^{\text{LCSR}} = 1.9653$ GeV agrees with the measured value $m_{D_s}^{\text{PDG}} = 1.9685$ GeV. In order to show the degree of stability of the TFFs versus the Borel parameter, we present the curve of TFFs in Fig. 5, in which the shaded region shows the errors from all input parameters. The solid line with blue shaded band represents $f_+^{\eta}(0)$ and the dashed line with green band represents $f_+^{\eta^{\prime}}(0)$. This figure shows that $f_+^{\eta^{(\prime)}}(0)$ changes less than 0.5% within the range of $M^2 \in [23, 27]$ GeV^2, which satisfies the third term of the criteria. More definitely, we put the errors caused by different input parameters in the following,

$$f_+^{\eta}(0) = 0.476 + \left(^{+0.011}_{-0.012}\right)_{s_0} + \left(^{+0.001}_{-0.001}\right)_{M^2} + \left(^{+0.036}_{-0.032}\right)_{m_c, f_{D_s}}$$
$$+ \left(^{+0.011}_{-0.011}\right)_{f_\eta} + \left(^{+0.004}_{-0.003}\right)_{a^2_{2;\eta}} + \left(^{+0.000}_{-0.000}\right)_{a^4_{2;\eta}}$$

$$+ \left(^{+0.000}_{-0.000}\right)_{a^6_{2;\eta}} = 0.476^{+0.040}_{-0.036} \tag{58}$$

$$f_+^{\eta^{\prime}}(0) = 0.544 + \left(^{+0.015}_{-0.016}\right)_{s_0} + \left(^{+0.001}_{-0.001}\right)_{M^2} + \left(^{+0.042}_{-0.037}\right)_{m_c, f_{D_s}}$$
$$+ \left(^{+0.010}_{-0.010}\right)_{f_{\eta^{\prime}}} + \left(^{+0.006}_{-0.005}\right)_{a^2_{2;\eta^{\prime}}} + \left(^{+0.000}_{-0.001}\right)_{a^4_{2;\eta^{\prime}}}$$
$$+ \left(^{+0.000}_{-0.000}\right)_{a^6_{2;\eta^{\prime}}} = 0.544^{+0.046}_{-0.042} \tag{59}$$

According to Eq. (4), when the Gegenbauer moments are taken up to 2nd, 4th and 6th order levels, the central values of TFFs $f_+^{\eta^{(\prime)}}(0)$ are

$$f_+^{\eta}(0)|_{2\text{nd}} = 0.4745,$$
$$f_+^{\eta}(0)|_{4\text{th}} = 0.4755,$$
$$f_+^{\eta}(0)|_{6\text{th}} = 0.4763,$$
$$f_+^{\eta^{\prime}}(0)|_{2\text{nd}} = 0.5435,$$
$$f_+^{\eta^{\prime}}(0)|_{4\text{th}} = 0.5434,$$
$$f_+^{\eta^{\prime}}(0)|_{6\text{th}} = 0.5436.$$

In comparing with the 2nd-order Gegenbauer moment's contribution, the 4th, 6th-order contributions shall be changed by about 0.211%, 0.379% for $f_+^{\eta}(0)$ and -0.018%, 0.018% for $f_+^{\eta^{\prime}}(0)$, respectively. These ratios are really small, indicating the Gegenbauer series has good convergence over the moment expansion. Then, we list the TFFs for $D_s \to \eta^{(\prime)}$ at large recoil point, i.e. $f_+^{\eta^{(\prime)}}(0)$, in Table 3, in which the uncertainties are from the squared average of all the mentioned error sources. As a comparison, we also present other theoretical and experimental predictions, such as the BESIII [12], the LQCD [13], the LFQM [14], the CQM [17], the CCQM [18,19], the QCD SR [22], the LCSR at 2013 and 2015 [20,21], respectively. Our results agree with the BESIII, the CCQM, the LCSR, the LQCD within errors, but are lack of agreement with the Lattice QCD results.

Table 3 The TFFs $f_+^{\eta^{(\prime)}}(0)$ at the large recoil point $q^2 = 0$. As a comparison, we also present the predictions from various experimental and theoretical groups

	References	$f_+^{\eta}(0)$	$f_+^{\eta^{\prime}}(0)$
Experimental results	BESIII [12]	0.4576(70)	0.490(51)
	LQCD-I [13]	0.542(13)	0.404(25)
	LQCD-II [13]	0.564(11)	0.437(18)
Theoretical predictions	This work (LCSR)	$0.476^{+0.040}_{-0.036}$	$0.544^{+0.046}_{-0.042}$
	LFQM [14]	0.76	–
	CQM [17]	0.78	0.78
	CCQM [18]	0.78(12)	0.73(11)
	CCQM [19]	0.49(7)	0.59(9)
	LCSR 2013 [20]	0.432(33)	0.520(80)
	LCSR 2015 [21]	$0.495^{+0.029}_{-0.030}$	$0.558^{+0.047}_{-0.045}$
	QCD SR [22]	0.50(4)	–

The physically allowable ranges for the TFFs are $m_\ell^2 \leq q^2 \leq (m_{D_s} - m_\eta)^2 \approx 2$ GeV^2 and $m_\ell^2 \leq q^2 \leq (m_{D_s} - m_{\eta'})^2 \approx 1$ GeV^2. Theoretically, the LCSRs approach for $D_s \to \eta^{(\prime)}$ TFFs are applicable in low and intermediate q^2-regions, i.e. $q^2 \in [0, 1.2]$ GeV^2 of η-meson, $q^2 \in [0, 0.6]$ GeV^2 of η'-meson. One can extrapolate it to whole q^2-regions via a rapidly $z(q^2, t)$ converging series expansion (SE) [102]:

$$f_+^{\eta^{(\prime)}}(q^2) = \frac{1}{B(q^2)\phi_+^{\eta^{(\prime)}}(q^2)} \sum_k^{K-1} \alpha_k z^k(q^2, t_0). \tag{60}$$

Normally, the parameter K stands for the order of expansion. The $z(q^2, t)$ is the function:

$$z(q^2, t) = \frac{\sqrt{t_+ - q^2} - \sqrt{t_+ - t}}{\sqrt{t_+ - q^2} + \sqrt{t_+ - t}}, \tag{61}$$

where $t = (t_0^{\eta^{(\prime)}}, t_-^{\eta^{(\prime)}}, m_{D_s})$ with $t_\pm^{\eta^{(\prime)}} = (m_{D_s} \pm m_{\eta^{(\prime)}})^2$. Here, the $0 \leq t_0^{\eta^{(\prime)}} \leq t_-^{\eta^{(\prime)}}$ is a free parameter which can be optimised to reduce the maximum value of $|z(q^2, t_0^{\eta^{(\prime)}})|$ in the physical TFFs range, $t_0^{\eta^{(\prime)}}|_{\text{opt.}} = t_+^{\eta^{(\prime)}}(1 - \sqrt{1 - t_-^{\eta^{(\prime)}}/t_+^{\eta^{(\prime)}}})$. Here, we list the value of $z(q^2, t_0^{\eta^{(\prime)}})$ with different q^2 cases in Table 4. The function $\phi_+^{\eta^{(\prime)}}(q^2)$ can be expressed as

$$\phi_+^{\eta^{(\prime)}}(q^2) = \sqrt{\frac{\varsigma}{48\pi \chi_+^{\eta^{(\prime)}}(n)}} \frac{q^2 - t_+}{(t_+ - t_0)^{1/4}}$$
$$\times \left(\frac{z(q^2, 0)}{-q^2}\right)^{(3+n)/2} \left(\frac{z(q^2, t_0)}{t_0 - q^2}\right)^{-1/2}$$
$$\times \left(\frac{z(q^2, t_-)}{t_- - q^2}\right)^{-3/4}\bigg|_{n=2}, \tag{62}$$

where $\varsigma = 1$ is an isospin-degeneracy factor for a given channel and $B(q^2) = \prod_i z(q^2, m_{D_s^i}^2)$ stands for the Blaschke factor. The $m_{D_s^i}$ stands for the mass of each resonance state with $J^P = 0^-, 0^+, 1^- \ldots$, respectively, which can be found in PDG [91]. For the coefficients $\chi_+^{\eta^{(\prime)}}(n)$, it can be calculated by using QCD sum rules including perturbative LO and NLO results as well as the condensate contributions, which can be expressed as [102]

$$\chi_+^{\eta^{(\prime)}} = \frac{3}{32\pi^2 m_c^2}\left[1 + \frac{\alpha_s(m_c)C_F}{4\pi}\left(\frac{25}{6} + \frac{2\pi^2}{3}\right)\right]$$
$$- \frac{\langle q\bar{q}\rangle}{m_c^5} - \frac{\langle \alpha_s G^2\rangle}{12\pi m_c^6} - \frac{\langle \bar{q}Gq\rangle}{m_c^7}. \tag{63}$$

Furthermore, the coefficients α_k should satisfy the basic unitarity constraint,

$$\sum_k^{K-1} \alpha_k^2 < 1. \tag{64}$$

The simplified version of the series expansion (SSE) method is to replace the Blaschke factor $B(q^2)$ by a simple pole $P(q^2)$ to account for low-lying resonances, i.e. [103]

$$f_+^{\eta^{(\prime)}}(q^2) = \frac{1}{P(t)} \sum_k^{K-1} \beta_k z^k(q^2, t_0). \tag{65}$$

As for the SSE parameterization, imposing the unitarity bound and by comparing the SE and SSE parameterizations

$$\alpha_i = \sum_{k=0}^{\min[K-1,i]} \zeta_{i-k}\beta_k, \quad 0 \leq i \leq K - 1, \tag{66}$$

we obtain the unitarity bound of the SSE

$$\sum_{j,k=0}^{\min[K-1]} C_{jk}\beta_j\beta_k \leq 1, \tag{67}$$

with the positive defined matrix

$$C_{jk} = \sum_{i=0}^{K-1-\max[j,k]} \zeta_i \zeta_{j-k}. \tag{68}$$
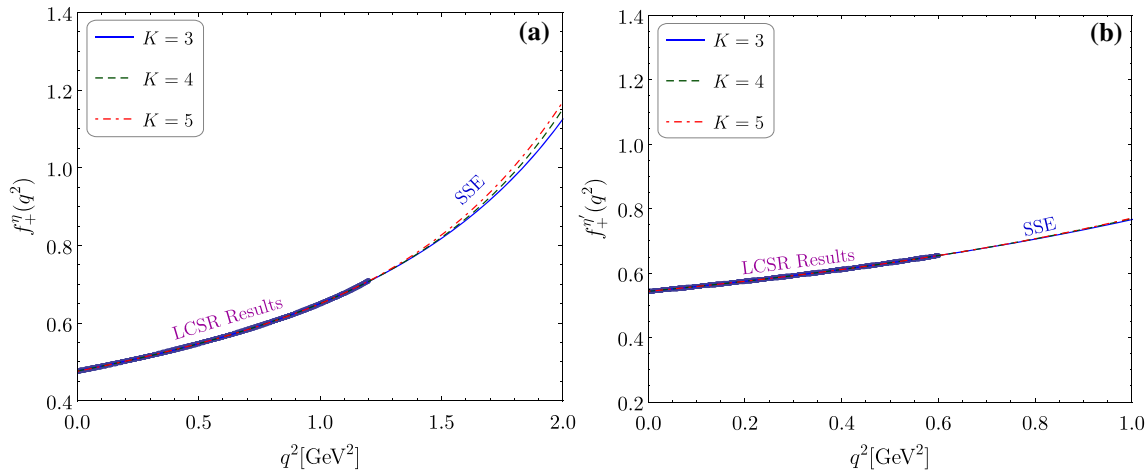
Theoretically, the order K can be taken up to infinite order. It has been proven that the higher order expansion shall give the same result with very small errors. We take $K = 3, 4, 5$ as explicit examples, which are shown in Fig. 6. It is found that three SSE curves with $K = 3, 4, 5$ for the TFFs $f_+^{\eta^{(\prime)}}(q^2)$ are almost coincide with each other. So, we will take $K = 3$ to do our expansion in the following calculations, which also agrees with the choices of most of the theoretical groups. At the same time, the α_k of SE and β_k of SSE should also satisfy the condition $\Delta < 1\%$. From which, the parameter Δ is used to measure the quality of extrapolation, which is defined as

$$\Delta = \frac{\sum_t |F_i(t) - F_i^{\text{fit}}(t)|}{\sum_t |F_i(t)|} \times 100, \tag{69}$$

where $t \in [0, 1/100, \ldots, 100/100] \times 1.2$ GeV for η-meson, $t \in [0, 1/100, \ldots, 100/100] \times 0.6$ GeV for η'-meson. Numerical values of α_k, β_k with $k = (0, 1, 2)$ for central values, upper and lower limit of $f_+^{\eta^{(\prime)}}(q^2)$ are listed in Table 5. Here, the $\sum \alpha_k^2$ for SE unitarity bound and $\sum C_{i,j}\beta_i\beta_j$ for SSE are less than 1. The quality of extrapolation Δ are less than 0.13%. Since there have good unitary bound and a small

Table 4 The fitting parameters $z(q^2, t_0^{\eta^{(\prime)}})$ of SSE for TFFs $f_+^{\eta^{(\prime)}}(q^2)$

η-meson	$q^2(\text{GeV}^2)$	0	0.4	0.8	1.2	1.6	2.0
	$z(q^2, t_0^{\eta})$	0.048	0.032	0.014	-0.005	-0.025	-0.047
η'-meson	$q^2(\text{GeV}^2)$	0	0.2	0.4	0.6	0.8	1.0
	$z(q^2, t_0^{\eta'})$	0.016	0.004	-0.009	-0.022	-0.036	-0.051

Fig. 6 The SSE for the TFFs $f_+^{\eta}(q^2)$ and $f_+^{\eta'}(q^2)$ up to $K = 3, 4, 5$ order

Table 5 The fitting parameters for the central TFFs $f_+^{\eta^{(\prime)}(C)}(q^2)$, the upper TFFs $f_+^{\eta^{(\prime)}(U)}(q^2)$ and the lower TFFs $f_+^{\eta^{(\prime)}(L)}(q^2)$

	$f_+^{\eta(C)}(q^2)$	$f_+^{\eta(U)}(q^2)$	$f_+^{\eta(L)}(q^2)$	$f_+^{\eta'(C)}(q^2)$	$f_+^{\eta'(U)}(q^2)$	$f_+^{\eta'(L)}(q^2)$
α_0	-0.0003	-0.0003	-0.0003	-0.00001	-0.00001	-0.00001
α_1	-0.0015	-0.0017	-0.0015	-0.00017	-0.00018	-0.00016
α_2	-0.0061	-0.0074	-0.0052	-0.00134	-0.00143	-0.00127
$\sum \alpha_k^2$	3.9×10^{-5}	5.8×10^{-5}	2.9×10^{-5}	1.8×10^{-6}	2.4×10^{-6}	1.6×10^{-6}
β_0	0.512	0.555	0.476	0.563	0.611	0.519
β_1	-1.450	-1.211	-0.976	-1.653	-1.801	-1.534
β_2	17.26	12.24	8.73	28.95	30.61	27.98
$\sum C_{i,j}\beta_i\beta_j$	0.020	0.019	0.008	0.005	0.005	0.004
Δ	0.075%	0.129%	0.099%	0.005%	0.004%	0.007%

Δ value, the SSE results are in high agreement with our LCSR results.
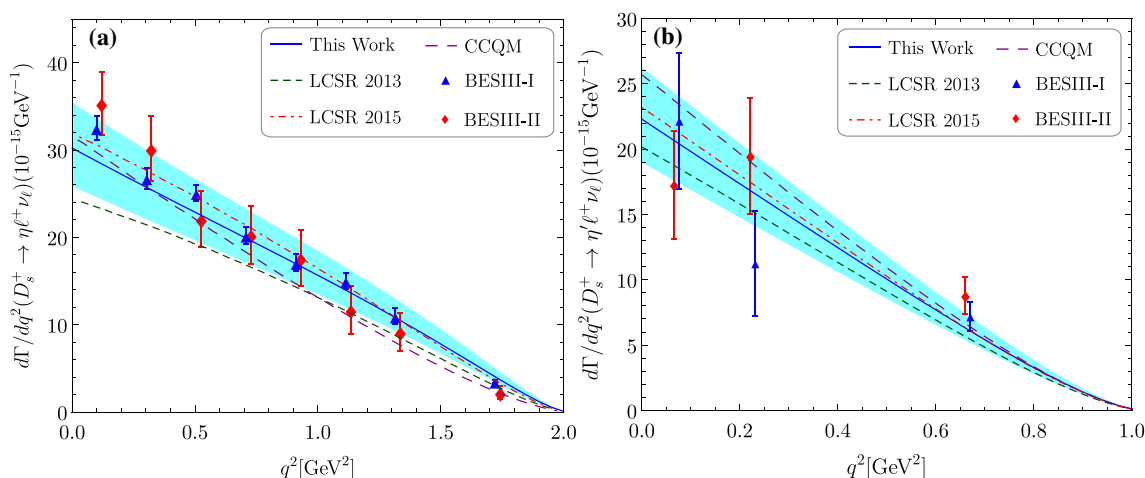
The extrapolated TFFs in the whole q^2-region is shown in Fig. 7, other theoretical and experimental results, such as those of the BESIII [12], the LCSR 2013 [20], the LCSR 2015 [21] and the CCQM [19] are present as a comparison. Two sets of BESIII are from the two different $\eta^{(\prime)}$ decay channels. For η-meson, the blue triangle stands for $\eta \to \gamma\gamma$ channel and the red diamond stands for $\eta \to \pi^0\pi^+\pi^-$ channel. For η'-meson the blue triangle stands for $\eta' \to \gamma\rho^0$ channel and red diamond stands for $\eta' \to \eta_{\gamma\gamma}\pi^+\pi^-$ channel. To compare with other theoretical and experimental groups, our results have the following characteristics,

- Comparing with $f_+^{\eta}(q^2)$, the $f_+^{\eta'}(q^2)$ is more flat in the whole q^2 region.
- Our predictions of $f_+^{\eta}(q^2)$ are in good agreement with the recent BESIII predictions for the $\eta \to \gamma\gamma$ channel.
- In the LCSR q^2-region, our results have good agreement with the LCSR 2013 and 2015, the CCQM, and the two sets of BES-III predictions within errors.
- The SSE of $f_+^{\eta}(q^2)$ in the region of $q^2 \in [1.2, 2.0]\,\text{GeV}^2$ have agreement with the LCSR in 2015 results within errors. However, our predictions are larger than the LCSR in 2013 and CCQM predictions due to the different η-meson distribution amplitudes or different method.

Fig. 7 The TFFs $f_+^{\eta^{(')}}(q^2)$ together with its uncertainties. Results of the LCSR 2013 [20], the LCSR 2015 [21], the CCQM [19] and the BESIII [12] are also given as the comparison

Fig. 8 Decay width for the $D_s^+ \to \eta^{(')}\ell^+\nu_\ell (\ell = e, \mu)$ versus q^2 within uncertainties. The LCSR in 2013 [20] and 2015 [21], the CCQM [19], and two sets of BESIII collaboration [12] predictions are also present as a comparison

3.4 Decay widthes and branching fractions for the semileptonic decay $D_s^+ \to \eta^{(')}\ell^+\nu_\ell$

One can get the differential decay widths by using the formula (50). For the CKM matrix element $|V_{cs}|$, we take it to be the average value of leptonic and semileptonic decay $c \to s$ processes coming from PDG [93], i.e. $|V_{cs}| = 0.987 \pm 0.011$. After taking the derived $D_s \to \eta^{(')}$ TFFs into the decay widths, we present the differential decay widths in Fig. 8. As a comparison, we also give the LCSR in 2013 [20] and 2015 [21], the CCQM [19], and two sets of BESIII collaboration [12] predictions. The LCSR and the CCQM results are calculated by applying their TFFs into the width formula. Those figures show that our prediction for $D_s^+ \to \eta\ell^+\nu_\ell$ is in agreement with LCSR 2015, CCQM, the BESIII-I and the BESIII-II results within errors, and the $D_s^+ \to \eta'\ell^+\nu_\ell$ agrees with the LCSR 2013 and 2015, the CCQM,

the BESIII-I and BESIII-II predictions within errors. All the results are convergence to zero at the small recoil region $q^2_{max} = (m_{D_s} - m_{\eta^{(')}})^2$, which indicates that our results are reasonable.

After integrating over the whole $m_\ell^2 \leq q^2 \leq (m_{D_s} - m_{\eta^{(')}})^2$ region for the differential decay widths, we obtain the total decay widths for $D_s^+ \to \eta^{(')}\ell^+\nu_\ell$ with two different channel $\Gamma(D_s^+ \to \eta^{(')}e^+\nu_e)$ and $\Gamma(D_s^+ \to \eta^{(')}\mu^+\nu_\mu)$, i.e.,

$$\Gamma(D_s^+ \to \eta e^+\nu_e) = 30.634^{+5.453}_{-4.323} \times 10^{-15} \text{ GeV},$$
$$\Gamma(D_s^+ \to \eta\mu^+\nu_\mu) = 30.298^{+5.395}_{-4.275} \times 10^{-15} \text{ GeV},$$
$$\Gamma(D_s^+ \to \eta'e^+\nu_e) = 10.345^{+1.844}_{-1.534} \times 10^{-15} \text{ GeV},$$
$$\Gamma(D_s^+ \to \eta'\mu^+\nu_\mu) = 10.096^{+1.800}_{-1.498} \times 10^{-15} \text{ GeV}. \quad (70)$$

Then, by using the lifetime of the initial state D_s^+-meson, $\tau_{D_s^+} = (0.504 \pm 0.007)$ ps [91], the branching fractions for the two different semileptonic decay channels $D_s \to$

Table 6 Branching factions of $D_s^+ \to \eta^{(\prime)}\ell^+\nu_\ell$ with $\ell = e$ and μ (in unit 10^{-2}). The errors are squared averages of all the mentioned error sources. As a comparison, we also present the predictions for various methods
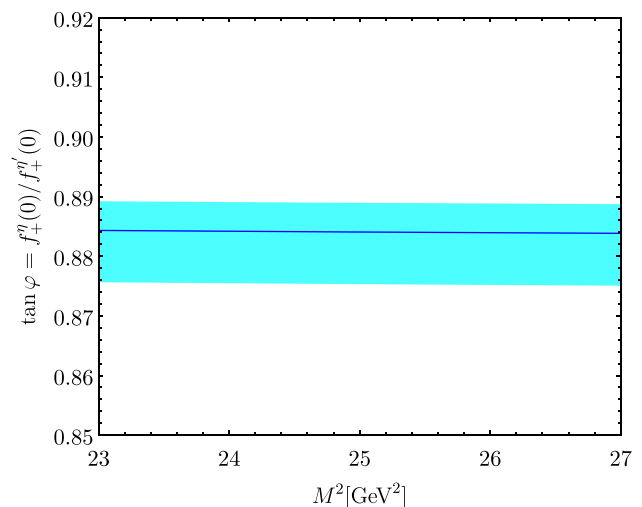
	Mode	$\mathcal{B}(D_s^+ \to \eta e^+\nu_e)$	$\mathcal{B}(D_s^+ \to \eta\mu^+\nu_\mu)$
Experimental results	BESIII [11,12]	$2.323 \pm 0.063 \pm 0.063$	$2.42 \pm 0.46 \pm 0.11$
	CLEO [8]	$2.28 \pm 0.14 \pm 0.19$	–
	CLEO [9]	$2.48 \pm 0.29 \pm 0.13$	–
	PDG [91]	2.32 ± 0.08	2.4 ± 0.5
Theoretical predictions	This work (LCSR)	$2.346^{+0.418}_{-0.331}$	$2.320^{+0.413}_{-0.327}$
	LFQM [15]	2.26 ± 0.21	2.22 ± 0.20
	CCQM [19]	2.24	2.18
	LCSR [20]	2.00 ± 0.32	–
	LCSR [21]	2.40 ± 0.28	–
	QCD SR-I [22]	2.6 ± 0.7	–
	QCD SR-II [22]	2.3 ± 0.4	–
	Mode	$\mathcal{B}(D_s^+ \to \eta'e^+\nu_e)$	$\mathcal{B}(D_s^+ \to \eta'\mu^+\nu_\mu)$
Experimental results	BESIII [11,12]	$0.824 \pm 0.073 \pm 0.027$	$1.06 \pm 0.54 \pm 0.07$
	CLEO [8]	$0.68 \pm 0.15 \pm 0.06$	–
	CLEO [9]	$0.91 \pm 0.33 \pm 0.05$	–
	PDG [91]	0.80 ± 0.07	1.1 ± 0.5
Theoretical predictions	This work (LCSR)	$0.792^{+0.141}_{-0.118}$	$0.773^{+0.138}_{-0.115}$
	LFQM [15]	0.89 ± 0.09	0.85 ± 0.08
	CCQM [19]	0.83	0.79
	LCSR [20]	0.75 ± 0.23	–
	LCSR [21]	0.79 ± 0.14	–
	QCD SR-I [22]	0.89 ± 0.34	–
	QCD SR-II [22]	1.0 ± 0.2	–

$\eta^{(\prime)}\ell^+\nu_\ell$ with $\ell = (e, \mu)$ can be obtained, which are presented in Table 6. Here, we also listed the BESIII [11,12], the PDG [91], the CLEO [9] for the experimental results, and the CCQM [19], the LFQM [15], the QCDSR-I, II [22], the LCSR [20,21] for theoretical predictions. Our results are closer to the BESIII, PDG, CLEO results, all of which are within 1σ uncertainties.

After substituting the corresponding terms of Eq. (3), one can get the mixing angle of $\eta - \eta'$. The mixing angle $\tan\varphi$ with the parameter of Borel parameter M^2 are shown in Fig. 9. In the whole Borel parameter M^2 region, the mixing angle is changed slightly, which also indicates that there have a stable Borel window for $\tan\varphi$. Numerical results for the single mixing angle φ are present in Table 7. Our result is closer to the KLOE [48] and the LCSR predictions [21,49], which is slightly larger than other LFQM [16] and QCD SR [22] predictions.

Furthermore, it is useful to study the ratio for the different decay channel $\mathcal{R}^\ell_{\eta'/\eta}$ related to the mixing angle, which has the basic definition

$$\mathcal{R}^\ell_{\eta'/\eta} = \frac{\mathcal{B}(D_s \to \eta'\ell^+\nu_\ell)}{\mathcal{B}(D_s \to \eta\ell^+\nu_\ell)}. \qquad (71)$$

Fig. 9 $f_+^\eta(0)/f_+^{\eta'}(0)$ as a function of the Borel parameter M^2, where the shaded band is induced by the variations of squared average of all input parameters

Numerical results together with different experimental and theoretical predictions are given in Table 7. Our results are in agreement with the CLEO [7] and the BESIII [10] predictions, and the LCSR predictions [21,49]. This can be con-

Table 7 The φ with respect to mixing angle, $\mathcal{R}^{\ell}_{\eta'/\eta}$ for different models and experimental values. As a comparison, we also present the experimental and theoretical predictions

Mode	Angle φ	$\mathcal{R}^{\ell}_{\eta'/\eta}$
This work (LCSR) with $\ell = e$	$41.2°^{+0.05}_{-0.06}$	$0.338^{+0.057}_{-0.051}$
This work (LCSR) with $\ell = \mu$	$41.2°^{+0.05}_{-0.06}$	$0.333^{+0.050}_{-0.058}$
CLEO [7]	–	$0.35 \pm 0.09 \pm 0.07$
BESIII [10]	–	$0.40 \pm 0.14 \pm 0.02$
LFQM [16]	$39°$	0.39
LCSR [21]	$41.8°$	0.33 ± 0.07
QCD SR [22]	$40°$	0.44 ± 0.01
KLOE [48]	$41.4°$	–
LCSR-I [49]	$39.7°$	0.32 ± 0.02
LCSR-II [49]	$41.5°$	0.27 ± 0.01

sidered as a good test of the correctness of the considered internal structure for the D_s-meson as well as the mixing angle between η and η' states.

4 Summary

In this paper, we have calculated the moments $\langle \xi^n_{2;\eta^{(\prime)}} \rangle|_\mu$ of $\eta^{(\prime)}$-meson LCDA with $n = (2, 4, 6)$ up to NLO correction and completely dimension-six condensates within BFTSR, which are shown in Eq. (33). Due to the $\eta^{(\prime)}$-meson should be considered as $s\bar{s}$ component in $D_s \to \eta^{(\prime)}$ decay processes, we have also taken the $I_{m_s^2}(n, M^2)$ corrections into consideration, i.e. Eq. (34), the detailed terms of OPE are listed in the Appendix B.

Then, we have sought a reasonable continuum threshold s_0 and stable Borel windows for $\langle \xi^n_{2;\eta^{(\prime)}} \rangle|_\mu$ with $n = (2, 4, 6)$ by using the traditional three criteria for the SVZ sum rules, which are present in Figs. 1 and 2 and Table 1. By using the expression between two different Gegenbauer and LCDA moments, i.e. Eq. (37), we have presented the first three Gegenbauer and LCDA moments $a^n_{2;\eta^{(\prime)}}(\mu_0)$ and $\langle \xi^n_{2;\eta^{(\prime)}} \rangle|_{\mu_0}$ with $n = (2, 4, 6)$ for the $\phi_{2;\eta^{(\prime)}}(u, \mu_0)$ within errors in Table 2. Our results are in agreement with the CLEO fit and the BABAR fit predictions. Meanwhile, we have exhibited the curves of $\phi_{2;\eta^{(\prime)}}(u, \mu_0)$ of our prediction with $n = (2, 4, 6)$ and compare with others.

Furthermore, the TFFs $f^{\eta^{(\prime)}}_+(q^2)$ have been given in Eq. (46) up to NLO QCD corrections for twist-2, 3 LCDA contributions. The TFFs at large recoil region have been presented in Table 3 with respect to other theoretical predictions. After extrapolating it to the whole physical q^2-region via simplified series expansion, we have shown the behavior of TFFs in Fig. 7. The differential/total decay widths and branching fractions in this work have also been given. Our results are in agreement with the BESIII and the PDG average value within errors. Finally, we have presented the mixing angle $\tan \varphi$ and

ratio for different decay channel $\mathcal{R}^{\ell}_{\eta'/\eta}$, which agree with theoretical and experimental results within errors. Thus, the QCDSR within BFTSR can be considered a good approach in dealing with the heavy-to-light semileptonic processes, and we hope more data can be achieved in the near future for more precise studies.

Appendix A: Quark propagators and vertex for background field theory framework

A1. Quark propagators

Quarks field and its propagators satisfy the equation Eq. (11) in the BFT, solve to Eq. (11), we have the following form

$$S_F(x,0) = (i\not{D} + m)\mathcal{D}(x,0), \tag{A1}$$

where $\mathcal{D}(x,0)$ satisfies the equation

$$(\partial^2 - \mathcal{P}_\mu \partial^\mu - \mathcal{Q} + m^2)\mathcal{D}(x,0) = \delta^4(x), \tag{A2}$$

with $\mathcal{P}_\mu = 2i\mathcal{A}_\mu$, $\mathcal{Q} = \gamma^\nu \gamma^\mu [\mathcal{A}_\nu(x)\mathcal{A}_\mu(x) + i\partial_\nu \mathcal{A}_\mu(x)]$. After using above equation up here we can get quark propagator $S_F(x,0)$ subexpression

$$
\begin{aligned}
S_F(x,0) = {}& S_F^0(x,0) + S_F^2(x,0) \\
& + S_F^3(x,0) + \sum_{i=1}^{2} S_F^{4(i)}(x,0) \\
& + \sum_{i=1}^{3} S_F^{5(i)}(x,0) + \sum_{i=1}^{5} S_F^{6(i)}(x,0).
\end{aligned} \tag{A3}
$$

In order to have a clear look at the detailed quark propagator $S_F(x,0)$ separately, we list the expression of $S_F^d(x,0)$ with $d \le 6$ as follows,

$$S_F^0(x,0) = i\int \frac{d^4p}{(2\pi)^4} e^{-ip\cdot x}\left[-\frac{m+\not{p}}{m^2-p^2}\right], \tag{A4}$$

$$S_F^2(x,0) = i\int \frac{d^4p}{(2\pi)^4} e^{-ip\cdot x}\left[-\frac{i}{2}\frac{\gamma^\mu(m-\not{p})\gamma^\nu}{(m^2-p^2)^2}G_{\mu\nu}\right], \tag{A5}$$

$$
\begin{aligned}
S_F^3(x,0) = {}& i\int \frac{d^4p}{(2\pi)^4} e^{-ip\cdot x}\left\{-\frac{2}{3}\left[\frac{(\gamma^\mu p^\rho + \gamma^\rho p^\mu)(m-\not{p})}{(m^2-p^2)^3}\right.\right. \\
& \left.\left.-\frac{g^{\mu\rho}}{(m^2-p^2)^2}\right]\gamma^\nu G_{\mu\nu;\rho}\right\},
\end{aligned} \tag{A6}
$$

$$
\begin{aligned}
S_F^{4(1)}(x,0) = {}& i\int \frac{d^4p}{(2\pi)^4} e^{-ip\cdot x}\left\{\frac{1}{4}\left[\frac{\gamma^\mu(m-\not{p})}{(m^2-p^2)^3}\right.\right. \\
& \left.-\frac{2p^\mu}{(m^2-p^2)^3}\right]\gamma^\nu\gamma^\rho\gamma^\sigma + \frac{1}{2}\left[\frac{(m+\not{p})\gamma^\mu}{(m^2-p^2)^3}g^{\nu\sigma}\right. \\
& \left.\left.+4\frac{\gamma^\mu(m-\not{p})}{(m^2-p^2)^4}p^\nu p^\sigma\right]\gamma^\rho\right\}G_{\mu\nu}G_{\rho\sigma},
\end{aligned} \tag{A7}
$$

$$
\begin{aligned}
S_F^{4(2)}(x,0) = {}& i\int \frac{d^4p}{(2\pi)^4} e^{-ip\cdot x}\left\{\frac{i}{4}\left[\frac{g^{\{\mu\rho}\gamma^{\sigma\}}(m-\not{p})}{(m^2-p^2)^3}\right.\right. \\
& \left.\left.-\frac{2g^{\{\mu\rho}p^{\sigma\}}}{(m^2-p^2)^3}+4\frac{\gamma^{\{\mu}p^\rho p^{\sigma\}}(m-\not{p})}{(m^2-p^2)^4}\right]\gamma^\nu \times G_{\mu\nu;\rho\sigma}\right\},
\end{aligned} \tag{A8}
$$

$$
\begin{aligned}
S_F^{5(1)}(x,0) = {}& i\int \frac{d^4p}{(2\pi)^4} e^{-ip\cdot x} \\
& \times\left\{-\frac{i}{3}\left[\left(3\frac{\gamma^\mu(m-\not{p})\gamma^\nu}{(m^2-p^2)^4}(p^\lambda\gamma^\rho + p^\rho\gamma^\lambda)\right.\right.\right.
\end{aligned}
$$

$$
\begin{aligned}
& \left.-\frac{\gamma^\nu(g^{\mu\lambda}\gamma^\rho + g^{\mu\rho}\gamma^\lambda)}{(m^2-p^2)^3}\right)\cdot\gamma^\sigma + 4\left(\frac{\gamma^\mu(m-\not{p})}{(m^2-p^2)^4}g^{\{\nu\sigma}p^{\lambda\}}\right. \\
& \left.\left.+2\frac{p^\mu g^{\{\nu\sigma}p^{\lambda\}}}{(m^2-p^2)^4}+6\frac{\gamma^\mu(m-\not{p})}{(m^2-p^2)^5}p^\nu p^\sigma p^\lambda\right)\gamma^\rho\right]G_{\mu\nu} \\
& \times G_{\rho\sigma;\lambda}\bigg\},
\end{aligned} \tag{A9}
$$

$$
\begin{aligned}
S_F^{5(2)}(x,0) = {}& i\int \frac{d^4p}{(2\pi)^4} e^{-ip\cdot x} \\
& \times\left\{\frac{2i}{3}\left[\left(\frac{g^{\mu\lambda}}{(m^2-p^2)^3}+6\frac{p^\mu p^\lambda}{(m^2-p^2)^4}\right)\right.\right. \\
& \times\gamma^\nu\gamma^\rho\gamma^\sigma - 2\left(\frac{\gamma^\mu(m-\not{p})}{(m^2-p^2)^4}\times g^{\{\nu\sigma}p^{\lambda\}}+2\frac{p^\mu g^{\{\nu\sigma}p^{\lambda\}}}{(m^2-p^2)^4}\right. \\
& \left.\left.+6\frac{\gamma^\mu(m-\not{p})}{(m^2-p^2)^5}p^\nu p^\sigma p^\lambda\right)\gamma^\rho\right]G_{\mu\nu;\lambda}G_{\rho\sigma}\bigg\},
\end{aligned} \tag{A10}
$$

$$
\begin{aligned}
S_F^{5(3)}(x,0) = {}& i\int \frac{d^4p}{(2\pi)^4} e^{-ip\cdot x}\frac{4}{15} \\
& \times\left[\frac{g^{\{\rho\sigma}p^\lambda\gamma^{\mu\}}(m-\not{p})}{(m^2-p^2)^4}-\frac{2g^{\{\rho\sigma}p^\lambda p^{\mu\}}}{(m^2-p^2)^4}\right. \\
& \left.+6\frac{\gamma^{\{\mu}p^\rho p^\sigma p^{\lambda\}}(m-\not{p})}{(m^2-p^2)^5}-\frac{g^{(\mu\nu\sigma\lambda)}}{(m^2-p^2)^3}\right]\gamma^\nu G_{\mu\nu;\rho\sigma\lambda},
\end{aligned} \tag{A11}
$$

$$
\begin{aligned}
S_F^{6(1)}(x,0) = {}& i\int \frac{d^4p}{(2\pi)^4} e^{-ip\cdot x}\frac{i}{8}\left\{\left[\frac{\gamma^\mu(m-\not{p})}{(m^2-p^2)^4}\right.\right. \\
& \left.-4\frac{p^\mu}{(m^2-p^2)^4}\right]\gamma^\nu\gamma^\rho\gamma^\sigma\gamma^\lambda\gamma^\tau +2\left[\frac{3\gamma^\mu(m-\not{p})}{(m^2-p^2)^4}\right. \\
& \times g^{\sigma\tau}+16\frac{\gamma^\mu(m-\not{p})}{(m^2-p^2)^5}p^\sigma p^\tau \\
& \left.-4\frac{g^{\mu\sigma}p^\tau + g^{\mu\tau}p^\sigma}{(m^2-p^2)^4}\right]\gamma^\nu\gamma^\rho\gamma^\lambda\bigg\}G_{\mu\nu}G_{\rho\sigma}G_{\lambda\tau},
\end{aligned} \tag{A12}
$$

$$
\begin{aligned}
S_F^{6(2)}(x,0) = {}& i\int \frac{d^4p}{(2\pi)^4} e^{-ip\cdot x}\left(-\frac{1}{8}\right) \\
& \times\left\{\left[3\frac{\gamma^\mu(m-\not{p})\gamma^\nu}{(m^2-p^2)^4}g^{\{\lambda\tau}\gamma^{\rho\}}\right.\right. \\
& \left.+16\frac{\gamma^\mu(m-\not{p})\gamma^\nu}{(m^2-p^2)^5}\gamma^{\{\rho}p^\lambda p^{\tau\}}-4\frac{\gamma^\nu}{(m^2-p^2)^4}g^{\mu\{\lambda}p^\tau\gamma^{\rho\}}\right]\gamma^\sigma \\
& +4\left[\frac{m+\not{p}}{(m^2-p^2)^4}g^{(\nu\sigma\tau\lambda)}+6\frac{m+\not{p}}{(m^2-p^2)^5}g^{\{\nu\sigma}p^\tau p^{\lambda\}}\right. \\
& \left.\left.+48\frac{m+\not{p}}{(m^2-p^2)^6}p^\nu p^\sigma p^\tau p^\lambda\right]\gamma^\mu\gamma^\rho\right\}G_{\mu\nu}G_{\rho\sigma;\lambda\tau},
\end{aligned} \tag{A13}
$$

$$
\begin{aligned}
S_F^{6(3)}(x,0) = {}& i\int \frac{d^4p}{(2\pi)^4} e^{-ip\cdot x}\left(-\frac{2}{9}\right) \\
& \times\left\{3\left[\left(2\frac{\gamma^\mu(m-\not{p})}{(m^2-p^2)^5}p^\lambda p^\tau\right.\right.\right. \\
& \left.-\frac{g^{\{\mu\lambda}p^{\tau\}}}{(m^2-p^2)^4}-\frac{4p^\mu p^\lambda p^\tau}{(m^2-p^2)^5}\right) \\
& \left.\cdot\gamma^\nu\gamma^\rho + (\mu\leftrightarrow\lambda) + (\rho\leftrightarrow\tau) + (\mu\leftrightarrow\lambda, \rho\leftrightarrow\tau)\right]\gamma^\sigma \\
& +4\left[\frac{m+\not{p}}{(m^2-p^2)^4}g^{(\nu\lambda\sigma\tau)}+6\times\frac{m+\not{p}}{(m^2-p^2)^5}g^{\{\nu\lambda}p^\sigma p^{\tau\}}\right. \\
& \left.+48\frac{m+\not{p}}{(m^2-p^2)^6}p^\nu p^\lambda p^\sigma p^\tau\right]\gamma^\mu\gamma^\rho\bigg\}G_{\mu\nu;\lambda}G_{\rho\sigma;\tau},
\end{aligned} \tag{A14}
$$

$$S_F^{6(4)}(x,0) = i\int \frac{d^4p}{(2\pi)^4} e^{-ip\cdot x}\left(-\frac{1}{2}\right)$$

$$\times \left\{ \left[\frac{m+\not p}{(m^2-p^2)^4} g^{\{\nu\tau\lambda\sigma\}} + 6\frac{m+\not p}{(m^2-p^2)^5} g^{\{\nu\tau} p^\lambda p^\sigma\}} + 48 \right. \right.$$

$$\times \frac{(m+\not p) p^\nu p^\tau p^\lambda p^\sigma}{(m^2-p^2)^6} \Bigg]$$

$$\times \gamma^\mu\gamma^\rho - 3\left[\frac{g^{\{\mu\lambda} p^{\tau\}}}{(m^2-p^2)^4} + \frac{8 p^\mu p^\lambda p^\tau}{(m^2-p^2)^5} \right] \gamma^\nu\gamma^\rho\gamma^\sigma \Bigg\} G_{\mu\nu;\lambda\tau} G_{\rho\sigma}, \tag{A15}$$

$$S_F^{6(5)}(x,0) = i\int \frac{d^4p}{(2\pi)^4} e^{-ip\cdot x}$$

$$\times \Bigg\{ -\frac{i}{18}\left[\frac{g^{[\rho\sigma\lambda\tau} \gamma^{\mu]}(m-\not p)}{(m^2-p^2)^4} \right.$$

$$-4\frac{g^{\{\rho\sigma\lambda\tau} p^{\mu\}}}{(m^2-p^2)^4} + 6 g^{\{\rho\sigma} p^\lambda p^\tau \gamma^{\mu\}}$$

$$\times \frac{m-\not p}{(m^2-p^2)^5} - 12\frac{g^{\{\rho\sigma} p^\lambda p^\tau p^{\mu\}}}{(m^2-p^2)^5}$$

$$+48\frac{p^{\{\rho} p^\sigma p^\lambda p^\tau p^{\mu\}}(m-\not p)}{(m^2-p^2)^6} \Bigg] \gamma^\nu G_{\mu\nu;\rho\sigma\lambda\tau} \Bigg\}. \tag{A16}$$

The Feynman diagrams for the quark propagators Eqs. (A4)-(A16) that with various gauge invariant tensors are shown in Fig. 10, where thirteen figures, i.e. Fig. 10a–m, correspond to $S_F^0(x,0), \ldots, S_F^{6(5)}(x,0)$, respectively. The symbol "×" attached to the gluon line indicates the tensor of the local gluon background field with "n" stands for n-th order covariant derivative. For quark propagator from x to 0, the following relation can be used,

$$S_F(0,x|\mathcal{A}) = C S_F^T(x,0|-\mathcal{A}^T) C^{-1}. \tag{A17}$$

The detailed expression are

$$S_F^0(0,x) = i\int \frac{d^4p}{(2\pi)^4} e^{-ip\cdot x}\left[-\frac{m-\not p}{m^2-p^2} \right], \tag{A18}$$

$$S_F^2(0,x) = i\int \frac{d^4p}{(2\pi)^4} e^{-ip\cdot x}\left[\frac{i}{2}\frac{\gamma^\nu(m+\not p)\gamma^\mu}{(m^2-p^2)^2} G_{\mu\nu} \right], \tag{A19}$$

$$S_F^3(0,x) = i\int \frac{d^4p}{(2\pi)^4} e^{-ip\cdot x}\left\{ \frac{2}{3}\gamma^\nu\left[\frac{(m+\not p)(\gamma^\mu p^\rho + \gamma^\rho p^\mu)}{(m^2-p^2)^3} \right. \right.$$

$$+ \frac{g^{\mu\rho}}{(m^2-p^2)^2} \Bigg] G_{\mu\nu;\rho} \Bigg\}, \tag{A20}$$

$$S_F^{4(1)}(0,x) = i\int \frac{d^4p}{(2\pi)^4} e^{-ip\cdot x}\left\{ \frac{1}{4}\gamma^\sigma\gamma^\rho\gamma^\nu \right.$$

$$\times \left[\frac{(m+\not p)\gamma^\mu}{(m^2-p^2)^3} + \frac{2p^\mu}{(m^2-p^2)^3} \right] + \frac{1}{2}\gamma^\rho$$

$$\times \left[\frac{\gamma^\mu(m-\not p)}{(m^2-p^2)^3} g^{\nu\sigma} + 4\frac{(m+\not p)\gamma^\mu}{(m^2-p^2)^4} p^\nu p^\sigma \right] \Bigg\} G_{\rho\sigma} G_{\mu\nu}, \tag{A21}$$

$$S_F^{4(2)}(0,x) = i\int \frac{d^4p}{(2\pi)^4} e^{-ip\cdot x}$$

$$\times \left\{ -\frac{i}{4}\gamma^\nu\left[\frac{(m+\not p)g^{\{\mu\rho}\gamma^{\sigma\}}}{(m^2-p^2)^3} + \frac{2g^{\{\mu\rho} p^{\sigma\}}}{(m^2-p^2)^3} \right. \right.$$

$$+ 4\frac{(m+\not p)\gamma^{\{\mu} p^\rho p^{\sigma\}}}{(m^2-p^2)^4} \Bigg] \times G_{\mu\nu;\rho\sigma} \Bigg\}, \tag{A22}$$

$$S_F^{5(1)}(0,x) = i\int \frac{d^4p}{(2\pi)^4} e^{-ip\cdot x}\left\{ -\frac{i}{3}\left[\gamma^\sigma \right. \right.$$

$$\times \left(-3(p^\lambda\gamma^\rho + p^\rho\gamma^\lambda)\frac{\gamma^\nu(m+\not p)\gamma^\mu}{(m^2-p^2)^4} \right.$$

$$- \frac{(g^{\mu\lambda}\gamma^\rho + g^{\mu\rho}\gamma^\lambda)}{(m^2-p^2)^3} \cdot \gamma^\nu \Bigg) + 4\gamma^\rho$$

$$\times \left(\frac{\gamma^\mu(m-\not p)}{(m^2-p^2)^4} g^{\{\nu\sigma} p^{\lambda\}} + 2\frac{p^\mu g^{\{\nu\sigma} p^{\lambda\}}}{(m^2-p^2)^4} \right.$$

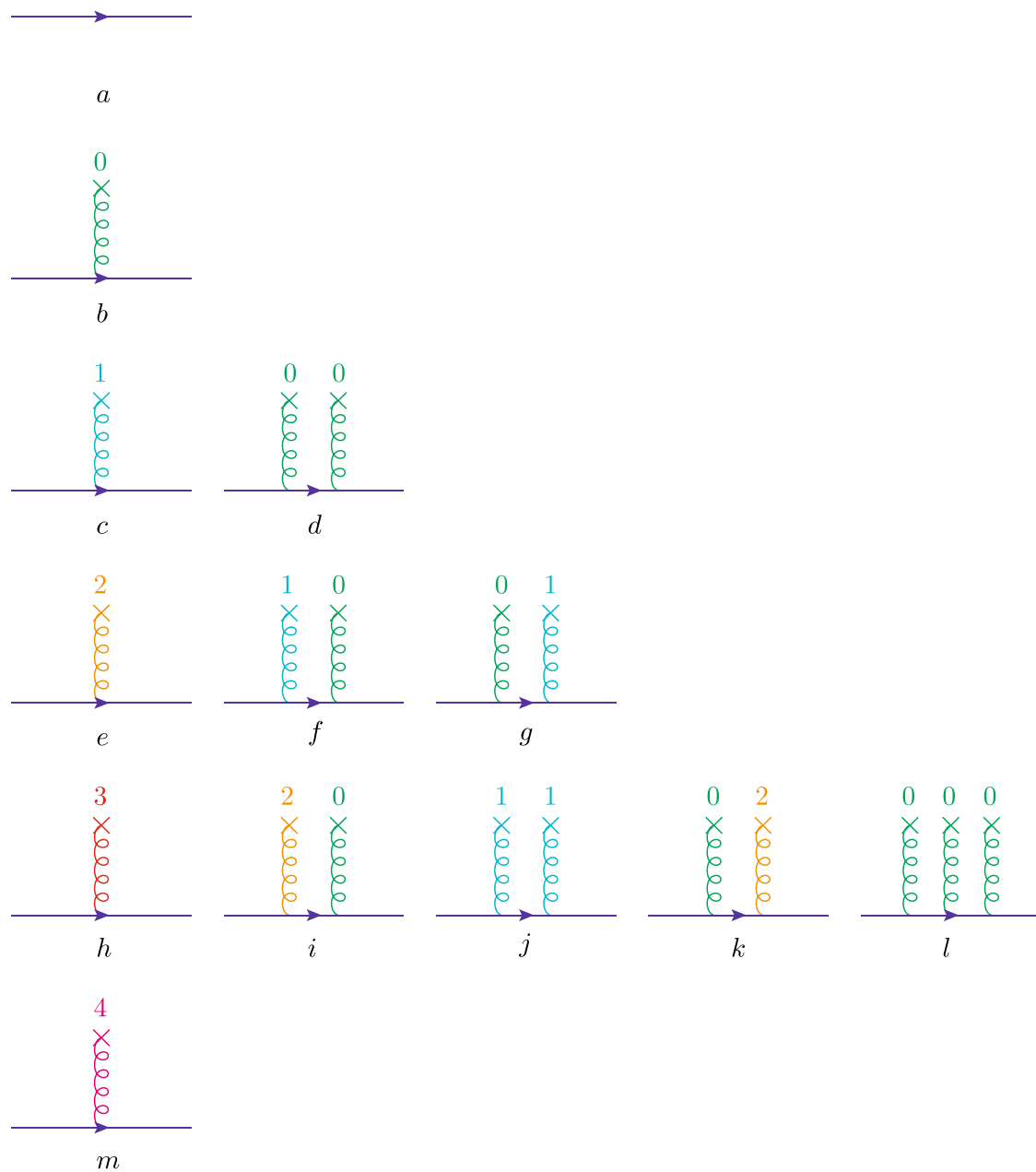$$+ 6\frac{\gamma^\mu(m-\not p)}{(m^2-p^2)^5} p^\nu p^\sigma p^\lambda \Bigg) \Bigg] G_{\rho\sigma;\lambda} \times G_{\mu\nu} \Bigg\}, \tag{A23}$$

$$S_F^{5(2)}(0,x) = i\int \frac{d^4p}{(2\pi)^4} e^{-ip\cdot x} \frac{2i}{3}\left[\gamma^\sigma\gamma^\rho\gamma^\nu\left(\frac{g^{\mu\lambda}}{(m^2-p^2)^3} \right. \right.$$

$$+ 6\frac{p^\mu p^\lambda}{(m^2-p^2)^4} \Bigg) - 2\gamma^\rho\left(-\frac{(m+\not p)\gamma^\mu}{(m^2-p^2)^4} \right.$$

$$\times g^{\{\nu\sigma} p^{\lambda\}} - 2\frac{p^\mu g^{\{\nu\sigma} p^{\lambda\}}}{(m^2-p^2)^4}$$

$$- 6\frac{(m+\not p)\gamma^\mu}{(m^2-p^2)^5} p^\nu p^\sigma p^\lambda \Bigg) \Bigg] G_{\rho\sigma} G_{\mu\nu;\lambda}, \tag{A24}$$

$$S_F^{5(3)}(0,x) = i\int \frac{d^4p}{(2\pi)^4} e^{-ip\cdot x} \frac{4}{15}\gamma^\nu\left[-\frac{(m+\not p)g^{\{\rho\sigma} p^\lambda\gamma^{\mu\}}}{(m^2-p^2)^4} \right.$$

$$- \frac{2g^{\{\rho\sigma} p^\lambda p^{\mu\}}}{(m^2-p^2)^4} - 6\frac{(m-\not p)}{(m^2-p^2)^5} \cdot \gamma^{\{\mu} p^\rho p^\sigma p^{\lambda\}}$$

$$- \frac{g^{\{\mu\nu\sigma\lambda\}}}{(m^2-p^2)^3} \Bigg] G_{\mu\nu;\rho\sigma\lambda}, \tag{A25}$$

$$S_F^{6(1)}(0,x) = i\int \frac{d^4p}{(2\pi)^4} e^{-ip\cdot x}\left(-\frac{i}{8} \right)\left\{ \gamma^\tau\gamma^\lambda\gamma^\sigma\gamma^\rho\gamma^\nu \right.$$

$$\times \left[\frac{(m+\not p)\gamma^\mu}{(m^2-p^2)^4} + 4\frac{p^\mu}{(m^2-p^2)^4} \right] + 2\gamma^\lambda\gamma^\rho\gamma^\nu$$

$$\times \left[\frac{3(m+\not p)\gamma^\mu}{(m^2-p^2)^4} g^{\sigma\tau} \right.$$

$$+ 16\frac{(m+\not p)\gamma^\mu}{(m^2-p^2)^5} p^\sigma p^\tau + 4\frac{g^{\mu\sigma} p^\tau + g^{\mu\tau} p^\sigma}{(m^2-p^2)^4} \Bigg] \Bigg\} G_{\lambda\tau} G_{\rho\sigma} G_{\mu\nu}, \tag{A26}$$

$$S_F^{6(2)}(0,x) = i\int \frac{d^4p}{(2\pi)^4} e^{-ip\cdot x}\left(-\frac{1}{8} \right)$$

$$\times \Bigg\{ \gamma^\sigma\left[3g^{\{\lambda\tau}\gamma^{\rho\}}\frac{\gamma^\nu(m+\not p)\gamma^\mu}{(m^2-p^2)^4} \right.$$

$$+ 16\gamma^{\{\rho} p^\lambda p^{\tau\}}\frac{\gamma^\nu(m+\not p)\gamma^\mu}{(m^2-p^2)^5} + 4\frac{g^{\mu\{\lambda} p^\tau\gamma^{\rho\}}\gamma^\nu}{(m^2-p^2)^4} \Bigg]$$

$$+ 4\gamma^\rho\gamma^\mu\left[\frac{m-\not p}{(m^2-p^2)^4} g^{\{\nu\sigma\tau\lambda\}} + 6\frac{m-\not p}{(m^2-p^2)^5} g^{\{\nu\sigma} p^\tau p^{\lambda\}} \right.$$

$$+ 48\frac{m-\not p}{(m^2-p^2)^6} p^\nu p^\sigma p^\tau p^\lambda \Bigg] \Bigg\} G_{\rho\sigma;\lambda\tau} G_{\mu\nu}, \tag{A27}$$

$$S_F^{6(3)}(0,x) = i\int \frac{d^4p}{(2\pi)^4} e^{-ip\cdot x}\left(-\frac{2}{9} \right)\left\{ 3\gamma^\sigma \right.$$

$$\times \left[\gamma^\rho\gamma^\nu\left(2\frac{(m+\not p)\gamma^\mu}{(m^2-p^2)^5} p^\lambda p^\tau \right. \right.$$

$$+ \frac{g^{\{\mu\lambda} p^{\tau\}}}{(m^2-p^2)^4} 4p^\mu p^\lambda p^\tau$$

$$\times \frac{1}{(m^2-p^2)^5} \Bigg) + (\mu \leftrightarrow \lambda) + (\rho \leftrightarrow \tau)$$

$$+ (\mu \leftrightarrow \lambda, \rho \leftrightarrow \tau) \Bigg] + 4\gamma^\rho\gamma^\mu\left[\frac{m-\not p}{(m^2-p^2)^4} \right.$$

Fig. 10 Feynman diagrams for the quark propagator within the background field theory which shall results in operators up to dimension-six. The symbol "×" attached to the gluon line indicates the tensor of the local gluon background field, in which "n" stands for n-th order covariant derivative

$$\times \, g^{(\nu\lambda\sigma\tau)} + 6 \frac{m - \not{p}}{(m^2 - p^2)^5} g^{\{\nu\lambda} p^\sigma p^{\tau\}}$$

$$+ 48 \frac{m - \not{p}}{(m^2 - p^2)^6} p^\nu p^\lambda p^\sigma p^\tau \Bigg] \Bigg\} G_{\rho\sigma;\tau} G_{\mu\nu;\lambda},$$ (A28)

$$S_F^{6(4)}(0, x) = i \int \frac{d^4 p}{(2\pi)^4} e^{-ip\cdot x} \left(-\frac{1}{2} \right) \Bigg\{ \gamma^\rho \gamma^\mu$$

$$\times \Bigg[\frac{m - \not{p}}{(m^2 - p^2)^4} g^{\{\nu\tau\lambda\sigma\}} + 6 \frac{m - \not{p}}{(m^2 - p^2)^5} g^{\{\nu\tau} p^\lambda p^{\sigma\}}$$

$$+ 48 \frac{(m - \not{p}) p^\nu p^\tau p^\lambda p^\sigma}{(m^2 - p^2)^6} \Bigg] + 3 \gamma^\sigma \gamma^\rho \gamma^\nu$$

$$\times \Bigg[\frac{g^{\{\mu\lambda} p^{\tau\}}}{(m^2 - p^2)^4} + \frac{8 p^\mu p^\lambda p^\tau}{(m^2 - p^2)^5} \Bigg] \Bigg\} G_{\rho\sigma} G_{\mu\nu;\lambda\tau},$$ (A29)

$$S_F^{6(5)}(0, x) = i \int \frac{d^4 p}{(2\pi)^4} e^{-ip\cdot x} \Bigg\{ -\frac{i}{18} \gamma^\nu \Bigg[\frac{(m + \not{p}) g^{[\rho\sigma\lambda\tau} \gamma^{\mu]}}{(m^2 - p^2)^4}$$

$$+ 4 \frac{g^{\{\rho\sigma\lambda\tau} p^{\mu\}}}{(m^2 - p^2)^4} + 6 \frac{(m + \not{p})}{(m^2 - p^2)^5}$$

$$\cdot \, g^{\{\rho\sigma} p^\lambda p^\tau \gamma^{\mu\}} + 12 \frac{g^{\{\rho\sigma} p^\lambda p^\tau p^{\mu\}}}{(m^2 - p^2)^5}$$

$$- 48 \frac{p^{\{\rho} p^\sigma p^\lambda p^\tau p^{\mu\}} (m + \not{p})}{(m^2 - p^2)^6} \Bigg] G_{\mu\nu;\rho\sigma\lambda\tau} \Bigg\}.$$ (A30)

where

$$g^{[\mu\nu\rho\sigma} p^{\lambda]} = g^{(\mu\nu\rho\sigma)} p^{\lambda} + g^{(\lambda\nu\rho\sigma)} p^{\mu}$$
$$+ g^{(\mu\lambda\rho\sigma)} p^{\nu} + g^{(\mu\nu\lambda\sigma)} p^{\rho} + g^{(\mu\nu\rho\lambda)} p^{\sigma}, \quad (A31)$$

$$g^{\{\mu\nu} p^{\rho} p^{\sigma} p^{\lambda\}} = g^{\mu\nu} p^{\rho} p^{\sigma} p^{\lambda} + g^{\mu\rho} p^{\nu} p^{\sigma} p^{\lambda}$$
$$+ g^{\mu\sigma} p^{\rho} p^{\nu} p^{\lambda} + g^{\mu\lambda} p^{\rho} p^{\sigma} p^{\nu} + g^{\nu\rho} p^{\mu} p^{\sigma} p^{\lambda}$$
$$+ g^{\nu\sigma} p^{\rho} p^{\mu} p^{\lambda} + g^{\nu\lambda} p^{\rho} p^{\sigma} p^{\mu}$$
$$+ g^{\rho\sigma} p^{\mu} p^{\nu} p^{\lambda} + g^{\rho\lambda} p^{\mu} p^{\sigma} p^{\nu} + g^{\sigma\lambda} p^{\rho} p^{\mu} p^{\nu}, \quad (A32)$$

$$g^{\{\mu\rho} \gamma^{\sigma\}} = g^{\mu\rho} \gamma^{\sigma} + g^{\mu\sigma} \gamma^{\rho} + g^{\rho\sigma} \gamma^{\mu}, \quad (A33)$$

$$g^{[\rho\sigma\lambda\tau} \gamma^{\mu]} = \gamma^{\mu} g^{(\rho\sigma\lambda\tau)}$$
$$+ (\mu \leftrightarrow \rho) + (\mu \leftrightarrow \sigma) + (\mu \leftrightarrow \lambda) + (\mu \leftrightarrow \tau), \quad (A34)$$

$$g^{\{\rho\sigma} p^{\lambda} \gamma^{\mu\}} = \gamma^{\mu} g^{\{\rho\sigma} p^{\lambda\}}$$
$$+ (\mu \leftrightarrow \rho) + (\mu \leftrightarrow \sigma) + (\mu \leftrightarrow \lambda), \quad (A35)$$

$$g^{\{\rho\sigma} p^{\lambda} p^{\tau} \gamma^{\mu\}} = \gamma^{\mu} g^{\{\rho\sigma} p^{\lambda} p^{\tau\}}$$
$$+ (\mu \leftrightarrow \rho) + (\mu \leftrightarrow \sigma) + (\mu \leftrightarrow \lambda) + (\mu \leftrightarrow \tau), \quad (A36)$$

$$\gamma^{\{\mu} p^{\rho} p^{\sigma\}} = \gamma^{\mu} p^{\rho} p^{\sigma}$$
$$+ \gamma^{\rho} p^{\mu} p^{\sigma} + \gamma^{\sigma} p^{\mu} p^{\rho}, \quad (A37)$$

$$\gamma^{\{\mu} p^{\rho} p^{\sigma} p^{\lambda\}} = \gamma^{\mu} p^{\rho} p^{\sigma} p^{\lambda}$$
$$+ (\mu \leftrightarrow \rho) + (\mu \leftrightarrow \sigma) + (\mu \leftrightarrow \lambda), \quad (A38)$$

$$\gamma^{\{\mu} p^{\rho} p^{\sigma} p^{\lambda} p^{\tau\}} = \gamma^{\mu} p^{\rho} p^{\sigma} p^{\lambda} p^{\tau}$$
$$+ (\mu \leftrightarrow \rho) + (\mu \leftrightarrow \sigma) + (\mu \leftrightarrow \lambda) + (\mu \leftrightarrow \tau), \quad (A39)$$

$$g^{\mu\{\lambda} p^{\tau} \gamma^{\rho\}} = g^{\mu\lambda} p^{\tau} \gamma^{\rho} + g^{\mu\tau} p^{\lambda} \gamma^{\rho} + g^{\mu\rho} p^{\tau} \gamma^{\lambda}$$
$$+ g^{\mu\tau} p^{\rho} \gamma^{\lambda} + g^{\mu\rho} p^{\lambda} \gamma^{\tau} + g^{\mu\lambda} p^{\rho} \gamma^{\tau}. \quad (A40)$$

In these expressions, the mass term is retained explicitly, which application not only in the case of light quarks, but also in the case of heavy quarks.

A2. Vertex operator

The vertex operator $(z \cdot \overset{\leftrightarrow}{D})^n$ is encountered when we calculate the distributed amplitude of moment with the SVZ sum rule. Here it is only the dimension $d \leq 6$ terms are retained, vertex operator $(z \cdot \overset{\leftrightarrow}{D})^n$ in dimension-six order, the results are as follows

$$(z \cdot \overset{\leftrightarrow}{D})_0^n = (z \cdot \overset{\leftrightarrow}{\partial})^n, \quad (A41)$$

$$(z \cdot \overset{\leftrightarrow}{D})_2^n = -i(z \cdot \overset{\leftrightarrow}{\partial})^{n-1} \underline{x}^{\mu} z^{\nu} G_{\mu\nu}, \quad (A42)$$

$$(z \cdot \overset{\leftrightarrow}{D})_3^n = -\frac{2i}{3}(z \cdot \overset{\leftrightarrow}{\partial})^{n-1} \underline{x}^{\mu} \underline{x}^{\rho} z^{\nu} G_{\mu\nu;\rho}, \quad (A43)$$

$$(z \cdot \overset{\leftrightarrow}{D})_{4(1)}^n = -\frac{n(n-1)}{2}(z \cdot \overset{\leftrightarrow}{\partial})^{n-2} \underline{x}^{\mu} \underline{x}^{\rho} z^{\nu} z^{\sigma} G_{\mu\nu} G_{\rho\sigma}, \quad (A44)$$

$$(z \cdot \overset{\leftrightarrow}{D})_{4(2)}^n = \Big[-\frac{i}{4} n(z \cdot \overset{\leftrightarrow}{\partial})^{n-2} \underline{x}^{\mu} \underline{x}^{\rho} \underline{x}^{\sigma}$$

$$-\frac{i}{12}(n-1)(n-2)(z \cdot \overset{\leftrightarrow}{\partial})^{n-3} \underline{x}^{\mu} z^{\rho} z^{\sigma} z^{\nu} \Big]$$
$$\times G_{\mu\nu;\rho\sigma}, \quad (A45)$$

$$(z \cdot \overset{\leftrightarrow}{D})_{5(1)}^n = -\frac{n(n-1)}{3}(z \cdot \overset{\leftrightarrow}{\partial})^{n-2} \underline{x}^{\mu} \underline{x}^{\rho} \underline{x}^{\sigma} \underline{x}^{\lambda} z^{\nu} z^{\sigma}$$
$$\times G_{\mu\nu} G_{\rho\sigma;\lambda}, \quad (A46)$$

$$(z \cdot \overset{\leftrightarrow}{D})_{5(2)}^n = -\frac{n(n-1)}{3}(z \cdot \overset{\leftrightarrow}{\partial})^{n-2} \underline{x}^{\mu} \underline{x}^{\rho} \underline{x}^{\sigma} \underline{x}^{\lambda} z^{\nu} z^{\sigma}$$
$$\times G_{\mu\nu;\lambda} G_{\rho\sigma}, \quad (A47)$$

$$(z \cdot \overset{\leftrightarrow}{D})_{5(3)}^n = \Big[-\frac{i}{15} n(z \cdot \overset{\leftrightarrow}{\partial})^{n-1} \underline{x}^{\mu} \underline{x}^{\rho} \underline{x}^{\sigma} \underline{x}^{\lambda} z^{\nu}$$

$$-\frac{i}{45} n(n-1)(n-2)(z \cdot \overset{\leftrightarrow}{\partial})^{n-2} \underline{x}^{\mu} (\underline{x}^{\rho} z^{\sigma} z^{\lambda}$$
$$+ \underline{x}^{\sigma} z^{\rho} z^{\lambda} + \underline{x}^{\lambda} z^{\sigma} z^{\rho}) z^{\nu} \Big] G_{\mu\nu;\rho\sigma\lambda}, \quad (A48)$$

$$(z \cdot \overset{\leftrightarrow}{D})_{6(1)}^n = \frac{i}{6} n(n-1)(n-2)(z \cdot \overset{\leftrightarrow}{\partial})^{n-3} \underline{x}^{\mu}$$
$$\times \underline{x}^{\rho} \underline{x}^{\lambda} z^{\nu} z^{\sigma} z^{\tau} G_{\mu\nu} G_{\rho\sigma} G_{\lambda\tau}, \quad (A49)$$
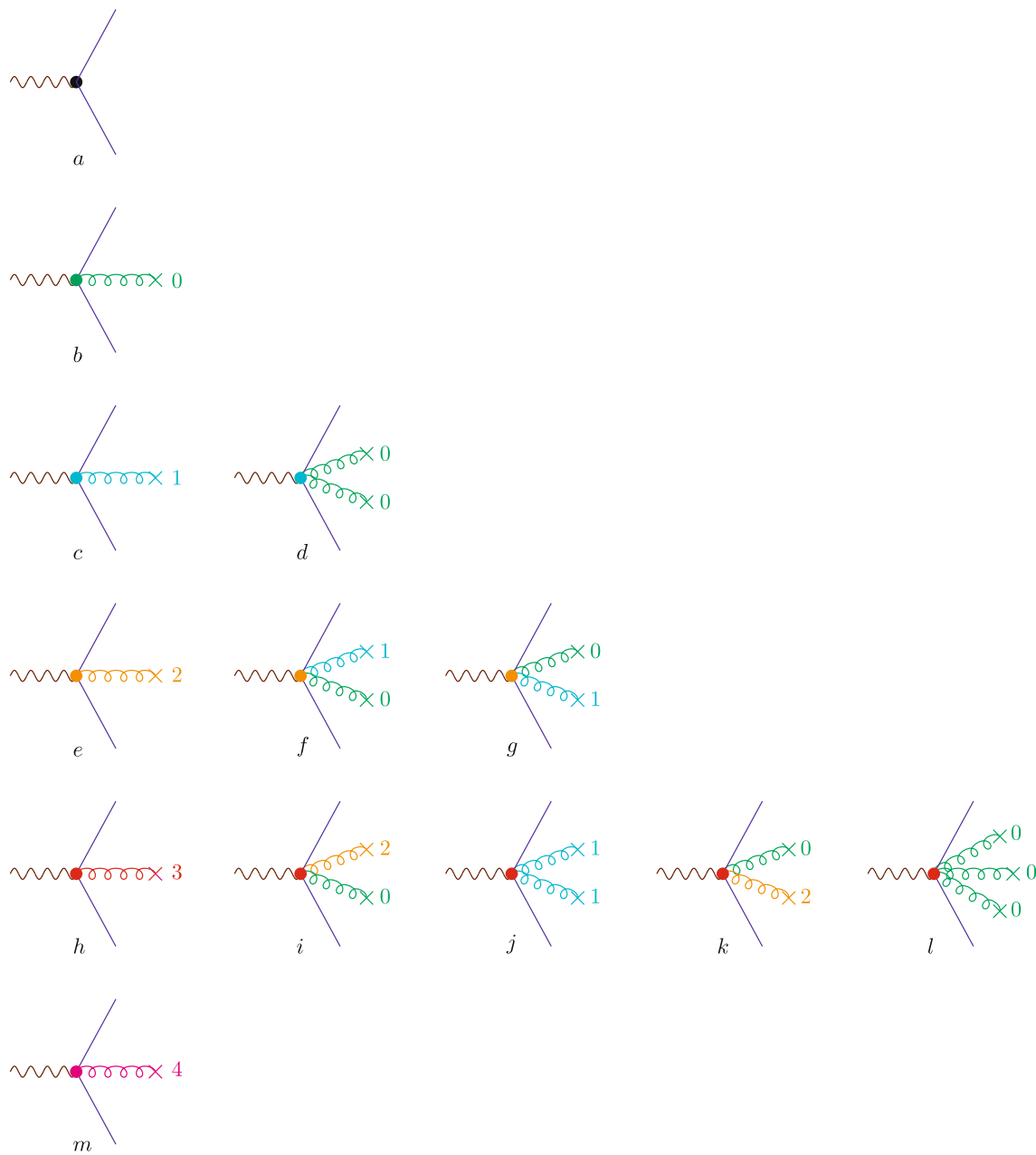
$$(z \cdot \overset{\leftrightarrow}{D})_{6(2)}^n = \Big[-\frac{n(n-1)}{8}(z \cdot \overset{\leftrightarrow}{\partial})^{n-2} \underline{x}^{\mu} \underline{x}^{\rho} \underline{x}^{\lambda} \underline{x}^{\tau} z^{\nu} z^{\sigma}$$

$$-\frac{1}{12} n(n-1)(n-2)(n-3)(z \cdot \overset{\leftrightarrow}{\partial})^{n-4}$$
$$\times \underline{x}^{\mu} \underline{x}^{\rho} z^{\lambda} z^{\tau} z^{\nu} z^{\sigma} \Big] G_{\mu\nu} G_{\rho\sigma;\lambda\tau}, \quad (A50)$$

$$(z \cdot \overset{\leftrightarrow}{D})_{6(3)}^n = -\frac{2}{9} n(n-1)(z \cdot \overset{\leftrightarrow}{\partial})^{n-2} \underline{x}^{\mu}$$
$$\times \underline{x}^{\rho} \underline{x}^{\lambda} \underline{x}^{\tau} z^{\nu} z^{\sigma} G_{\mu\nu;\lambda} G_{\rho\sigma;\tau},$$

$$(z \cdot \overset{\leftrightarrow}{D})_{6(4)}^n = -\frac{n(n-1)}{8}(z \cdot \overset{\leftrightarrow}{\partial})^{n-2} \underline{x}^{\mu}$$
$$\times \underline{x}^{\rho} \underline{x}^{\lambda} \underline{x}^{\tau} z^{\nu} z^{\sigma} G_{\mu\nu;\lambda\tau} G_{\rho\sigma}, \quad (A51)$$

$$(z \cdot \overset{\leftrightarrow}{D})_{6(5)}^n = \Big[-\frac{i}{72} \times (z \cdot \overset{\leftrightarrow}{\partial})^{n-1} \underline{x}^{\mu} \underline{x}^{\rho} \underline{x}^{\lambda} \underline{x}^{\tau} z^{\nu}$$

$$-\frac{i}{216} n(n-1)(n-2)(z \cdot \overset{\leftrightarrow}{\partial})^{n-3} \underline{x}^{\mu}$$
$$\times \Big(z^{\rho} z^{\sigma} \underline{x}^{\lambda} \underline{x}^{\tau} + z^{\rho} \underline{x}^{\sigma} z^{\lambda} \underline{x}^{\tau} + z^{\rho} \underline{x}^{\sigma} \underline{x}^{\tau} z^{\tau}$$
$$+ \underline{x}^{\rho} z^{\sigma} z^{\lambda} \underline{x}^{\tau} + \underline{x}^{\rho} z^{\sigma} \underline{x}^{\lambda} z^{\tau}$$
$$+ \underline{x}^{\rho} \underline{x}^{\sigma} z^{\lambda} z^{\tau} \Big) z^{\nu} - \frac{i}{360} n(n-1)$$
$$\times (n-2)(n-3)(n-4)(z \cdot \overset{\leftrightarrow}{\partial})^{n-5} \underline{x}^{\mu} z^{\rho} z^{\sigma}$$
$$\times z^{\lambda} z^{\tau} z^{\nu} \Big] G_{\mu\nu;\lambda\tau\rho\sigma}. \quad (A52)$$

where the subscript $k(m)$ with $k = (1, \ldots, 6)$ stands for the dimension of the operator, in which (m) stands for the m-th type of the operator with same dimension. For example, there is two type of dimension four operators, three type of dimension five operators and five type of dimension-six

Fig. 11 Feynman diagrams for the vertex operator $\Gamma(z \cdot \overset{\leftrightarrow}{D})^n$ under the background field theory up to dimension-six. The symbol "×" attached to the gluon line indicates the tensor of the local gluon background field, in which "n" stands for n-th order covariant derivative

operators. Figure 11 represents the Feynman diagrams for the vertex operator $\Gamma(z \cdot \overset{\leftrightarrow}{D})^n$ under the background field theory, where thirteen figures, i.e. Fig. 11a–m, correspond to $\Gamma(z \cdot \overset{\leftrightarrow}{D})_1^n, \ldots, \Gamma(z \cdot \overset{\leftrightarrow}{D})_{6(5)}^n$, respectively. The symbol "×" attached to the gluon line indicates the tensor of the local gluon background field with "n" stands for the n-th order covariant derivative.

A3. Vacuum matrix elements

In addition to quark propagators $S_F(x, 0)$ and vertex operators $(z \cdot \overset{\leftrightarrow}{D})^n$, one may also encounter vacuum condensation in the process of calculation, which are the basic input parameter. The specific expression for vacuum matrix element in the D-dimension space have the following forms,

$$\langle 0|G_{\mu\nu}^a G_{\rho\sigma}^b|0\rangle = \frac{1}{96}\delta^{ab}\langle G^2\rangle[g_{\mu\rho}g_{\nu\sigma} - (\sigma \leftrightarrow \rho)],$$
(A53)

$$\text{Tr}\langle 0|G_{\mu\nu}G_{\rho\sigma}|0\rangle = \frac{\pi}{6}\langle \alpha_s G^2\rangle[g_{\mu\rho}g_{\nu\sigma} - (\sigma \leftrightarrow \rho)],$$
(A54)

$$\langle 0|G_{\mu\nu;\lambda}^a G_{\rho\sigma;\tau}^b|0\rangle = -\frac{1}{648}\sum_{u,d,s}\delta^{ab}\langle g_s\bar{\psi}\psi\rangle^2$$

$$\times [2g_{\lambda\tau}(g_{\mu\rho}g_{\nu\sigma} - g_{\mu\sigma}g_{\nu\rho})$$
$$+ g_{\lambda\rho}(g_{\tau\mu}g_{\sigma\nu} - g_{\tau\nu}g_{\sigma\mu}) - g_{\lambda\sigma}(g_{\tau\mu}g_{\rho\nu} - g_{\tau\nu}g_{\rho\mu})],$$
(A55)

$$\text{Tr}\langle 0|G_{\mu\nu;\lambda}G_{\rho\sigma;\tau}|0\rangle = -\frac{1}{162}\sum_{u,d,s}\langle g_s^2\bar{\psi}\psi\rangle^2$$

$$\times [2g_{\lambda\tau}(g_{\mu\rho}g_{\nu\sigma} - g_{\mu\sigma}g_{\nu\rho})$$
$$+ g_{\lambda\rho}(g_{\tau\mu}g_{\sigma\nu} - g_{\tau\nu}g_{\sigma\mu}) - g_{\lambda\sigma}(g_{\tau\mu}g_{\rho\nu} - g_{\tau\nu}g_{\rho\mu})],$$
(A56)

$$\langle 0|G_{\mu\nu}^a G_{\rho\sigma}^b G_{\lambda\tau}^c|0\rangle$$
$$= \frac{1}{576}f^{abc}\langle G^a G^b G^c\rangle\{[g_{\mu\rho}(g_{\nu\lambda}g_{\sigma\tau} - g_{\nu\tau}g_{\sigma\lambda})$$
$$- g_{\mu\sigma}(g_{\nu\lambda}g_{\rho\tau} - g_{\nu\tau}g_{\rho\lambda})] - (\mu \leftrightarrow \nu)\},$$
(A57)

$$\text{Tr}\langle 0|G_{\mu\nu}G_{\rho\sigma}G_{\lambda\tau}|0\rangle$$
$$= \frac{i}{96}\langle g_s^3 f G^3\rangle\{[g_{\mu\rho}(g_{\nu\lambda}g_{\sigma\tau} - g_{\nu\tau}g_{\sigma\lambda})$$
$$- g_{\mu\sigma}(g_{\nu\lambda}g_{\rho\tau} - g_{\nu\tau}g_{\rho\lambda})] - (\mu \leftrightarrow \nu)\},$$
(A58)

$$\langle 0|G_{\mu\nu}^a G_{\rho\sigma;\lambda\tau}^b|0\rangle = \delta^{ab}$$
$$\times \left\{\left(-\frac{1}{1296}\sum_{u,d,s}\langle g_s\bar{\psi}\psi\rangle^2 - \frac{1}{384}\langle g_s f G^3\rangle\right)\right.$$
$$\times [2g_{\lambda\tau}(g_{\mu\sigma}g_{\nu\rho} - g_{\mu\rho}g_{\nu\sigma})$$
$$+ g_{\rho\tau}(g_{\mu\sigma}g_{\nu\lambda} - g_{\mu\lambda}g_{\nu\sigma})$$
$$- g_{\sigma\tau}(g_{\mu\lambda}g_{\nu\rho} - g_{\mu\rho}g_{\nu\lambda})]$$
$$+ \left(-\frac{1}{1296}\sum_{u,d,s}\langle g_s\bar{\psi}\psi\rangle^2 + \frac{1}{384}\langle g_s f G^3\rangle\right)$$
$$\left. \times [g_{\mu\tau}(g_{\rho\nu}g_{\sigma\lambda} - g_{\rho\lambda}g_{\nu\sigma}) + (\mu \leftrightarrow \nu)]\right\},$$
(A59)

$$\text{Tr}\langle 0|G_{\mu\nu}G_{\rho\sigma;\lambda\tau}|0\rangle = 4\left(-\frac{1}{1296}g_s^2\sum_{u,d,s}\langle g_s\bar{\psi}\psi\rangle^2\right.$$
$$\left. -\frac{1}{384}\langle g_s^3 f G^3\rangle\right)$$
$$\times [2g_{\lambda\tau}(g_{\mu\sigma}g_{\nu\rho} - g_{\mu\rho}g_{\nu\sigma})$$
$$+ g_{\rho\tau}(g_{\mu\sigma}g_{\nu\lambda} - g_{\mu\lambda}g_{\nu\sigma})$$
$$- g_{\sigma\tau}(g_{\mu\lambda}g_{\nu\rho} - g_{\mu\rho}g_{\nu\lambda})]$$
$$+ 4\left(-\frac{1}{1296}g_s^2\sum_{u,d,s}\langle g_s\bar{\psi}\psi\rangle^2 + \frac{1}{384}\langle g_s^3 f G^3\rangle\right)$$
$$\times [g_{\mu\tau}(g_{\rho\nu}g_{\sigma\lambda} - g_{\rho\lambda}g_{\nu\sigma}) + (\mu \leftrightarrow \nu)],$$
(A60)

$$\langle 0|\bar{\psi}_\alpha^a(x)\psi_\beta^b(y)|0\rangle = \delta^{ab}\left\{\langle\bar{\psi}\psi\rangle\right.$$

$$\times \left[\frac{1}{12}g_{\beta\alpha} + \frac{im_s}{48}(\not{x} - \not{y})_{\beta\alpha} - \frac{m_s^2}{96}(x-y)^2 g_{\beta\alpha}\right.$$
$$\left. -\frac{im_s^3}{576}(x-y)^2(\not{x} - \not{y})_{\beta\alpha}\right]$$
$$+ g_s\langle\bar{\psi}TG\psi\rangle\left[\frac{1}{192}(x-y)^2 g_{\beta\alpha}\right.$$
$$\left.\left. +\frac{im_s}{864}(x-y)^2(\not{x} - \not{y})_{\beta\alpha}\right]\right\}$$
(A61)

$$\langle 0|\bar{\psi}_\alpha^a(x)\psi_\beta^b(y)G_{\mu\nu}^A|0\rangle$$
$$= \frac{1}{192}\langle\bar{\psi}TG\psi\rangle(\sigma_{\mu\nu})_{\beta\alpha}(T^A)^{ba} + \left\{-\frac{1}{864}g_s\langle\bar{\psi}\psi\rangle^2\right.$$
$$\times (g_{\mu\rho}\gamma_\nu - g_{\nu\rho}\gamma_\mu)_{\beta\alpha}(x+y)^\rho$$
$$+ i(x-y)^\rho\left[\frac{1}{864}g_s\langle\bar{\psi}\psi\rangle^2\right.$$
$$\left.\left. +\frac{m_s}{384}\langle\bar{\psi}TG\psi\rangle\right](\epsilon_{\rho\mu\nu\sigma}\gamma_5\gamma^\sigma)_{\beta\alpha}\right\}(T^A)^{ba}$$
(A62)

$$\langle 0|\bar{\psi}_\alpha^a(0)\psi_\beta^b(0)G_{\mu\nu;\rho}^A|0\rangle$$
$$= \frac{1}{432}g_s\langle\bar{\psi}\psi\rangle^2(g_{\mu\rho}\gamma_\nu - g_{\nu\rho}\gamma_\mu)_{\beta\alpha}(T^A)^{ba}$$
(A63)

the symbol "Tr" stands for tracing to the colour matrixes. Obviously,

$$\langle 0|G_{\rho\sigma;\lambda\tau}^B G_{\mu\nu}^A|0\rangle = \langle 0|G_{\mu\nu}^A G_{\rho\sigma;\lambda\tau}^B|0\rangle.$$
(A64)

As a final remark, by making use of the equation

$$[\tilde{D}_\mu, \tilde{D}_\nu]^{AB} = -g_s f^{ABC}G_{\mu\nu}^C,$$
(A65)

we can obtain a useful relation

$$\langle g_s^3 f G^3\rangle = \frac{8}{27}\sum_{u,d,s}\langle g_s^2\bar{\psi}\psi\rangle^2.$$
(A66)

which, can also be referred to our previous work [60].

Appendix B: Detailed expressions for $I_{m_s^0}(n, M^2)$ and $I_{m_s^2}(n, M^2)$ in BFTSR for $\langle\xi_{2;\eta^{(\prime)}}^n\rangle|_\mu$

According to the Feynman rule, we can obtain the following detailed expressions within $I_{m_s^0}(n, M^2)$ and $I_{m_s^2}(n, M^2)$ for the final BFTSR, i.e. Eq. (33). Some of the terms have the symmetric structure, we can combined these terms together. Here, we only list the key expression for the last step of the BFTSR. Firstly, we give the $I_{m_s^0}(n, M^2)$ terms which are expressed as,

$$\hat{\mathcal{B}}_{M^2}I_{000} = \frac{3}{8\pi^2}\frac{1 + (-1)^n}{(n+1)(n+3)},$$
(B1)

$$\hat{\mathcal{B}}_{M^2}I_{006+600} = \frac{g_s^2\sum\langle g_s\bar{q}q\rangle^2}{M^6}[1 + (-1)^n]\frac{-17}{324\pi^2}$$

$$\times \left\{ \left[(2n+1)\left(-\ln\frac{M^2}{\mu^2}\right) - (n+2) \right] \right.$$
$$+ \theta(n-2)\left[\frac{1}{2}(2n+1)\left(\psi\left(\frac{n+1}{2}\right)\right. \right.$$
$$\left. \left. \left. - \psi\left(\frac{n}{2}\right) + \ln 4\right) - \frac{(n+1)^2}{n} \right] \right\}, \tag{B2}$$

$$\hat{\mathcal{B}}_{M^2} I_{024+420} = \frac{g_s^2 \sum\langle g_s\bar{q}q\rangle^2}{M^6}[1+(-1)^n]$$
$$\times \frac{-1}{162\pi^2}\theta(n-2)\left\{ n\left(-\ln\frac{M^2}{\mu^2}\right) + \left[\frac{n}{2}\left(\psi\left(\frac{n+1}{2}\right)\right.\right.\right.$$
$$\left.\left.\left. - \psi\left(\frac{n}{2}\right) + \ln 4\right) - 1\right] \right\}, \tag{B3}$$

$$\hat{\mathcal{B}}_{M^2} I_{033+330} = \frac{g_s^2 \sum\langle g_s\bar{q}q\rangle^2}{M^6}[1+(-1)^n]$$
$$\times \frac{2}{243\pi^2}\theta(n-2)\left\{ n\left(-\ln\frac{M^2}{\mu^2} - \frac{1}{2}\right) + \left[\frac{n}{2}\right.\right.$$
$$\left.\left. \times \left(\psi\left(\frac{n+1}{2}\right) - \psi\left(\frac{n}{2}\right) + \ln 4\right) - 1\right] \right\}, \tag{B4}$$

$$\hat{\mathcal{B}}_{M^2} I_{202+040} = \frac{\langle\alpha_s G^2\rangle}{M^4}\frac{1+n\theta(n-2)}{24\pi(n+1)}[1+(-1)^n], \tag{B5}$$

$$\hat{\mathcal{B}}_{M^2} I_{060} = \frac{16g_s^2 \sum\langle g_s\bar{q}q\rangle^2 - 81\langle g_s^3 fG^3\rangle}{M^6}$$
$$\times \frac{n}{7776\pi^2}[1+(-1)^n]\theta(n-2), \tag{B6}$$

$$\hat{\mathcal{B}}_{M^2} I_{204+402} = \frac{g_s^2 \sum\langle g_s\bar{q}q\rangle^2}{M^6}[1+(-1)^n]$$
$$\times \frac{1}{324\pi^2}\left\{ \left(-\ln\frac{M^2}{\mu^2}\right) + \theta(n-2)\right.$$
$$\times \left[\frac{1}{2}\left(\psi\left(\frac{n+1}{2}\right)\right.\right.$$
$$\left.\left.\left. - \psi\left(\frac{n}{2}\right) + \ln 4\right) - \frac{1}{n}\right] \right\}, \tag{B7}$$

$$\hat{\mathcal{B}}_{M^2} I_{303(1)+303(3)} = \frac{g_s^2 \sum\langle g_s\bar{q}q\rangle^2}{M^6}[1+(-1)^n]$$
$$\times \frac{-2}{243\pi^2}\left\{ \left(-\ln\frac{M^2}{\mu^2}\right) + \theta(n-2)\left[\frac{1}{2}\right.\right.$$
$$\left.\left. \times \left(\psi\left(\frac{n+1}{2}\right) - \psi\left(\frac{n}{2}\right) + \ln 4\right) - \frac{1}{n}\right] \right\}, \tag{B8}$$

$$\hat{\mathcal{B}}_{M^2} I_{303(2)} = \frac{g_s^2 \sum\langle g_s\bar{q}q\rangle^2}{M^6}[1+(-1)^n]\frac{1}{162\pi^2}$$
$$\times \left\{ \left(-\ln\frac{M^2}{\mu^2} + \frac{1}{2}\right) + \frac{\theta(n-2)}{2}\left(\psi\left(\frac{n+1}{2}\right)\right.\right.$$
$$\left.\left. - \psi\left(\frac{n}{2}\right) + \ln 4\right) \right\}. \tag{B9}$$

In which, the subscript a, b, c, m in $\hat{\mathcal{B}}_{M^2} I_{abc(m)}$ for Eqs. (B1)–(B9) have the meaning that, a, b, c stand for a, b, cth-order of the propagator, vertex and propagator, while m means the mth terms of $I_{abc}^{m_s^2}$. Then, we give the expression for $I_{m_s^2}(n, M^2)$ terms separately,

$$\hat{\mathcal{B}}_{M^2} I_{004+400}^{m_s^2} = \frac{\langle\alpha_s G^2\rangle}{M^6}m_s^2\frac{-1}{12\pi}[1+(-1)^n]$$

$$\times \left\{ \left[(2n+1)\left(-\ln\frac{M^2}{\mu^2} + \psi(n+1) + 2\gamma_E\right) - n \right.\right.$$
$$\left. - 2 \right] + \theta(n-2)\left[\frac{2n+1}{2}\left(\psi\left(\frac{n+1}{2}\right)\right.\right.$$
$$\left.\left.\left. - \psi\left(\frac{n}{2}\right) + \ln 4\right) - \frac{(n+1)^2}{n}\right] \right\}, \tag{B10}$$

$$\hat{\mathcal{B}}_{M^2} I_{006(1)+600(1)}^{m_s^2} = \frac{\langle g_s^2\bar{q}q\rangle^2}{M^8}m_s^2$$
$$\times \frac{17}{324\pi^2}[1+(-1)^n]\left\{ \delta^{n0} + 2n\left(-\ln\frac{M^2}{\mu^2} + \psi(n+1) + 2\gamma_E\right)\right.$$
$$- n - 3 + \theta(n-2)$$
$$\left. \times \left[n\left(\psi\left(\frac{n+1}{2}\right) - \psi\left(\frac{n}{2}\right) + \ln 4\right) - (n+1) \right] \right\}, \tag{B11}$$

$$\hat{\mathcal{B}}_{M^2} I_{006(2)+600(2)}^{m_s^2} = \frac{8\langle g_s^2\bar{q}q\rangle^2 - 3\langle g_s^3 fG^3\rangle}{M^8}m_s^2\frac{1}{144\pi^2}[1+(-1)^n]$$
$$\times \left\{ \frac{1}{2}\delta^{n0} - \left[2n^2\left(-\ln\frac{M^2}{\mu^2}\right.\right.\right.$$
$$\left.\left. + \psi(n+1) + 2\gamma_E\right) - \frac{7n^2 + 19n + 2}{4}\right]\right\}$$
$$+ \left\{ \theta(n-3)\left[-n^2\left(\psi\left(\frac{n+1}{2}\right)\right.\right.\right.$$
$$\left.\left.\left. - \psi\left(\frac{n}{2}\right) + \frac{1}{4}(5n^2 + 5n + 2)\right] \right\}, \tag{B12}$$

$$\hat{\mathcal{B}}_{M^2} I_{024(1)+420(1)}^{m_s^2} = \frac{\langle g_s^2\bar{q}q\rangle^2}{M^8}m_s^2$$
$$\times \frac{n}{162\pi^2}[1+(-1)^n]\left\{ \theta(n-1)\left(-\ln\frac{M^2}{\mu^2} + \psi(n+1) + 2\gamma_E\right.\right.$$
$$\left.\left. - \frac{1}{n}\right) + \frac{1}{2}\theta(n-2)\left[\psi\left(\frac{n+1}{2}\right) - \psi\left(\frac{n}{2}\right) + \ln 4\right] \right\}, \tag{B13}$$

$$\hat{\mathcal{B}}_{M^2} I_{024(2)+420(2)}^{m_s^2} = \frac{8\langle g_s^2\bar{q}q\rangle^2 - 27\langle g_s^3 fG^3\rangle}{M^8}m_s^2$$
$$\times \frac{-n}{3888\pi^2}[1+(-1)^n]\left\{ \theta(n-1)\left[(2n-1)\right.\right.$$
$$\times \left.\left(-\ln\frac{M^2}{\mu^2} + \psi(n+1) + 2\gamma_E\right) - n - 3 + \frac{1}{n}\right]$$
$$+ \theta(n-3)\left[\frac{2n-1}{2}\right.$$
$$\left.\left. \times \left(\psi\left(\frac{n+1}{2}\right) - \psi\left(\frac{n}{2}\right) + \ln 4\right) - (n+1)\right] \right\}, \tag{B14}$$

$$\hat{\mathcal{B}}_{M^2} I_{033(1)+330(1)}^{m_s^2} = \frac{\langle g_s^2\bar{q}q\rangle^2}{M^8}m_s^2$$
$$\times \frac{-2n}{243\pi^2}[1+(-1)^n]\left\{ \theta(n-1)\left[(2n-1)\left(-\ln\frac{M^2}{\mu^2} + \psi(n+1)\right.\right.\right.$$
$$\left.\left. + 2\gamma_E\right) - n - 3 + \frac{1}{n}\right] + \theta(n-3)\left[\frac{2n-1}{2}\right.$$
$$\times \left(\psi\left(\frac{n+1}{2}\right) - \psi\left(\frac{n}{2}\right) + \ln 4\right)$$
$$\left.\left. - (n+1)\right] \right\}, \tag{B15}$$

$$\hat{\mathcal{B}}_{M^2} I_{033(2,1)+330(2,1)}^{m_s^2} = \frac{\langle g_s^2\bar{q}q\rangle^2}{M^8}m_s^2\frac{-[1+(-1)^n]2n^2\theta(n-1)}{243\pi^2}, \tag{B16}$$

$$\hat{\mathcal{B}}_{M^2} I^{m_s^2}_{033(2,2)+330(2,2)} = \frac{\langle g_s^2 \bar{q}q \rangle^2}{M^8} m_s^2$$

$$\times \frac{2n}{243\pi^2} [1 + (-1)^n] \left\{ \theta(n-1) \left[(2n-1) \left(-\ln\frac{M^2}{\mu^2} \right. \right. \right.$$

$$\left. + \psi(n+1) + 2\gamma_E \right) + n - 3 + \frac{1}{n} \right]$$

$$+ \theta(n-3) \left[\frac{2n-1}{2} \left(\psi\left(\frac{n+1}{2}\right) \right. \right.$$

$$\left. \left. \left. - \psi\left(\frac{n}{2}\right) + \ln 4 \right) - (n+1) \right] \right\}, \tag{B17}$$

$$\hat{\mathcal{B}}_{M^2} I^{m_s^2}_{033(3,1)+330(3,1)} = \frac{\langle g_s^2 \bar{q}q \rangle^2}{M^8} m_s^2 \frac{[1 + (-1)^n] n\theta(n-1)}{243\pi^2}, \tag{B18}$$

$$\hat{\mathcal{B}}_{M^2} I^{m_s^2}_{033(3,2)+330(3,2)} = \frac{\langle g_s^2 \bar{q}q \rangle^2}{M^8} m_s^2$$

$$\times \frac{-2n}{243\pi^2} [1 + (-1)^n] \left\{ \theta(n-1) \left(-\ln\frac{M^2}{\mu^2} + \psi(n+1) \right. \right.$$

$$\left. \left. + 2\gamma_E - \frac{1}{n} \right) + \frac{1}{2}\theta(n-2) \left[\psi\left(\frac{n+1}{2}\right) - \psi\left(\frac{n}{2}\right) + \ln 4 \right] \right\}, \tag{B19}$$

$$\hat{\mathcal{B}}_{M^2} I^{m_s^2}_{040(1)+040(2)} = \frac{\langle \alpha_s G^2 \rangle}{(m^2)^3} m_s^2 \frac{-[1 + (-1)^n] n\theta(n-2)}{12\pi}, \tag{B20}$$

$$\hat{\mathcal{B}}_{M^2} I^{m_s^2}_{060(1)+060(2)}$$
$$= \frac{16\langle g_s^2 \bar{q}q \rangle^2 - 81\langle g_s^3 f G^3 \rangle}{M^8} m_s^2 \frac{-[1 + (-1)^n] n\theta(n-2)}{3888\pi^2}, \tag{B21}$$

$$\hat{\mathcal{B}}_{M^2} I^{m_s^2}_{202(1)+202(2)} = \frac{\langle \alpha_s G^2 \rangle}{(m^2)^3} m_s^2 \frac{1}{12\pi} [1 + (-1)^n]$$

$$\times \left\{ \left(-\ln\frac{M^2}{\mu^2} + \psi(n+1) + 2\gamma_E \right) + \theta(n-1) \right.$$

$$\left. \times \frac{1}{2} \left[\psi\left(\frac{n+1}{2}\right) - \psi\left(\frac{n}{2}\right) + \ln 4 - \frac{2}{n} \right] \right\}, \tag{B22}$$

$$\hat{\mathcal{B}}_{M^2} I^{m_s^2}_{204(1)} = \frac{\langle g_s^2 \bar{q}q \rangle^2}{M^8} m_s^2 \frac{1}{324\pi^2} [1 + (-1)^n]$$

$$\times \left\{ -\left(-\ln\frac{M^2}{\mu^2} + \psi(n+1) + 2\gamma_E \right) + \frac{\theta(n-1)}{n} \right.$$

$$\left. - \theta(n-2)\frac{1}{2} \left[\psi\left(\frac{n+1}{2}\right) - \psi\left(\frac{n}{2}\right) + \ln 4 \right] \right\}, \tag{B23}$$

$$\hat{\mathcal{B}}_{M^2} I^{m_s^2}_{402(1)} = \frac{\langle g_s^2 \bar{q}q \rangle^2}{M^8} m_s^2 \frac{1}{324\pi^2} [1 + (-1)^n]$$

$$\times \left\{ -\left(-\ln\frac{M^2}{\mu^2} + \psi(n+1) + 2\gamma_E \right) + \frac{\theta(n-1)}{n} \right.$$

$$\left. - \theta(n-2)\frac{1}{2} \left[\psi\left(\frac{n+1}{2}\right) - \psi\left(\frac{n}{2}\right) + \ln 4 \right] \right\}, \tag{B24}$$

$$\hat{\mathcal{B}}_{M^2} I^{m_s^2}_{204(2)} = \frac{\langle g_s^2 \bar{q}q \rangle^2}{M^8} m_s^2 \frac{1}{243\pi^2} [1 + (-1)^n]$$

$$\times \left\{ -\left(-\ln\frac{M^2}{\mu^2} + \psi(n+1) + 2\gamma_E \right) + \frac{\theta(n-1)}{n} \right.$$

$$\left. - \theta(n-2)\frac{1}{2} \left[\psi\left(\frac{n+1}{2}\right) - \psi\left(\frac{n}{2}\right) + \ln 4 \right] \right\}, \tag{B25}$$

$$\hat{\mathcal{B}}_{M^2} I^{m_s^2}_{402(2)} = \frac{\langle g_s^2 \bar{q}q \rangle^2}{M^8} m_s^2 \frac{1}{243\pi^2} [1 + (-1)^n]$$

$$\times \left\{ -\left(-\ln\frac{M^2}{\mu^2} + \psi(n+1) + 2\gamma_E \right) + \frac{\theta(n-1)}{n} \right.$$

$$\left. - \theta(n-2)\frac{1}{2} \left[\psi\left(\frac{n+1}{2}\right) - \psi\left(\frac{n}{2}\right) + \ln 4 \right] \right\}, \tag{B26}$$

$$\hat{\mathcal{B}}_{M^2} I^{m_s^2}_{204(3)+402(3)} = \frac{4\langle g_s^2 \bar{q}q \rangle^2 - 27\langle g_s^3 f G^3 \rangle}{M^8}$$

$$\times m_s^2 \frac{1}{3888\pi^2} [1 + (-1)^n] \left\{ \delta^{n0} + 2n \left(-\ln\frac{M^2}{\mu^2} \right. \right.$$

$$\left. + \psi(n+1) + 2\gamma_E \right) - n - 3 + \theta(n-2)$$

$$\times \left[n \left(\psi\left(\frac{n+1}{2}\right) - \psi\left(\frac{n}{2}\right) + \ln 4 \right) \right.$$

$$\left. \left. - (n+1) \right] \right\}, \tag{B27}$$

$$\hat{\mathcal{B}}_{M^2} I^{m_s^2}_{303(1)+303(2)} = \frac{\langle g_s^2 \bar{q}q \rangle^2}{M^8} m_s^2$$

$$\times \frac{-5}{486\pi^2} [1 + (-1)^n] \left\{ \delta^{n0} + 2n \left(-\ln\frac{M^2}{\mu^2} + \psi(n+1) + 2\gamma_E \right) \right.$$

$$- n - 3 + \theta(n-2)$$

$$\left. \times \left[n \left(\psi\left(\frac{n+1}{2}\right) - \psi\left(\frac{n}{2}\right) + \ln 4 \right) - (n+1) \right] \right\}, \tag{B28}$$

$$\hat{\mathcal{B}}_{M^2} I^{m_s^2}_{303(3)+303(4)} = \frac{\langle g_s^2 \bar{q}q \rangle^2}{M^8} m_s^2$$

$$\times \frac{-1}{81\pi^2} [1 + (-1)^n] \left\{ \delta^{n0} + 2n \left(-\ln\frac{M^2}{\mu^2} + \psi(n+1) + 2\gamma_E \right) \right.$$

$$- n - 3 + \theta(n-2)$$

$$\left. \times \left[n \left(\psi\left(\frac{n+1}{2}\right) - \psi\left(\frac{n}{2}\right) + \ln 4 \right) - (n+1) \right] \right\}, \tag{B29}$$

$$\hat{\mathcal{B}}_{M^2} I^{m_s^2}_{303(5)} = \frac{\langle g_s^2 \bar{q}q \rangle^2}{M^8} m_s^2$$

$$\times \frac{-2}{243\pi^2} [1 + (-1)^n] \left\{ -\left(-\ln\frac{M^2}{\mu^2} + \psi(n+1) + 2\gamma_E \right) \right.$$

$$+ \frac{\theta(n-1)}{n}$$

$$\left. - \theta(n-2)\frac{1}{2} \left[\psi\left(\frac{n+1}{2}\right) - \psi\left(\frac{n}{2}\right) + \ln 4 \right] \right\}, \tag{B30}$$

$$\hat{\mathcal{B}}_{M^2} I^{m_s^2}_{303(6)} = \frac{\langle g_s^2 \bar{q}q \rangle^2}{M^8} m_s^2 \frac{-2}{243\pi^2} [1 + (-1)^n]$$

$$\times \left\{ -\left(-\ln\frac{M^2}{\mu^2} + \psi(n+1) + 2\gamma_E \right) + \frac{\theta(n-1)}{n} \right.$$

$$\left. - \theta(n-2)\frac{1}{2} \left[\psi\left(\frac{n+1}{2}\right) - \psi\left(\frac{n}{2}\right) + \ln 4 \right] \right\}, \tag{B31}$$

$$\hat{\mathcal{B}}_{M^2} I^{m_s^2}_{303(7)} = \frac{\langle g_s^2 \bar{q}q \rangle^2}{M^8} m_s^2 \frac{-7}{162\pi^2} [1 + (-1)^n]$$

$$\times \left\{ -\left(-\ln\frac{M^2}{\mu^2} + \psi(n+1) + 2\gamma_E \right) + \frac{\theta(n-1)}{n} \right.$$

$$\left. - \theta(n-2)\frac{1}{2} \left[\psi\left(\frac{n+1}{2}\right) - \psi\left(\frac{n}{2}\right) + \ln 4 \right] \right\}, \tag{B32}$$

$$\hat{\mathcal{B}}_{M^2} I^{m_s^2}_{303(8,1)+303(9,1)} = \frac{\langle g_s^2 \bar{q}q \rangle^2}{M^8} m_s^2 \frac{4}{162\pi^2} [1 + (-1)^n]$$

$$\times \left\{ -2\delta^{n0} \left(-\ln\frac{M^2}{\mu^2} + \psi(n+1) + 2\gamma_E \right. \right.$$

$$+ 1 \Big) + 2\delta^{n1} \left(-\ln \frac{M^2}{\mu^2} + \psi(n+1) + 2\gamma_E - 2 \right)$$

$$- \theta(n-2) \frac{n^2 + 4n - 2}{n}$$

$$+ \theta(n-3) \left[(n-1) \left(\psi\left(\frac{n+1}{2}\right) - \psi\left(\frac{n}{2}\right) + \ln 4 \right) - n \right] \Big\},$$
(B33)

$$\hat{\mathcal{B}}_{M^2} I^{m_s^2}_{303(8,2)+303(9,2)} = \frac{\langle g_s^2 \bar{q} q \rangle^2}{M^8} m_s^2$$

$$\times \frac{1}{162\pi^2} [1 + (-1)^n] \left(2n - 2 + 2\delta^{n1}\right).$$
(B34)

Here the subscript a, b, c, m, n in $\hat{\mathcal{B}}_{M^2} I^{m_s^2}_{abc(m,n)}$ in the expression within BFTSR, i.e. Eqs. (B10)–(B34) have following meaning. a, b, c stand for the a, b, cth-order of the propagator, vertex and propagator, while m means the mth terms of $I^{m_s^2}_{abc}$ and n means the nth subterm of $I^{m_s^2}_{abc(m)}$. Meanwhile, for the perturbative part we have

$$\mathrm{Im} I_{\mathrm{pert.}}(s) = \frac{3v^{n+1}}{8\pi(n+1)(n+3)}$$

$$\times \left\{ [1 + (-1)^n](n+1)\frac{1-v^2}{2} + [1 + (-1)^n] \right\}. \quad (B35)$$

Considering n is even, then $1 + (-1)^n = 2$, $\delta^{n1} = 0$, $\theta(n-1) = \theta(n-2)$, $\theta(n-3) = \theta(n-4)$. Add up all the above expressions we obtain the moment of distributed amplitude Eq. (33).

Appendix C: Matrix elements of $\eta^{(\prime)}$-meson twist-2, 3, 4 LCDAs

The expression of twist-2, 3, 4 LCDAs matrix elements used in the OPE calculation of LCSR have the following forms [99,100]

$$\langle \eta^{(\prime)}(p)|\bar{s}(x)\gamma_\mu\gamma_5 s(0)|0\rangle$$

$$= -ip_\mu f_{\eta^{(\prime)}} \int_0^1 du e^{iup\cdot x} [\phi_{2;\eta^{(\prime)}}(u, \mu) + x^2\psi_{4;\eta^{(\prime)}}(u)]$$

$$+ f_{\eta^{(\prime)}} \left(x_\mu - \frac{x^2 p_\mu}{p\cdot x} \right) \times \int_0^1 du e^{iup\cdot x} \phi_{4;\eta^{(\prime)}}(u), \quad (C1)$$

$$\langle \eta^{(\prime)}(p)|\bar{s}(x)i\gamma_5 s(0)|0\rangle = \frac{m_{\eta^{(\prime)}}^2 f_{\eta^{(\prime)}}}{2m_s} \int_0^1 du e^{iup\cdot x} \phi^p_{3;\eta^{(\prime)}}(u),$$
(C2)

$$\langle \eta^{(\prime)}(p)|\bar{s}(x)\sigma_{\mu\nu}\gamma_5 s(0)|0\rangle = i(p_\mu x_\nu - p_\nu x_\mu)$$

$$\times \frac{m_{\eta^{(\prime)}}^2 f_{\eta^{(\prime)}}}{12m_s} \int_0^1 du e^{iup\cdot x} \phi^\sigma_{3;\eta^{(\prime)}}(u),$$
(C3)

$$\langle \eta^{(\prime)}(p)|\bar{s}(x)\sigma_{\mu\nu}\gamma_5 g_s G_{\alpha\beta}(vx)s(0)|0\rangle$$

$$= i\frac{m_{\eta^{(\prime)}}^2 f_{\eta^{(\prime)}}}{2m_s}$$

$$\times \left(p_\alpha p_\mu g^\perp_{\nu\beta} - p_\alpha p_\nu g^\perp_{\mu\beta} - (\alpha \leftrightarrow \beta) \right) \Phi_{3;\eta^{(\prime)}}(v, p\cdot x)$$
(C4)

$$\langle \eta^{(\prime)}(p)|\bar{s}(x)\gamma_\mu\gamma_5 g_s G_{\alpha\beta}(vx)s(0)|0\rangle$$

$$= f_{\eta^{(\prime)}} \left[\frac{p_\mu}{p\cdot x}(p_\alpha x_\beta - p_\beta x_\alpha) \right.$$

$$\times \Phi_{4;\eta^{(\prime)}}(v, p\cdot x) + (p_\beta g^\perp_{\alpha\mu} - p_\alpha g^\perp_{\beta\mu})$$

$$\times \left. \Psi_{4;\eta^{(\prime)}}(v, p\cdot x) \right],$$
(C5)

$$\langle \eta^{(\prime)}(p)|\bar{s}(x)\gamma_\mu g_s \widetilde{G}_{\alpha\beta}(vx)s(0)|0\rangle$$

$$= i f_{\eta^{(\prime)}} \left[\frac{p_\mu}{p\cdot x}(p_\alpha x_\beta - p_\beta x_\alpha) \right.$$

$$\times \tilde{\Phi}_{4;\eta^{(\prime)}}(v, p\cdot x) + (p_\beta g^\perp_{\alpha\mu} - p_\alpha g^\perp_{\beta\mu})$$

$$\times \left. \tilde{\Psi}_{4;\eta^{(\prime)}}(v, p\cdot x) \right].$$
(C6)

In which, we have set

$$g^\perp_{\mu\nu} = g_{\mu\nu} - \frac{p_\mu x_\nu + p_\nu x_\mu}{p\cdot x};$$

$$K(v, p\cdot x) = \int_0^1 d\alpha_1 d\alpha_2 d\alpha_3 \delta(1 - \alpha_1 - \alpha_2 - \alpha_3)$$

$$\times e^{-i(\alpha_2 - \alpha_1 + v\alpha_3)p\cdot x} K(\alpha_i).$$
(C7)

References

1. B. Aubert et al. (BaBar), Study of the decay $D_s^+ \to K^+ K^- e^+ \nu_e$. Phys. Rev. D **78**, 051101 (2008). https://doi.org/10.1103/PhysRevD.78.051101. arXiv:0807.1599
2. J. Yelton et al. (CLEO), Absolute branching fraction measurements for exclusive $D_{(s)}$ semileptonic decays. Phys. Rev. D **80**, 052007 (2009). https://doi.org/10.1103/PhysRevD.80.052007. arXiv:0903.0601
3. K.M. Ecklund et al. (CLEO), Study of the semileptonic decay $D_s^+ \to f_0(980)e^+\nu$ and implications for $B_s^0 \to J/\psi f_0$. Phys. Rev. D **80**, 052009 (2009). https://doi.org/10.1103/PhysRevD.80.052009. arXiv:0907.3201
4. M. Ablikim et al. (BESIII), Measurements of the branching fractions for the semi-leptonic decays $D_s^+ \to \phi e^+\nu_e, \phi\mu^+\nu_\mu, \eta\mu^+\nu_\mu$ and $\eta'\mu^+\nu_\mu$. Phys. Rev. D **97**, 012006 (2018). https://doi.org/10.1103/PhysRevD.97.012006. arXiv:1709.03680
5. M. Ablikim et al. (BESIII), First measurement of the form factors in $D_s^+ \to K^0 e^+\nu_e$ and $D_s^+ \to K^{*0}e^+\nu_e$ decays. Phys. Rev. Lett. **122**, 061801 (2019). https://doi.org/10.1103/PhysRevLett.122.061801. arXiv:1811.02911
6. M. Ablikim et al. (BESIII), Measurement of the absolute branching fraction of inclusive semielectronic D_s^+ decays. Phys. Rev. D **104**, 012003 (2021). https://doi.org/10.1103/PhysRevD.104.012003. arXiv:2104.07311
7. G. Brandenburg et al. (CLEO Collaboration), Measurements of the ratios $\mathcal{B}(D_s^+ \to \eta\ell^+\nu)/\mathcal{B}(D_s^+ \to \eta'\ell^+\nu)$ and $\mathcal{B}(D_s^+ \to \eta'\ell^+\nu)/\mathcal{B}(D_s^+ \to \eta\ell^+\nu)$. Phys. Rev. Lett.

75, 3804 (1995). https://doi.org/10.1103/PhysRevLett.75.3804. arXiv:hep-ex/9508009

8. J. Hietala, D. Cronin-Hennessy, T. Pedlar and I. Shipsey (CLEO Collaboration), Exclusive D_s semileptonic branching fraction measurements, Phys. Rev. D **92**, 012009 (2015). https://doi.org/10.1103/PhysRevD.92.012009. arXiv:1505.04205

9. J. Yelton et al. (CLEO Collaboration), Absolute branching fraction measurements for exclusive $D_{(s)}$ semileptonic decays. Phys. Rev. D **80** (2009) 052007. https://doi.org/10.1103/PhysRevD.80.052007. arXiv:0903.0601

10. M. Ablikim et al. (BESIII Collaboration), Measurements of the absolute branching fractions for $D_s^+ \rightarrow \eta e^+ \nu_e$ and $D_s^+ \rightarrow \eta' e^+ \nu_e$. Phys. Rev. D **94**, 112003 (2016). https://doi.org/10.1103/PhysRevD.94.112003. arXiv:1608.06484

11. M. Ablikim et al. (BESIII Collaboration), Measurements of the branching fractions for the semi-leptonic decays $D_s^+ \rightarrow \phi e^+ \nu_e$, $\phi \mu^+ \nu_\mu$, $\eta \mu^+ \nu_\mu$ and $\eta' \mu^+ \nu_\mu$. Phys. Rev. D **97**, 012006 (2017). https://doi.org/10.1103/PhysRevD.97.012006. arXiv:1709.03680

12. M. Ablikim et al. (BESIII Collaboration), Measurement of the dynamics of the decays $D_s^+ \rightarrow \eta^{(\prime)} e^+ \nu_e$. Phys. Rev. Lett. **122**, 121801 (2019). https://doi.org/10.1103/PhysRevLett.122.121801. arXiv:1901.02133

13. G.S. Bali, S. Collins, S. Dürr, I. Kanamori, $D_s \rightarrow \eta, \eta'$ semileptonic decay form factors with disconnected quark loop contributions. Phys. Rev. D **91**, 014503 (2015). https://doi.org/10.1103/PhysRevD.91.014503. arXiv:1406.5449

14. R.C. Verma, Decay constants and form factors of S-wave and P-wave mesons in the covariant light-front quark model. J. Phys. G **39**, 025005 (2012). https://doi.org/10.1088/0954-3899/39/2/025005. arXiv:1103.2973

15. H.Y. Cheng, X.W. Kang, Branching fractions of semileptonic D and D_s decays from the covariant light-front quark model. Eur. Phys. J. C **77**, 587 (2017). https://doi.org/10.1140/epjc/s10052-017-5170-5. arXiv:1707.02851

16. Z.T. Wei, H.W. Ke, X.F. Yang, Interpretation of the "f_{D_s} puzzle" in SM and beyond. Phys. Rev. D **80**, 015022 (2009). https://doi.org/10.1103/PhysRevD.80.015022. arXiv:0905.3069

17. D. Melikhov, B. Stech, Weak form-factors for heavy meson decays: an update. Phys. Rev. D **62**, 014006 (2000). https://doi.org/10.1103/PhysRevD.62.014006. arXiv:hep-ph/0001113

18. N.R. Soni, M.A. Ivanov, J.G. Körner, J.N. Pandya, P. Santorelli, C.T. Tran, Semileptonic $D_{(s)}$-meson decays in the light of recent data. Phys. Rev. D **98**, 114031 (2018). https://doi.org/10.1103/PhysRevD.98.114031. arXiv:1810.11907

19. M.A. Ivanov, J.G. Körner, J.N. Pandya, P. Santorelli, N.R. Soni, C.T. Tran, Exclusive semileptonic decays of D and D_s mesons in the covariant confining quark model. Front. Phys. (Beijing) **14**, 64401 (2019). https://doi.org/10.1007/s11467-019-0908-1. arXiv:1904.07740

20. N. Offen, F.A. Porkert, A. Schäfer, Light-cone sum rules for the $D_s \rightarrow \eta^{(\prime)} \ell \nu_\ell$ form factor. Phys. Rev. D **88**, 034023 (2013). https://doi.org/10.1103/PhysRevD.88.034023. arXiv:1307.2797

21. G. Duplancic, B. Melic, Form factors of B, $B_s \rightarrow \eta'$ and D, $D_s \rightarrow \eta'$ transitions from QCD light-cone sum rules. JHEP **1511**, 138 (2015). https://doi.org/10.1007/JHEP11(2015)138. arXiv:1508.05287

22. P. Colangelo, F. De Fazio, $D_{(s)}$ decays to η and η' final states: a phenomenological analysis. Phys. Lett. B **520**, 78–86 (2001). https://doi.org/10.1016/S0370-2693(01)01112-1. arXiv:hep-ph/0107137

23. D.S. Du, J.W. Li, M.Z. Yang, Form-factors and semileptonic decay of $D_s^+ \rightarrow \phi \ell \nu$ from QCD sum rule. Eur. Phys. J. C **37**, 173–184 (2004). https://doi.org/10.1140/epjc/s2004-01979-9. arXiv:hep-ph/0308259

24. M.Z. Yang, Semileptonic decay of B and $D \rightarrow K_0^*(1430) \bar{\ell} \nu$ from QCD sum rule. Phys. Rev. D **73**, 034027 (2006). https://doi.org/10.1103/PhysRevD.73.079901. arXiv:hep-ph/0509103

25. J.P. Singh, S.D. Patel, Eta-nucleon and eta-prime-nucleon coupling constants in QCD and the role of gluons. Phys. Lett. B **791**, 249 (2019). https://doi.org/10.1016/j.physletb.2019.02.048. arXiv:1812.06275

26. H.B. Fu, L. Zeng, R. Lü, W. Cheng, X.G. Wu, The $D \rightarrow \rho$ semileptonic and radiative decays within the light-cone sum rules. Eur. Phys. J. C **80**, 194 (2020). https://doi.org/10.1140/epjc/s10052-020-7758-4. arXiv:1808.06412

27. S. Momeni, R. Khosravi, Semileptonic $D_{(s)} \rightarrow A \ell^+ \nu$ and non-leptonic $D \rightarrow K_1(1270, 1400)\pi$ decays in LCSR. J. Phys. G **46**, 105006 (2019). https://doi.org/10.1088/1361-6471/ab35d0. arXiv:1903.00860

28. G. Duplancic, A. Khodjamirian, T. Mannel, B. Melic, N. Offen, Light-cone sum rules for $B \rightarrow \pi$ form factors revisited. JHEP **0804**, 014 (2008). https://doi.org/10.1088/1126-6708/2008/04/014. arXiv:0801.1796

29. S. Descotes-Genon, A. Khodjamirian, J. Virto, Light-cone sum rules for $B \rightarrow K\pi$ form factors and applications to rare decays. JHEP **1912**, 083 (2019). https://doi.org/10.1007/JHEP12(2019)083. arXiv:1908.02267

30. S. Cheng, J.M. Shen, $\bar{B}_s \rightarrow f_0(980)$ form factors and the width effect from light-cone sum rules. Eur. Phys. J. C **80**, 554 (2020). https://doi.org/10.1140/epjc/s10052-020-8124-2. arXiv:1907.08401

31. S. Momeni, Helicity form factors for $D_{(s)} \rightarrow A \ell \nu$ process in the light-cone QCD sum rules approach. Eur. Phys. J. C **80**, 553 (2020). https://doi.org/10.1140/epjc/s10052-020-8084-6. arXiv:2004.02522

32. M. Emmerich, M. Strohmaier, A. Schäfer, $B \rightarrow f_2(1270)$ form factors with light-cone sum rules. Phys. Rev. D **98**, 014008 (2018). https://doi.org/10.1103/PhysRevD.98.014008. arXiv:1804.02953

33. S. Momeni, R. Khosravi, Semileptonic $B_{(s)} \rightarrow \alpha_1(K_1)\ell^+ \ell^-$ decays via the light-cone sum rules with B-meson distribution amplitudes. Phys. Rev. D **96**, 016018 (2017). https://doi.org/10.1103/PhysRevD.96.016018. arXiv:1804.04844

34. Y.L. Shen, Y.B. Wei, C.D. Lü, Renormalization group analysis of $B \rightarrow \pi$ form factors with B-meson light-cone sum rules. Phys. Rev. D **97**, 054004 (2018). https://doi.org/10.1103/PhysRevD.97.054004. arXiv:1607.08727

35. A. Bharucha, D.M. Straub, R. Zwicky, $B \rightarrow V \ell^+ \ell^-$ in the standard model from light-cone sum rules. JHEP **08**, 098 (2016). https://doi.org/10.1007/JHEP08(2016)098. arXiv:1503.05534

36. Y.J. Sun, Z.G. Wang, T. Huang, $B \rightarrow A$ transitions in the light-cone QCD sum rules with the chiral current. Chin. Phys. C **36**, 1046 (2012). https://doi.org/10.1088/1674-1137/36/11/003. arXiv:1106.4915

37. Z.G. Wang, Analysis of the $B \rightarrow K_2^*(1430)$, $a_2(1320)$, $f_2(1270)$ form-factors with light-cone QCD sum rules. Mod. Phys. Lett. A **26**, 2761 (2011). https://doi.org/10.1142/S0217732311037133. arXiv:1011.3200

38. Z.G. Wang, Analysis of the $B \rightarrow a_1(1260)$ form-factors with light-cone QCD sum rules. Phys. Lett. B **666**, 477 (2008). https://doi.org/10.1016/j.physletb.2008.08.014. arXiv:0804.0907

39. M. Beneke, V.M. Braun, Y. Ji, Y.B. Wei, Radiative leptonic decay $B \rightarrow \gamma \ell \nu_\ell$ with subleading power corrections. JHEP **07**, 154 (2018). https://doi.org/10.1007/JHEP07(2018)154. arXiv:1804.04962

40. V.V. Anisovich, D.V. Bugg, D.I. Melikhov, V.A. Nikonov, $\eta - \eta'$ glueball mixing from photon meson transition form-factors and decay ratio $D_s \rightarrow \eta \ell \nu / \eta' \ell \nu$. Phys. Lett. B **404**, 166–172 (1997). https://doi.org/10.1016/S0370-2693(97)00607-2. arXiv:hep-ph/9702383

41. P. Ball, J.M. Frere, M. Tytgat, Phenomenological evidence for the gluon content of η and η'. Phys. Lett. B **365**, 367 (1996). https://doi.org/10.1016/0370-2693(95)01287-7. arXiv:hep-ph/9508359

42. T. Feldmann, Quark structure of pseudoscalar mesons. Int. J. Mod. Phys. A **15**, 159 (2000). https://doi.org/10.1142/S0217751X00000082. arXiv:hep-ph/9907491

43. T. Huang, X.G. Wu, Determination of the η and η' mixing angle from the pseudoscalar transition form factors. Eur. Phys. J. C **50**, 771 (2007). https://doi.org/10.1140/epjc/s10052-007-0245-3. arXiv:hep-ph/0612007

44. H.W. Ke, X.Q. Li, Z.T. Wei, Determining the $\eta - \eta'$ mixing by the newly measured $\mathcal{B}(D(D_s) \to \eta(\eta')\ell\nu_l)$. Eur. Phys. J. C **69**, 133 (2010). https://doi.org/10.1140/epjc/s10052-010-1383-6. arXiv:0912.4094

45. F. De Fazio, M.R. Pennington, Radiative ϕ-meson decays and $\eta - \eta'$ mixing: a QCD sum rule analysis. JHEP **0007**, 051 (2000). https://doi.org/10.1088/1126-6708/2000/07/051. arXiv:hep-ph/0006007

46. H.M. Choi, Exclusive rare $B_s \to (K, \eta, \eta')\ell^+\ell^-$ decays in the light-front quark model. J. Phys. G **37**, 085005 (2010). https://doi.org/10.1088/0954-3899/37/8/085005. arXiv:1002.0721

47. P. Ball, G.W. Jones, $B \to \eta^{(\prime)}$ form factors in QCD. JHEP **0708**, 025 (2007). https://doi.org/10.1088/1126-6708/2007/08/025. arXiv:0706.3628

48. F. Ambrosino et al. (KLOE Collaboration), Measurement of the pseudoscalar mixing angle and eta-prime gluonium content with KLOE detector. Phys. Lett. B **648**, 267–273 (2007). https://doi.org/10.1016/j.physletb.2007.03.032. arXiv:hep-ex/0612029

49. K. Azizi, R. Khosravi, F. Falahati, Exclusive $D_s \to (\eta, \eta')\ell\nu$ decays in light cone QCD. J. Phys. G **38**, 095001 (2011). https://doi.org/10.1088/0954-3899/38/9/095001. arXiv:1011.6046

50. J. Gronberg et al. (CLEO Collaboration), Measurements of the meson-photon transition form-factors of light pseudoscalar mesons at large momentum transfer. Phys. Rev. D **57**, 33 (1998). https://doi.org/10.1103/PhysRevD.57.33. arXiv:hep-ex/9707031

51. P. del Amo Sanchez et al. (BaBar Collaboration), Measurement of the $\gamma\gamma^* \to \eta$ and $\gamma\gamma^* \to \eta'$ transition form factors. Phys. Rev. D **84**, 052001 (2011). https://doi.org/10.1103/PhysRevD.84.052001. arXiv:1101.1142

52. P. Kroll, K. Passek-Kumericki, The $\eta \, (\eta')\gamma$ transition form factor and the gluon–gluon distribution amplitude. J. Phys. G **40**, 075005 (2013). https://doi.org/10.1088/0954-3899/40/7/075005. arXiv:1206.4870

53. P. Ball, R. Zwicky, New results on $B \to \pi, K, \eta$ decay formfactors from light-cone sum rules. Phys. Rev. D **71**, 014015 (2005). https://doi.org/10.1103/PhysRevD.71.014015. arXiv:hep-ph/0406232

54. T. Huang, Z. Huang, Quantum chromodynamics in background fields. Phys. Rev. D **39**, 1213 (1989). https://doi.org/10.1103/PhysRevD.39.1213

55. T. Huang, X.N. Wang, X.D. Xiang, S.J. Brodsky, The quark mass and spin effects in the mesonic structure. Phys. Rev. D **35**, 1013 (1987). https://doi.org/10.1103/PhysRevD.35.1013

56. M.A. Shifman, A.I. Vainshtein, V.I. Zakharov, QCD and resonance physics: applications. Nucl. Phys. B **147**, 448 (1979). https://doi.org/10.1016/0550-3213(79)90023-3

57. J. Govaerts, F. de Viron, D. Gusbin, J. Weyers, Exotic mesons from QCD sum rules. Phys. Lett. B **128**, 262 (1983). https://doi.org/10.1016/0370-2693(84)92038-0

58. V.A. Novikov, M.A. Shifman, A.I. Vainshtein, V.I. Zakharov, Calculations in external fields in quantum chromodynamics. Technical review. Fortschr. Phys. **32**, 585 (1984)

59. W. Hubschmid, S. Mallik, Operator expansion at short distance in QCD. Nucl. Phys. B **207**, 29 (1982). https://doi.org/10.1016/0550-3213(82)90134-1

60. T. Zhong, X.G. Wu, Z.G. Wang, T. Huang, H.B. Fu, H.Y. Han, Revisiting the pion leading-twist distribution amplitude within the QCD background field theory. Phys. Rev. D **90**, 016004 (2014). https://doi.org/10.1103/PhysRevD.90.016004. arXiv:1405.0774

61. H.B. Fu, X.G. Wu, W. Cheng, T. Zhong, ρ-meson longitudinal leading-twist distribution amplitude within QCD background field theory. Phys. Rev. D **94**, 074004 (2016). https://doi.org/10.1103/PhysRevD.94.074004. arXiv:1607.04937

62. H.B. Fu, L. Zeng, W. Cheng, X.G. Wu, T. Zhong, Longitudinal leading-twist distribution amplitude of the J/ψ meson within the background field theory. Phys. Rev. D **97**, 074025 (2018). https://doi.org/10.1103/PhysRevD.97.074025. arXiv:1801.06832

63. T. Zhong, X.G. Wu, T. Huang, Heavy pseudoscalar leading-twist distribution amplitudes within QCD theory in background fields. Eur. Phys. J. C **75**, 45 (2015). https://doi.org/10.1140/epjc/s10052-015-3271-6. arXiv:1408.2297

64. T. Zhong, X.G. Wu, T. Huang, H.B. Fu, Heavy pseudoscalar twist-3 distribution amplitudes within QCD theory in background fields. Eur. Phys. J. C **76**, 509 (2016). https://doi.org/10.1140/epjc/s10052-016-4350-z. arXiv:1604.04709

65. T. Zhong, X.G. Wu, J.W. Zhang, Y.Q. Tang, Z.Y. Fang, New results on pionic twist-3 distribution amplitudes within the QCD sum rules. Phys. Rev. D **83**, 036002 (2011). https://doi.org/10.1103/PhysRevD.83.036002. arXiv:1101.3592

66. H.Y. Han, X.G. Wu, H.B. Fu, Q.L. Zhang, T. Zhong, Twist-3 distribution amplitudes of scalar mesons within the QCD sum rules and its application to the $B \to S$ transition form factors. Eur. Phys. J. A **49**, 78 (2013). https://doi.org/10.1140/epja/i2013-13078-7. arXiv:1301.3978

67. T. Huang, X.H. Wu, M.Z. Zhou, Twist three distribute amplitudes of the pion in QCD sum rules. Phys. Rev. D **70**, 014013 (2004). https://doi.org/10.1103/PhysRevD.70.014013. arXiv:hep-ph/0402100

68. T. Huang, M.Z. Zhou, X.H. Wu, Twist-3 distribution amplitudes of the pion and kaon from the QCD sum rules. Eur. Phys. J. C **42**, 271 (2005). https://doi.org/10.1140/epjc/s2005-02285-x. arXiv:hep-ph/0501032

69. T. Zhong, X.G. Wu, H.Y. Han, Q.L. Liao, H.B. Fu, Z.Y. Fang, Revisiting the twist-3 distribution amplitudes of K-meson within the QCD background field approach. Commun. Theor. Phys. **58**, 261 (2012). https://doi.org/10.1088/0253-6102/58/2/16. arXiv:1109.3127

70. Y. Zhang, T. Zhong, X.G. Wu, K. Li, H.B. Fu, T. Huang, Uncertainties of the $B \to D$ transition form factor from the D-meson leading-twist distribution amplitude. Eur. Phys. J. C **78**, 76 (2018). https://doi.org/10.1140/epjc/s10052-018-5551-4. arXiv:1709.02226

71. Y. Zhang, T. Zhong, H.B. Fu, W. Cheng, X.G. Wu, D_s-meson leading-twist distribution amplitude within the QCD sum rules and its application to the $B_s \to D_s$ transition form factor. Phys. Rev. D **103**, 114024 (2021). https://doi.org/10.1103/PhysRevD.103.114024. arXiv:2104.00180

72. D.D. Hu, H.B. Fu, T. Zhong, Z.H. Wu, X.G. Wu, Investigating $D \to a_1(1260)\ell^+\nu_\ell$ processes within QCD sum rules framework. arXiv:2107.02758

73. I.C. Cloët, L. Chang, C.D. Roberts, S.M. Schmidt, P.C. Tandy, Pion distribution amplitude from lattice QCD. Phys. Rev. Lett. **111**, 092001 (2013). https://doi.org/10.1103/PhysRevLett.111.092001. arXiv:1306.2645

74. M.V. Polyakov, H.D. Son, On the second Gegenbauer moment of ρ-meson distribution amplitude. Phys. Rev. D **102**, 114005 (2020). https://doi.org/10.1103/PhysRevD.102.114005. arXiv:2008.06270

75. S. Cheng, A. Khodjamirian, A.V. Rusov, Pion light-cone distribution amplitude from the pion electromagnetic form factor. Phys.

Rev. D **102**, 074022 (2020). https://doi.org/10.1103/PhysRevD.102.074022. arXiv:2007.05550

76. W. Wang, Y.M. Wang, J. Xu, S. Zhao, *B*-meson light-cone distribution amplitude from Euclidean quantities. Phys. Rev. D **102**, 011502 (2020). https://doi.org/10.1103/PhysRevD.102.011502. arXiv:1908.09933

77. J.H. Zhang, J.W. Chen, X. Ji, L. Jin, H.W. Lin, Pion distribution amplitude from lattice QCD. Phys. Rev. D **95**, 094514 (2017). https://doi.org/10.1103/PhysRevD.95.094514. arXiv:1702.00008

78. F. Zuo, T. Huang, Photon-to-pion transition form factor and pion distribution amplitude from holographic QCD. Eur. Phys. J. C **72**, 1813 (2012). https://doi.org/10.1140/epjc/s10052-011-1813-0. arXiv:1105.6008

79. X.G. Wu, T. Huang, An implication on the pion distribution amplitude from the pion-photon transition form factor with the new BABAR data. Phys. Rev. D **82**, 034024 (2010). https://doi.org/10.1103/PhysRevD.82.034024. arXiv:1005.3359

80. A. Khodjamirian, T. Mannel, N. Offen, Form-factors from light-cone sum rules with *B*-meson distribution amplitudes. Phys. Rev. D **75**, 054013 (2007). https://doi.org/10.1103/PhysRevD.75.054013. arXiv:hep-ph/0611193

81. F. Zuo, T. Huang, B_c (B) → $D\ell\nu$ form-factors in light-cone sum rules and the *D*-meson distribution amplitude. Chin. Phys. Lett. **24**, 61 (2007). https://doi.org/10.1088/0256-307X/24/1/017. arXiv:hep-ph/0611113

82. Y.M. Makeenko, A.A. Migdal, Exact equation for the loop average in multicolor QCD. Phys. Lett. B **88**, 135 (1979). https://doi.org/10.1016/0370-2693(79)90131-X [Erratum: Phys. Lett. B **89**, 437 (1980)]

83. M.A. Shifman, A.I. Vainshtein, M.B. Voloshin, V.I. Zakharov, η_c puzzle in quantum chromodynamics. Phys. Lett. B **77**, 80–83 (1978). https://doi.org/10.1016/0370-2693(78)90206-X

84. J. Ambjorn, R.J. Hughes, Canonical quantization in nonabelian background fields. Ann. Phys. **145**, 340 (1983). https://doi.org/10.1016/0003-4916(83)90187-2

85. J. Govaerts, F. de Viron, D. Gusbin, J. Weyers, Exotic mesons from QCD sum rules. Phys. Lett. B **128**, 262 (1983). https://doi.org/10.1016/0370-2693(84)92038-0

86. J. Ambjorn, R.J. Hughes, Ann. Phys. **145**, 340 (1983). https://doi.org/10.1016/0003-4916(83)90187-2

87. J. Ambjorn, R.J. Hughes, Nucl. Phys. B **217**, 336 (1983)

88. M.A. Shifman, Wilson loop in vacuum fields. Nucl. Phys. B **173**, 13–31 (1980)

89. T. Zhong, Z.H. Zhu, H.B. Fu, X.G. Wu, T. Huang, An improved light-cone harmonic oscillator model for the pionic leading-twist distribution amplitude. Phys. Rev. D **104**, 016021 (2021). https://doi.org/10.1103/PhysRevD.104.016021 arXiv:2102.03989

90. P. Ball, V.M. Braun, The ρ-meson light cone distribution amplitudes of leading twist revisited. Phys. Rev. D **54**, 2182 (1996). https://doi.org/10.1103/PhysRevD.54.2182. arXiv:hep-ph/9602323

91. P.A. Zyla et al. (Particle Data Group), Review of particle physics. PTEP **2020**, 083C01 (2020). https://doi.org/10.1093/ptep/ptaa104

92. A. Ali, G. Kramer, C.D. Lü, Experimental tests of factorization in charmless nonleptonic two-body B decays. Phys. Rev. D **58**, 094009 (1998). https://doi.org/10.1103/PhysRevD.58.094009. arXiv:hep-ph/9804363

93. S. Narison, Improved $f_{D^*_{(s)}}$, $f_{B^*_{(s)}}$ and f_{B_c} from QCD Laplace sum rules. Int. J. Mod. Phys. A **30**, 1550116 (2015). https://doi.org/10.1142/S0217751X1550116X. arXiv:1404.6642

94. P. Colangelo, A. Khodjamirian, QCD sum rules, a modern perspective. arXiv:hep-ph/0010175

95. K.C. Yang, W.Y.P. Hwang, E.M. Henley, L.S. Kisslinger, QCD sum rules and neutron proton mass difference. Phys. Rev. D **47**, 3001 (1993). https://doi.org/10.1103/PhysRevD.47.3001

96. W.Y.P. Hwang, K.C. Yang, QCD sum rules: $\Delta - N$ and $\Sigma^0 - \Lambda$ mass splittings. Phys. Rev. D **49**, 460 (1994). https://doi.org/10.1103/PhysRevD.49.460

97. C.D. Lü, Y.M. Wang, H. Zou, Twist-3 distribution amplitudes of scalar mesons from QCD sum rules. Phys. Rev. D **75**, 056001 (2007). https://doi.org/10.1103/PhysRevD.75.056001. arXiv:hep-ph/0612210

98. T. Huang, Z.H. Li, X.Y. Wu, Improved approach to the heavy to light form-factors in the light cone QCD sum rules. Phys. Rev. D **63**, 094001 (2001). https://doi.org/10.1103/PhysRevD.63.094001

99. P. Ball, V.M. Braun, A. Lenz, Higher-twist distribution amplitudes of the *K*-meson in QCD. JHEP **05**, 004 (2006). https://doi.org/10.1088/1126-6708/2006/05/004. arXiv:hep-ph/0603063

100. H.B. Fu, W. Cheng, R.Y. Zhou, L. Zeng, $D \to P(\pi, K)$ helicity form factors within light-cone sum rule approach. Chin. Phys. C **44**, 113103 (2020). https://doi.org/10.1088/1674-1137/abae4f. arXiv:2002.11279

101. H.B. Fu, X.G. Wu, H.Y. Han, Y. Ma, $B \to \rho$ transition form factors and the ρ-meson transverse leading-twist distribution amplitude. J. Phys. G **42**, 055002 (2015). https://doi.org/10.1088/0954-3899/42/5/055002. arXiv:1406.3892

102. A. Bharucha, T. Feldmann, M. Wick, Theoretical and phenomenological constraints on form factors for radiative and semi-leptonic *B*-meson decays. JHEP **1009**, 090 (2010). https://doi.org/10.1007/JHEP09(2010)090. arXiv:1004.3249

103. C. Bourrely, I. Caprini, L. Lellouch, Model-independent description of $B \to \pi l \nu$ decays and a determination of $|V_{ub}|$. Phys. Rev. D **79**, 013008 (2009). https://doi.org/10.1103/PhysRevD.82.099902. arXiv:0807.2722